THE ROLE OF *VIBRIO* BACTERIA IN DISEASE AND DYSBIOSIS OF THE THREATENED CARIBBEAN ELKHORN CORAL, *ACROPORA PALMATA*

by

KERI GOODMAN KEMP

(Under the Direction of Erin K. Lipp)

ABSTRACT

The critically endangered elkhorn coral, *Acropora palmata*, is affected by white pox disease (WPX) throughout the Florida Reef Tract and wider Caribbean. This dissertation examines the association of *Vibrio* bacteria with WPX occurrence in the Florida Keys, USA. The concentration of *Vibrio* was consistently greater in WPX samples compared to healthy samples across the three years (2012–2014). In summer 2015, we utilized a high resolution sampling approach (2–3 times per week) to examine changes in the *A. palmata* microbiome during WPX onset and progression. Microbial assemblages from new disease lesions (≤ 24 h) had higher levels of beta diversity (sample-to-sample) and lower levels of evenness and phylogenetic diversity. We also identifed the combination of low wind speed and high seawater temperature as important thresholds that may lead WPX lesion formation. WPX lesions healed rapidly, decreasing in size by ~29% after just 8–13 d and transitioned close the community composition of the "healthy" state within days. This suggests the coral and/or the commensal microbiota are resilient to ephemeral *Vibrio* blooms and that although *A. palmata* in the Florida Keys develop WPX signs, they may now be resistant to tissue-loss progression due to WPX.

We assessed the diversity of 69 *Vibrio* isolates collected from diseased and apparently healthy *A. palmata* colonies and the surrounding seawater by multilocus sequence analysis (MLSA) and found no strong association of particular *Vibrio* species with health status or sample type; however, 86% of total isolates were closely related to *Vibrio* species with known pathogenicity to corals. Taken together, these results indicate that *Vibrio* may be part of a non-specific, heterotrophic bloom in WPX disease lesions. Additionally, we sequenced and assembled draft genomes of the 69 *Vibrio* spp. isolates. The availability of these genomes will provide an important foundation for understanding *Vibrio* blooming in the coral microbiome.

INDEX WORDS: *Vibrio*, coral disease, microbiome, host-microbe interactions, dysbiosis, pathobiont, conditionally rare taxa (CRT)

THE ROLE OF *VIBRIO* BACTERIA IN DISEASE AND DYSBIOSIS OF THE THREATENED CARIBBEAN ELKHORN CORAL, *ACROPORA PALMATA*

by

KERI GOODMAN KEMP

B.S., Kansas State University, 2001

M.S., Georgia Institute of Technology, 2011

A Dissertation Submitted to the Graduate Faculty of The University of Georgia in Partial Fulfillment of the Requirements for the Degree

DOCTOR OF PHILOSOPHY

ATHENS, GEORGIA

2017

THE ROLE OF *VIBRIO* BACTERIA IN DISEASE AND DYSBIOSIS OF THE THREATENED CARIBBEAN ELKHORN CORAL, *ACROPORA PALMATA*

by

KERI GOODMAN KEMP

Major Professor: Erin K. Lipp
Committee: James W. Porter
John P. Wares
Eric V. Stabb
Mary Ann Moran

Electronic Version Approved:

Suzanne Barbour
Dean of the Graduate School
The University of Georgia
May 2017

DEDICATION

The love and support of my family made this work possible. I dedicate this dissertation to my parents, Doug and Jean Goodman and my husband, Dusty Kemp.

ACKNOWLEDGEMENTS

I would like to thank my advisor Erin Lipp for her continuous support and patience throughout the entire dissertation process. I also thank my committee members, James Porter, Eric Stabb, Mary Ann Moran and John Wares for their enthusiasm and guidance. I am thankful for the friendly support of everyone at MOTE Tropical Research Laboratory, especially Erich Bartels, Corey Walter, and Mark Knowels. Finally and most importantly I would like to thank my family, especially my husband, Dusty Kemp, who provided aid as a field assistant, laboratory assistant, and editor.

TABLE OF CONTENTS

Page

APPENDICES

LIST OF TABLES

Page

LIST OF FIGURES

Page

CHAPTER 1

INTRODUCTION

The health and immunity of reef-building corals is intimately intertwined with their microbial associates (Bourne *et al.*, 2016; Ainsworth *et al.*, 2010; Sweet and Brown, 2016; Blackall *et al.*, 2015). The term ‘‘holobiont’’ has been used to embody this symbiotic relationship and refers to the coral animal together with its intracellular micro-algae and diverse assemblage of bacteria, archaea, fungi, protists, and viruses (Rohwer *et al.*, 2002). Since corals lack the ability to produce antibodies and have no adaptive immune system, it is believed that their microbiota play an important role in disease resistance (Rosenberg *et al.*, 2007; Mao-Jones *et al.*, 2010; Krediet *et al.*, 2013b). Surface mucus layer (SML) microbes serve as a barrier to invading pathogens by competition and/or producing antimicrobial compounds (Mao-Jones *et al.*, 2010; Ritchie, 2006; Krediet *et al.*, 2013a).

The importance of coral-microbe associations is becoming increasingly apparent as coral reefs continue to decline worldwide. Caribbean reefs have lost more than 80% of their coral cover over the last three decades (Gardner *et al.*, 2003) due to rising sea temperatures, loss of herbivores, and the emergence of new marine diseases. Over 20 coral diseases have been described to date (Weil and Rogers, 2010; Sutherland *et al.*, 2004), and disease prevalence and severity is increasing with global climate change (Precht *et al.*, 2016; Ruiz-Moreno *et al.*, 2012; Sweet and Brown, 2016).

While bacterial etiological agents are believed to be associated with many coral diseases, only a few studies have shown that specific bacteria are capable of causing disease through fulfillment of Koch's and Hill's postulates (Sutherland *et al.*, 2016). There is a growing realization that application of these fundamental postulates is limited in coral disease (Sweet and Bulling, 2017; Sussman *et al.*, 2008) and other fields (Nelson *et al.*, 2012; Vayssier-Taussat, 2014) because they are largely based upon the 'one pathogen, one disease' framework. It is becoming increasingly clear that many infections in corals and other hosts have a polymicrobial etiology, in which several microorganisms are involved in disease origin and/or manifestation. (Sutherland *et al.*, 2016; Sweet and Bulling, 2017).

Sweet and Bulling (Sweet and Bulling, 2017) recently proposed that considering the coral 'pathobiome' (members within the microbiome that are directly involved in pathogenesis) offers a new framework for advancing coral disease research beyond the 'one pathogen, one disease' paradigm. In this view, pathogens live and interact with other microorganisms and these complex interactions influence or drive disease dynamics (Vayssier-Taussat, 2014). The pathobiome framework places a new emphasis on elucidating ecological interactions and spatiotemporal dynamics of these communities, drawing on ecological theory in community assembly and succession (Vayssier-Taussat, 2014; Nelson *et al.*, 2012; Byrd and Segre, 2016; Sweet and Bulling, 2017).

This dissertation investigates the role of *Vibrio* bacteria in disease of the critically endangered Caribbean elkhorn coral, *Acropora palmata*. Vibrios have received a great deal of attention in coral disease for their role in pathogenesis in white syndromes (Ushijima *et al.*, 2014; 2012; Sussman *et al.*, 2008), white band disease (Ritchie and

Smith, 1998; Gil-Agudelo *et al.*, 2006), *Porites* white patch and white spot diseases (Arboleda and Reichardt, 2010; Zhenyu *et al.*, 2013), and Caribbean yellow band disease (Cervino *et al.*, 2008). Until now, the role of *Vibrio* in white pox disease (WPX) of *A. palmata* has been uninvestigated. Documentation is provided here that shows *Vibrio* are present in low abundance within the *Acropora palmata* microbiome and can exhibit dramatic increases in relative abundance during WPX disease. This dissertation frames *Vibrio* spp. as 'pathobionts' in the coral microbiome, capable of eliciting disease under certain environmental conditions. Examining *Vibrio* from a pathobiome/pathobiont framework, emphasizing environmental thresholds that trigger changes in *Vibrio* population growth and virulence expression with potential consequences for microbiome and immune homeostasis can advance our understanding of the role *Vibrio* play in coral disease.

References

Ainsworth TD, Thurber R, Gates R. (2010). The future of coral reefs: a microbial perspective. *Trends Ecol Evol* **25**: 233–240.

Arboleda M, Reichardt WT. (2010). *Vibrio* sp. causing *Porites* ulcerative white spot disease. *Dis Aquat Org* **90**: 93–104.

Blackall LL, Wilson B, van Oppen MJH. (2015). Coral-the world's most diverse symbiotic ecosystem. *Mol Ecol* **24**: 5330–5347.

Bourne DG, Morrow KM, Webster NS. (2016). Insights into the coral microbiome: underpinning the health and resilience of reef ecosystems. *Annu Rev Microbiol* **70**: 317–340.

Byrd AL, Segre JA. (2016). Adapting Koch's postulates. *Science* **351**: 224–226.

Cervino JM, Thompson FL, Gomez-Gil B, Lorence EA, Goreau TJ, Hayes RL, *et al.* (2008). The *Vibrio* core group induces yellow band disease in Caribbean and Indo-Pacific reef-building corals. *J Appl Microbiol* **105**: 1658–1671.

Gardner T, Côté I, Gill J, Grant A, Watkinson A. (2003). Long-term region-wide declines in Caribbean corals. *Science* **301**: 958–960.

Gil-Agudelo DL, Smith GW, Weil E. (2006). The white band disease type II pathogen in Puerto Rico. *Rev Biol Trop* **54**: 59–67.

Krediet CJ, Ritchie KB, Alagely A, Teplitski M. (2013a). Members of native coral microbiota inhibit glycosidases and thwart colonization of coral mucus by an opportunistic pathogen. *ISME J* **7**: 980–990.

Krediet CJ, Ritchie KB, Paul VJ, Teplitski M. (2013b). Coral-associated micro-organisms and their roles in promoting coral health and thwarting diseases. *Proc R Soc B Biol Sci* **280**: 20122328.

Mao-Jones J, Ritchie KB, Ellner SP. (2010). How microbial community composition regulates coral disease development. *PLoS Biol* **8**: e1000345.

Nelson A, De Soyza A, Perry JD, Sutcliffe IC, Cummings SP. (2012). Polymicrobial challenges to Koch's postulates: ecological lessons from the bacterial vaginosis and cystic fibrosis microbiomes. *Innate Immun* **18**: 774–783.

Precht WF, Gintert BE, Robbart ML, Fura R, van Woesik R. (2016). Unprecedented disease-related coral mortality in Southeastern Florida. *Sci Rep* **6**: 31374–31311.

Ritchie KB. (2006). Regulation of microbial populations by coral surface mucus and mucus-associated bacteria. *Mar Ecol Prog Ser* **322**: 1–14.

Ritchie KB, Smith GW. (1998). Type II white-band disease. *Rev Biol Trop* **46**: 199–203.

Rohwer F, Seguritan V, Azam F, Knowlton N. (2002). Diversity and distribution of coral-associated bacteria. *Mar Ecol Prog Ser* **243**: 1–10.

Rosenberg E, Koren O, Reshef L, Efrony R, Zilber-Rosenberg I. (2007). The role of microorganisms in coral health, disease and evolution. *Nat Rev Micro* **5**: 355–362.

Ruiz-Moreno D, Willis BL, Page AC, Weil E, Croquer A, Vargas-Angel B, *et al.* (2012). Global coral disease prevalence associated with sea temperature anomalies and local factors. *Dis Aquat Org* **100**: 249–261.

Sussman M, Willis BL, Victor S, Bourne DG. (2008). Coral pathogens identified for White Syndrome (WS) epizootics in the Indo-Pacific. *PLoS One* **3**: e2393–14.

Sutherland KP, Berry B, Park A, Kemp DW, Kemp KM, Lipp EK, *et al.* (2016). Shifting white pox aetiologies affecting *Acropora palmata* in the Florida Keys, 1994-2014. *Philos Trans R Soc Lond B Biol Sci* **371**: 20150205.

Sutherland KP, Porter JW, Torres C. (2004). Disease and immunity in Caribbean and Indo-Pacific zooxanthellate corals. *Mar Ecol Prog Ser* **266**: 273–302.

Sweet MJ, Brown BE. (2016). Coral responses to anthropogenic stress in the twenty-first century: an ecophysiological perspective. *Oceanogr Mar Bio Ann Rev* **54**: 271–314.

Sweet MJ, Bulling MT. (2017). On the importance of the microbiome and pathobiome in coral health and disease. *Front Mar Sci* **4**: 2261–11.

Ushijima B, Smith A, Aeby GS, Callahan SM. (2012). *Vibrio owensii* Induces the tissue loss disease *Montipora* white syndrome in the Hawaiian reef coral *Montipora capitata*. *PLoS One* **7**: e46717–10.

Ushijima B, Videau P, Burger AH, Shore-Maggio A, Runyon CM, Sudek M, *et al.* (2014). *Vibrio coralliilyticus* strain ocn008 is an etiological agent of acute *Montipora* white syndrome. *Appl Environ Microbiol* **80**: 2102–2109.

Vayssier-Taussat M. (2014). Shifting the paradigm from pathogens to pathobiome: new concepts in the light of meta-omics. *Front Cell Infect Microbiol* **4**: 1–7.

Weil E, Rogers CS. (2010). Coral Reef Diseases in the Atlantic-Caribbean. In: Coral Reefs: An Ecosystem in Transition. *Coral Reefs: An Ecosystem in Transition*. Springer Netherlands: Dordrecht, pp 465–491.

Zhenyu X, Shaowen K, Chaoqun H, Zhixiong Z, Shifeng W, Yongcan Z. (2013). First characterization of bacterial pathogen, *Vibrio alginolyticus*, for *Porites andrewsi* white syndrome in the South China Sea. *PLoS One* **8**: e75425–8.

CHAPTER 2

LITERATURE REVIEW

Moving beyond the 'one pathogen, one disease' paradigm. Diseases in coral reef ecosystems have been studied for several decades (Bruckner, 2015); however, our understanding of coral disease epidemiology is limited and few etiologic agents have been identified (Sutherland *et al.*, 2016). In keeping with the 'one pathogen, one disease' paradigm, coral disease studies have historically focused on describing the relationship between specific microbial taxa and the disease state (Sweet and Bulling, 2017). The goal has been to identify taxa that are (1) present in disease samples while absent in healthy samples or (2) have increased abundance in disease samples compared to healthy samples. However, most of these investigations have failed to produce evidence for the association between a single pathogen and the disease state (Sutherland *et al.*, 2016).

Other fields examining disease in complex host-microbe systems have suffered the same challenges. This statement in a recent review of human inflammatory diseases echoes the failures in coral disease, "decades of microbiological study have failed to produce an inviolable association between any organism or group of organisms and periodontitis" (Lamont and Hajishengallis, 2015). It has become apparent that the etiology of many of diseases that initiate on mucosal membranes, including periodontitis, lung infections, bacterial vaginosis, and gastro-intestinal inflammatory diseases, do not involve monocultures of bacteria, but rather heterogeneous communities of organisms (Lamont and Hajishengallis, 2015; Nelson *et al.*, 2012). Pathogenesis of disease can arise

from polymicrobial synergy that results in disruption of microbiome homeostasis and normal immune responses. This realization has lead to a paradigm shift in the study of human inflammatory diseases, which calls into question the utility of Koch's postulates in polymicrobial diseases (Byrd and Segre, 2016; Nelson *et al.*, 2012; Vayssier-Taussat, 2014). These postulates favor the identification of the most abundance taxa present at the time of symptomatic infection, while ignoring the role of other (potentially less abundant) taxa prior to the development of disease signs. Second, these postulates and their later adaptations state that a pathogen should be absent or less abundant in the healthy state. Yet commensal (*e.g.*, *Clostridium difficile* (Kamada *et al.*, 2013b)) and even mutualistic microbes (*e.g.*, *Bifidiobacteria* (Pathak *et al.*, 2014)) that regularly occur in the microbiome can become pathogenic under certain conditions. These microbiome members with pathogenic potential have been termed 'pathobionts' (Chow *et al.*, 2011), and their switch in symbiosis status may occur due to an increase in relative abundance and/or activation and expression of virulence mechanisms.

The coral disease field has been arguably slower in adopting new frameworks to advance beyond the 'one pathogen, one disease' paradigm. However, Sweet and Bulling (2017) have recently advocated the application of the 'pathobiome' model to coral disease. In this view, pathogens live and interact with other microbiome members and these complex interactions influence or drive disease dynamics (Lamont and Hajishengallis, 2015; Hajishengallis *et al.*, 2012; Vayssier-Taussat, 2014; Kamada *et al.*, 2013b; 2013a). The pathobiome framework places a new emphasis on elucidating ecological interactions and spatiotemporal dynamics of these communities, drawing on ecological theory in community assembly and succession (Vayssier-Taussat, 2014). This

framework may be more applicable to coral diseases that do not appear to follow a contagion model of disease in which pathogens are transmitted directly from colony to colony, by biological vectors, or indirectly through the water column. Indeed, many common Caribbean coral diseases including white pox disease (WPX), yellow-band disease, dark-spot syndrome, and white plague do not display contagion properties *in situ* (Muller and van Woesik, 2012; 2014). Thus, adopting a non-contagion approach that emphasizes examination of environmental thresholds important for disease induction, disruption of microbiome homeostasis, and host organismal traits that affect susceptibility to biotic and abiotic stressors may provide insightful results (Muller and van Woesik, 2012; Sweet and Bulling, 2017).

Viewing *Vibrio* bacteria as 'pathobionts'. To date, ten different *Vibrio* species have also been implicated as etiologic agents in disease of reef-building corals (reviewed in Table 3.1). *Vibrio* relative abundance often increases significantly in the coral microbiome during disease (Ushijima *et al.*, 2012; Sussman *et al.*, 2008; Pantos and Bythell, 2006), temperature stress (Thurber *et al.*, 2009; Bourne *et al.*, 2007; Bourne and Munn, 2005; Tout *et al.*, 2015; Ziegler *et al.*, 2017), and low water flow (Lee *et al.*, 2017). However, *Vibrio* are found in low abundance in the microbiomes of apparently healthy corals (Alves *et al.*, 2010; Pollock *et al.*, 2016; Rubio-Portillo *et al.*, 2014). *Vibrio* isolates from coral mucus are capable of fixing N_2, and might function as coral mutualists during non-stressful conditions (Chimetto *et al.*, 2008; Benavides *et al.*, 2017). With environmental stress or when coral hosts are immunosuppressed, *Vibrio* may shift along the symbiotic spectrum from functioning as commensals or mutualists to functioning as potential pathogens. Thus, it can be useful to examine conditionally rare

Vibrio spp. in the coral microbiome as potential 'pathobionts'. The term 'pathobiont' was developed in the study of human inflammatory diseases to describe regularly occurring microbiome members that are normally innocuous and promote pathology only under conditions of disrupted homeostasis (Chow *et al.*, 2011).

Vibrio populations are increasing in coastal waters with rising sea surface temperatures, and it is expected that potentially pathogenic *Vibrio* populations will pose an even greater threat to human and marine animal health in the future (Vezzulli *et al.*, 2016). There is an urgent need to better understand biotic and abiotic conditions that promote *Vibrio* blooms in the coral microbiome and how *Vibrio* spp. influence coral health as coral disease poses an increasing threat to reef ecosystems (Precht *et al.*, 2016; Ruiz-Moreno *et al.*, 2012; Sweet and Brown, 2016; Weil and Rogers, 2011).

Investigating the pathogenic role of vibrios in coral disease is complicated because *Vibrio* virulence is often dissociated from phylogenetic relatedness. This is because *Vibrio* virulence genes are often contained in mobile genetic elements (including plasmids, pro-phages, and integrons) and can be easily lost, gained, and transferred. For example, closely related pathogenic *V. cholerae* strains can differ in their virulence properties depending on which sets of genes they carry for antibiotic resistance, toxin production and toxin secretion (Choi *et al.*, 2016). Rather than examining the presence/absence of certain *Vibrio* species with host health state, it has been argued that a functional approach— examining genome content and virulence potential— is needed to advance our understanding of the role *Vibrio* play in coral disease (Thurber *et al.*, 2009; Sweet and Bulling, 2017).

***Vibrio* interactions with the coral immune system.** A key hallmark of polymicrobial diseases is the interaction between microbes and their host's immune system. Particulars players in polymicrobial diseases may interact with and disrupt normal immune function, which in turn inhibits the host's ability to control its commensal microbial community (Lamont and Hajishengallis, 2015; Kamada *et al.*, 2013b). A prime example is the interaction between *Porphyromonas gingivalis*, the host immune system, and the commensal community during periodontal disease. In the mouse model of periodontitis, the keystone pathogen *Porphyromonas gingivalis* initiates an uncontrolled inflammatory response and impairs leukocyte killing cells, resulting in overgrowth of commensals (Hajishengallis *et al.*, 2012). Thus, *P. gingivalis* is capable of remodeling normally benign microbiota into a dysbiotic role by interrupting normal immune function. *P. gingivalis* fails to cause periodontitis in gene-knock out mice that lack the cellular receptors necessary for the bacterium to subvert leukocyte defenses and there is no uncontrolled bacterial growth leading to destructive inflammation. Thus, it is the interaction between *P. gingivalis* and the commensal microbiota, mediated by the host immune system, which leads to periodontal inflammatory disease. *P. gingivalis* has been termed a 'keystone pathogen' in this system because this bacterium is able to initiate disease even at very low colonization levels (<0.01% of the total bacterial count) (Hajishengallis *et al.*, 2012).

It is likely that similar mechanisms, involving polymicrobial synergy (Lamont and Hajishengallis, 2015), give rise to disease and dysbiosis in corals. Experimental studies are needed to further examine the interaction between *Vibrio* spp. and other potential coral pathogens, the host immune system, and coral microbiome. At least one

vibrio, *V. coralliilyticus*, has been shown to suppress coral innate immune pathways (Vidal-Dupiol *et al.*, 2014). The common pacific coral *Pocillopora damicornis* produces an antimicrobial peptide (Damicornin), which is housed within granular cells in the coral's ectoderm and is active against fungi and gram-positive bacteria (Vidal-Dupiol *et al.*, 2011). *V. coralliilyticus* is capable of entering ectodermal cells of the host, where it replicates and causes a 50-fold decrease in Damicornin concentration by some unknown process. Other *Vibrio* bacteria are known to cause transcriptional changes in their host (*i.e.*, *V. fisheri* suppresses host squid production of nitric oxide (Norsworthy and Visick, 2013)). Thus, it is proposed that once *V. coralliilyticus* enters coral cells, it is able to interfere with host transcription of Damicornin (Vidal-Dupiol *et al.*, 2011; 2014).

The production of antimicrobial peptides may have evolved as an ancient means by the innate immune system to control host-microbial specificity (Franzenburg *et al.*, 2013). Changes in the host production of antimicrobial peptides drastically alter the microbiome community composition of another cnidarian, the freshwater species *Hydra* (Franzenburg *et al.*, 2013; 2012). Thus, the reduction of Damicornin may lead to a diminished ability of *P. damicornis* to regulate its microbiome. Thus, *V. coralliilyticus*, may prove to be a keystone coral pathogen (Hajishengallis *et al.*, 2012), capable interrupting normal coral immune function to initiate disease and dysbiosis.

Describing disease onset and secondary dysbiotic stages. To capture the dynamic interactions during polymicrobial disease in corals, an appropriate sampling resolution must be applied. Sampling in coral disease has often been conducted in a cross-sectional manner, in which collections for microbiological comparisons of disease to healthy individuals are made at a single time point during a disease outbreak. Studies

that have included temporal sampling have done so in a seasonal manner, comparing samples collected at single time point within a given season (*i.e.*, summer versus winter) (Joyner *et al.*, 2015; Pollock *et al.*, 2016; Sussman *et al.*, 2008; Séré *et al.*, 2015). While these sampling schemes have yielded important information on seasonal shifts in the coral microbiome (Pollock *et al.*, 2016) and have led to the identification of several disease agents (Sussman *et al.*, 2008; Séré *et al.*, 2015), they often lack the resolution needed to distinguish initial pathogenesis from secondary disease stages. For example, corals are most frequently sampled after classic disease signs are already apparent, while the onset of disease is missed. Thus, many described microbial patterns typical of the disease state, such as increased abundance of Rhodobacteraceae (Sunagawa *et al.*, 2009; Cárdenas *et al.*, 2011; Roder *et al.*, 2014; Pollock *et al.*, 2016), may reflect secondary opportunistic stages rather than primary pathogenesis. The combination of appropriately scaled longitudinal studies and examination of biotic and abiotic thresholds that may serve as tipping points for disruption of microbiome and coral immune homeostasis will advance coral disease research.

References

Alves N, Neto OSM, Silva BSO, De Moura RL, Francini-Filho RB, Barreira e Castro C, *et al.* (2010). Diversity and pathogenic potential of vibrios isolated from Abrolhos Bank corals. *Environ Microbiol Rep* **2**: 90–95.

Benavides M, Bednarz VN, Ferrier-Pagès C. (2017). Diazotrophs: overlooked key players within the coral symbiosis and tropical reef ecosystems? *Front Mar Sci* **4**: 2261–17.

Bourne D, Iida Y, Uthicke S, Smith-Keune C. (2007). Changes in coral-associated microbial communities during a bleaching event. *ISME J* **2**: 350–363.

Bourne DG, Munn CB. (2005). Diversity of bacteria associated with the coral *Pocillopora damicornis* from the Great Barrier Reef. *Environ Microbiol* **7**: 1162–1174.

Bruckner AW. (2015). History of coral disease research. In: Downs CA, Bruckner AW, Porter JW, Galloway SB (eds). *Diseases of Coral*. John Wiley & Sons, Inc: Hoboken, NJ, pp 52–84.

Byrd AL, Segre JA. (2016). Adapting Koch's postulates. *Science* **351**: 224–226.

Cárdenas A, Rodriguez-R LM, Pizarro V, Cadavid LF, Arévalo-Ferro C. (2011). Shifts in bacterial communities of two caribbean reef-building coral species affected by white plague disease. *ISME J* **6**: 502–512.

Chimetto LA, Brocchi M, Thompson CC, Martins RCR, Ramos HR, Thompson FL. (2008). Vibrios dominate as culturable nitrogen-fixing bacteria of the Brazilian coral *Mussismilia hispida*. *Syst Appl Microbiol* **31**: 312–319.

Choi SY, Rashed SM, Hasan NA, Alam M, Islam T, Sadique A, *et al.* (2016). Phylogenetic diversity of *Vibrio cholerae* associated with endemic cholera in Mexico from 1991 to 2008. *mBio* **7**: e02160–15–9.

Chow J, Tang H, Mazmanian SK. (2011). Pathobionts of the gastrointestinal microbiota and inflammatory disease. *Curr Opin Immunol* **23**: 473–480.

Franzenburg S, Fraune S, Künzel S, Baines JF, Domazet-Loso T, Bosch TCG. (2012). MyD88-deficient Hydra reveal an ancient function of TLR signaling in sensing bacterial colonizers. *Proc Natl Acad Sci* **109**: 19374–19379.

Franzenburg S, Walter J, Künzel S, Wang J, Baines JF, Bosch TCG, *et al.* (2013). Distinct antimicrobial peptide expression determines host species-specific bacterial associations. *Proc Natl Acad Sci* **110**: E3730–E3738.

Hajishengallis G, Darveau RP, Curtis MA. (2012). The keystone-pathogen hypothesis. *Nat Rev Micro* **10**: 717–725.

Joyner JL, Sutherland KP, Kemp D, Berry B, Griffin A, Porter J, *et al.* (2015). Systematic analysis of white pox disease in *Acropora palmata* of the Florida Keys and the role of *Serratia marcescens*. *Appl Environ Microbiol* AEM.00116–15.

Kamada N, Chen GY, Inohara N, Núñez G. (2013a). Control of pathogens and pathobionts by the gut microbiota. *Nat Immunol* **14**: 685–690.

Kamada N, Seo S-U, Chen GY, Núñez G. (2013b). Role of the gut microbiota in immunity and inflammatory disease. *Nat Rev Immunol* **13**: 321–335.

Lamont RJ, Hajishengallis G. (2015). Polymicrobial synergy and dysbiosis in inflammatory disease. *Trends Mol Med* **21**: 172–183.

Lee STM, Davy SK, Tang S-L, Kench PS. (2017). Water flow buffers shifts in bacterial community structure in heat-stressed *Acropora muricata*. *Sci Rep* **7**: 43600.

Muller EM, van Woesik R. (2012). Caribbean coral diseases: primary transmission or secondary infection? *Global Change Biol* **18**: 3529–3535.

Muller EM, van Woesik R. (2014). Genetic susceptibility, colony size, and water temperature drive white-pox disease on the coral *Acropora palmata*. *PLoS One* **9**: e110759–5.

Nelson A, De Soyza A, Perry JD, Sutcliffe IC, Cummings SP. (2012). Polymicrobial challenges to Koch's postulates: ecological lessons from the bacterial vaginosis and cystic fibrosis microbiomes. *Innate Immun* **18**: 774–783.

Norsworthy AN, Visick KL. (2013). Gimme shelter: how *Vibrio fischeri* successfully navigates an animal's multiple environments. *Front Microbiol* **4**: 356.

Pantos O, Bythell JC. (2006). Bacterial community structure associated with white band disease in the elkhorn coral *Acropora palmata* determined using culture-independent 16S rRNA techniques. *Dis Aquat Org* **69**: 79–88.

Pathak P, Trilligan C, Rapose A. (2014). Bifidobacterium--friend or foe? A case of urinary tract infection with Bifidobacterium species. *BMJ Case Rep* **2014**: bcr2014205122–bcr2014205122.

Pollock FJ, Wada N, Torda G, Willis BL, Bourne DG. (2016). White syndrome-affected corals have a distinct microbiome at disease lesion fronts. *Appl Environ Microbiol* **83**: e02799–16–16–15.

Precht WF, Gintert BE, Robbart ML, Fura R, van Woesik R. (2016). Unprecedented disease-related coral mortality in Southeastern Florida. *Sci Rep* **6**: 31374–31311.

Roder C, Arif C, Bayer T, Aranda M, Daniels C, Shibl A, *et al.* (2014). Bacterial profiling of White Plague Disease in a comparative coral species framework. *ISME J* **8**: 31–39.

Rubio-Portillo E, Yarza P, alver CPN, aacute AAR-E, n JAO. (2014). New insights into *Oculina patagonica* coral diseases and their associated *Vibrio* spp. communities. *ISME J* **8**: 1794–1807.

Ruiz-Moreno D, Willis BL, Page AC, Weil E, Croquer A, Vargas-Angel B, *et al.* (2012). Global coral disease prevalence associated with sea temperature anomalies and local factors. *Dis Aquat Org* **100**: 249–261.

Séré MG, Tortosa P, Chabanet P, Quod J-P, Sweet MJ, Schleyer MH. (2015). Identification of a bacterial pathogen associated with *Porites* white patch syndrome in the Western Indian Ocean. *Mol Ecol* **24**: 4570–4581.

Sunagawa S, DeSantis TZ, Piceno YM, Brodie EL, DeSalvo MK, Voolstra CR, *et al.* (2009). Bacterial diversity and White Plague Disease-associated community changes in the Caribbean coral Montastraea faveolata. *ISME J* **3**: 512–521.

Sussman M, Willis BL, Victor S, Bourne DG. (2008). Coral pathogens identified for White Syndrome (WS) epizootics in the Indo-Pacific. *PLoS One* **3**: e2393–14.

Sutherland KP, Berry B, Park A, Kemp DW, Kemp KM, Lipp EK, *et al.* (2016). Shifting white pox aetiologies affecting *Acropora palmata* in the Florida Keys, 1994-2014. *Philos Trans R Soc Lond B Biol Sci* **371**: 20150205.

Sweet MJ, Brown BE. (2016). Coral responses to anthropogenic stress in the twenty-first century: an ecophysiological perspective. *Oceanogr Mar Bio Ann Rev* **54**: 271–314.

Sweet MJ, Bulling MT. (2017). On the importance of the microbiome and pathobiome in coral health and disease. *Front Mar Sci* **4**: 2261–11.

Thurber RV, Willner-Hall D, Rodriguez-Mueller B, Desnues C, Edwards RA, Angly F, *et al.* (2009). Metagenomic analysis of stressed coral holobionts. *Environ Microbiol* **11**: 2148–2163.

Tout J, Siboni N, Messer LF, Garren M, Stocker R, Webster NS, *et al.* (2015). Increased seawater temperature increases the abundance and alters the structure of natural *Vibrio* populations associated with the coral *Pocillopora damicornis*. *Front Microbiol* **6**: 403–12.

Ushijima B, Smith A, Aeby GS, Callahan SM. (2012). *Vibrio owensii* Induces the tissue loss disease *Montipora* white syndrome in the Hawaiian reef coral *Montipora capitata*. *PLoS One* **7**: e46717–10.

Vayssier-Taussat M. (2014). Shifting the paradigm from pathogens to pathobiome: new concepts in the light of meta-omics. *Front Cell Infect Microbiol* **4**: 1–7.

Vezzulli L, Grande C, Reid PC, Hélaouët P, Edwards M, Höfle MG, *et al.* (2016). Climate influence on *Vibrio* and associated human diseases during the past half-century in the coastal North Atlantic. *Proc Natl Acad Sci* **113**: E5062–E5071.

Vidal-Dupiol J, Dheilly NM, Rondon R, Grunau C, Cosseau C, Smith KM, *et al.* (2014). Thermal stress triggers broad *Pocillopora damicornis* transcriptomic remodeling, while *Vibrio coralliilyticus* infection induces a more targeted immuno-suppression response. *PLoS One* **9**: e107672.

Vidal-Dupiol J, Ladrière O, Destoumieux-Garzón D, Sautière P-E, Meistertzheim A-L, Tambutté E, *et al.* (2011). Innate immune responses of a scleractinian coral to vibriosis. *J Biol Chem* **286**: 22688–22698.

Weil E, Rogers CS. (2011). Coral reef diseases in the Atlantic-Caribbean. In: Dubinsky Z, Stambler N (eds). *Coral Reefs: An Ecosystem in Transition*. Springer Netherlands: Dordrecht, pp 465–491.

Ziegler M, Seneca FO, Yum LK, Palumbi SR, Voolstra CR. (2017). Bacterial community dynamics are linked to patterns of coral heat tolerance. *Nat Commun* **8**: 14213.

CHAPTER 3

DIVERSITY AND ABUNDANCE OF *VIBRIO* ASSOCIATED WITH DISEASED ELKHORN CORAL, *ACROPORA PALMATA*, OF THE FLORIDA KEYS

The critically endangered elkhorn coral, *Acropora palmata*, is affected by white pox disease (WPX) throughout the Florida Reef Tract and wider Caribbean. The bacterium *Serratia marcescens* was previously identified as one etiologic agent of WPX, but is no longer consistently detected in contemporary outbreaks. It is now believed that multiple etiologic agents cause WPX; however, to date, no other potential pathogens have been thoroughly investigated. This study examined the association of *Vibrio* bacteria with WPX occurrence from August 2012–2014 at Looe Key Reef in the Florida Keys, USA. The concentration of cultivable *Vibrio* was consistently greater in WPX samples compared to healthy samples. Based on quantitative real-time PCR (qPCR), the relative abundance of *Vibrio* bacteria to total bacteria was four times higher in samples from WPX lesions. The diversity of 69 *Vibrio* isolates collected from diseased and apparently healthy *A. palmata* colonies and the surrounding seawater was assessed by multilocus sequence analysis (MLSA). There was no strong association of particular *Vibrio* species with health status or sample type; however, 86% of total isolates were closely related to *Vibrio* species with known pathogenicity to corals. While the causative agent(s) of contemporary WPX outbreaks remain elusive, our results suggest that *Vibrio* may be part of a secondary opportunistic infection rather than acting as primary pathogens. This study

highlights the need for highly resolved temporal sampling *in situ* to further elucidate the role of *Vibrio* during WPX onset and progression.

Importance

Coral diseases are increasing worldwide and are now considered a major contributor to coral reef decline. The Caribbean, in particular, has been noted as a coral disease hotspot owing to the dramatic decline of framework-building acroporid corals to tissue loss diseases. The pathogenesis of contemporary white pox disease (WPX) outbreaks in *Acropora palmata* remains poorly understood. This study is the first to investigate the association of *Vibrio* bacteria with WPX.

Introduction

The health and function of reef-building corals is intricately intertwined with their symbiotic microbial associates. Corals host a diverse array of archaea, bacteria, fungi, viruses, protists, and photosynthetic microalgae in their surface mucus layer (SML), tissue, and skeleton (Ainsworth *et al.*, 2010; Bourne *et al.*, 2016). These microbial associates are collectively referred to as the 'microbiome', and they aid in nutrient cycling and host immunity. However, these symbiotic relationships can vary from mutualistic to potentially pathogenic depending on environmental factors such as sea temperature (Ben-Haim and Rosenberg, 2002; Cervino *et al.*, 2008; Ushijima *et al.*, 2014; Séré *et al.*, 2015; Randall and van Woesik, 2015), water flow (Lee *et al.*, 2017), and nutrient levels (Thurber *et al.*, 2009; Vega Thurber *et al.*, 2014; Bruno *et al.*, 2003). While bacterial etiological agents are believed to be associated with many coral diseases,

only a few studies have shown that specific bacteria are capable of causing disease through fulfillment of Koch's and Hill's postulates (Sutherland *et al.*, 2016). There is a growing realization that application of these fundamental postulates in coral disease (Sweet and Bulling, 2017; Sussman *et al.*, 2008) and other fields (Nelson *et al.*, 2012; Vayssier-Taussat, 2014) is limited, because they are largely based upon the 'one pathogen, one disease' framework. Mounting evidence suggests that many coral diseases may be caused by a consortium of pathogens (Sutherland *et al.*, 2016; Sweet and Bulling, 2017). There is an urgent need to develop new frameworks to investigate coral disease as it is recognized as an increasing threat to coral reef ecosystems due to global climate change and anthropogenic stressors (Precht *et al.*, 2016a; Ruiz-Moreno *et al.*, 2012; Sweet and Brown, 2016).

In the Caribbean, disease has contributed to a > 90% population decline of the framework-building elkhorn coral, *Acropora palmata* (Patterson *et al.*, 2002; Precht *et al.*, 2016b). Consequently, *A. palmata* is now listed as critically endangered on the International Union for Conservation of Nature (IUCN) Red List of Threatened Species, and as threatened under the US Endangered Species Act. The loss of *A. palmata*, and the complex architecture it once provided, has lead to a 'flattening' of Caribbean reefs with consequences for reef biodiversity and ecosystems functioning (Alvarez-Filip *et al.*, 2009). Living cover of *A. palmata* in the upper Florida Keys declined by 50% from 2004–2010 (Williams and Miller, 2011). Thirty-percent of this loss was attributable to partial mortality caused by white pox (WPX) and other tissue loss diseases. From 2009–2014, seasonal WPX prevalence rates ranged from 23% to 60% in a survey covering seven reefs throughout the Florida Keys National Marine Sanctuary (Sutherland *et al.*,

2016). Though the established WPX pathogen *Serratia marcescens* is still detected in *A. palmata* mucus and the reef environment, it is not consistently associated with contemporary WPX outbreaks in the Florida Keys (Joyner *et al.*, 2014). The bacterium was not detected in *A. palmata* displaying white pox signs in St. John, US Virgin Islands (May *et al.*, 2011) and the Bahamas (Lesser and Jarett, 2014). This lead to the conclusion that WPX signs are likely caused by multiple pathogens or environmental stressors (Sutherland *et al.*, 2016; Muller and van Woesik, 2014); however, to date, no other microbial taxa have been thoroughly investigated in relation to WPX. The aim of this study was to examine the association between WPX lesions and the bacterial genus *Vibrio*, which contains many species known to be pathogenic to corals, other marine organisms, and humans (Gomez-Gil *et al.*, 2014).

With more than 110 recognized species (http://www.bacterio.net/vibrio.html), *Vibrio* is one of the most diverse marine bacterial genera and is globally distributed in the coastal environment (Ceccarelli and Colwell, 2014). To date, ten different *Vibrio* species have been implicated as etiologic agents in coral disease through infection trials and fulfillment of Koch's and Hill's postulates (Table 3.1). *Vibrio mediterranei* (synonymous with *V. shiloi*) and various strains of *V. coralliilyticus* have been documented to cause bacterial bleaching disease in *Oculina patagonia* in the Mediterranean Sea (Rubio-Portillo *et al.*, 2014; Kushmaro *et al.*, 2001) and *Pocillopora damicornis* in the Indian Ocean . *Vibrio harveyi* (synonymous with *V. charachariae*) is one causative agent of white band disease in Caribbean *Acropora cervicornis* (Gil-Agudelo *et al.*, 2006; Ritchie and Smith, 1998) and a consortium of four *Vibrio* (*V. alginolyticus*, *V. harveyi*, *V. proteolyticus*, and *V. rotiferianus*) cause Caribbean yellow band disease in *Orbicella*

faveolata . White syndromes affecting multiple *Acropora*, *Porites* and *Montipora* corals throughout the Pacific have been associated with *Vibrio* spp. in the *Coralliilyticus*, *Harveyi* and *Orientalis* clades (Sussman *et al.*, 2008).

The association of *Vibrio* with WPX has not been thoroughly investigated, though screens for *V. coralliilyticus* and *V. shiloi* revealed these species had a higher detection rate in diseased samples compared to apparently healthy samples (May *et al.*, 2011). To further examine the relationship between *Vibrio* and WPX, we assessed the concentration and relative abundance of *Vibrio* spp. in WPX-affected *A. palmata* in the Florida Keys, USA. Enumeration of colony forming units (CFUs) on selective media and genus-specific quantitative real-time PCR showed a significantly higher abundance of *Vibrio* spp. in WPX lesions compared to apparently healthy samples. Additionally, we investigated the diversity *Vibrio* associated with diseased and apparently healthy *A. palmata* via multilocus sequencing analysis of 69 *Vibrio* spp. isolates. Both healthy and diseased *A. palmata* harbored *Vibrio* spp. closely related to species capable of causing disease in corals and other marine organisms. The lack of association between specific *Vibrio* species and coral health status, suggests that *Vibrio* may be part of a secondary, opportunistic infection.

Methods

Field surveys and sample collection. *Acropora palmata* colonies were sampled from Looe Key (3 m depth; N 24°32.724' W81°24.360'), located in the Florida Keys National Marine Sanctuary (FKNMS) three times per year (winter, spring, and summer) from August 2012 to August 2014. At each sampling, colonies were examined visually

for signs of white pox disease (WPX) defined as irregularly shaped lesions (at least 1 cm^2) with sloughing tissue and exposure of bright white skeleton (Sutherland *et al.*, 2016).

Non-destructive methods were used to collect the surface mucus layer (SML) of *A. palmata* with sterile, needleless 12-ml syringes (Kemp *et al.*, 2015; Zaneveld *et al.*, 2016). During each sampling period, SML samples were taken from apparently healthy *A. palmata* colonies displaying no visual signs of disease (n = 4–6; denoted as *H mucus*). We collected paired SML samples from colonies with WPX: one from the active margin of a disease lesion (n = 4–6; denoted *D mucus*) and one from an adjacent branch displaying no disease signs (n = 4–6; denoted *DH mucus*). Seawater was collected with 12-ml syringes from approximately 1 m above the *A. palmata* colonies (n = 2–6; denoted *reef water*) and from the first 10 cm of the sea surface (n = 4–6; denoted *surface water*). All samples were placed in bags, transported in a cooler filled with seawater at ambient temperature to the laboratory, and processed within 1 h of collection.

Quantification of cultivable *Vibrio* spp. Syringe contents were transferred into sterile 15 ml conical vials and vortexed for approximately 10 s. Then, 10 µl of SML from white pox lesions and 100 µl of all other sample types were spread in triplicate onto the *Vibrionaceae* selective media, thiosulfate-citrate-bile salts sucrose agar (TCBS; Oxoid) and incubated at 29 °C. TCBS colony forming units (CFUs) were enumerated after approximately 24 h and expressed as mean CFU ml^{-1}. All counts were log-transformed to allow for a normally distributed data set (verified by the Shapiro-Wilk test of normality). Differences in mean CFU ml^{-1} among sample type within each sampling period were examined using one-way analyses of variance (ANOVAs). An additional two-way

ANOVA was performed on late summer data to assess differences between years in addition to sample type. Significant groupings were determined by Tukey's pair-wise tests, accounting for multiple comparisons.

Quantitative PCR. We examined the relative abundance of *Vibrio* in relation to total bacteria during August 2014 among *H*, *DH*, and *D mucus* with quantitative real-time PCR (qPCR). DNA was obtained by pelleting duplicate 2-ml aliquots from each 12-ml syringe sample by centrifuging at 17,000 x g for 20 min. Supernatant fluids were decanted and pellets were stored at -80 °C until use. DNA was then extracted with the DNeasy blood and tissue kit (Qiagen, Valencia, CA) following the manufacturer's protocol for Gram-positive bacteria. The duplicate pellets were thawed and resuspended in 180 µl of lysis buffer (20 mM Tris-HCL, pH 8, 2 mM EDTA, and 1.2% Triton-X100) containing lysozyme (20 mg ml^{-1}, final concentration) and incubated at 37°C for 30 min followed by proteinase K digestion at 56°C for 1 h. Lysates of the duplicate 2-ml aliquots were combined onto a single DNeasy mini spin column for continuation of the DNeasy protocol. Purified DNA was eluted in 100 µl of Qiagen AE buffer. DNA was then diluted 1:10 in Qiagen AE buffer to reduce PCR inhibition.

Vibrio relative abundance was assessed by a SYBR-green quantitative real-time PCR (qPCR) method targeting the 16S rRNA gene previously described . The qPCR assay utilized *Vibrio*-specific primers targeting the V3-V4 region of the *Vibrio* 16S gene (Vib1 567f-5'-GGCGTAAAGCGCATGCAGGT-3' and Vib2 680r-5'-GAAATTCTACCCCCCTCTACAG-3',(Thompson *et al.*, 2004)) and general primers targeting the V6 region of the 16S gene for the domain *Bacteria* (967f-5'CAACGCG AAGAACCTTACC-3' and 1046r-5'CGACAGCCATGCANCACCT-3',). Each reaction

mixture contained 10 µl of PowerUp™ SYBR® Green Master Mix (Applied Biosystems, ThermoFisher Scientific), 0.3 µM of each primer and 5 µl of DNA template, with molecular grade water added for a total reaction volume of 20 µl. All reactions were run in triplicate on a StepOne real-time PCR system (Applied Biosystems, Life Technologies, Grand Isle, NY) with the following conditions: initial uracil-DNA glycosylase (UDG) activation at 50 °C for 2 min and polymerase activation at 95 °C for 2 min, followed by 40 cycles of denaturation at 95 °C for 15 s and annealing and elongation at 60 °C for the *Vibrio*-specific qPCR. The total bacteria qPCR had the same cycling conditions except the annealing and elongation were split into two steps: 61°C for 15 sec (annealing) and 72°C for 1 min (elongation). Each run was followed by a dissociation step (95°C for 30 sec and 60°C for 30 sec and 95°C for 30 sec) to determine a melt curve for analysis of specificity and included three replicate negative (no template) controls.

PCR standards were prepared from genomic DNA of *V. alginolyticus* (American Type Culture Collection strain 33839). The DNeasy blood and tissue kit (Qiagen, Valencia, CA) was used to extract DNA from an overnight culture according to the manufacturer's protocol for Gram-negative bacteria. Standards for the general bacterial assay were prepared from six serial dilutions of purified genomic DNA, factoring eleven copies of the 16S gene for *V. alginolyticus* ATCC strain 33839 (Stoddard *et al.*, 2015). The *Vibrio*-specific qPCR assay utilized linearized plasmid standards prepared from amplicon products of the Vib1 and Vib2 primers (described above). Briefly, amplicons were inserted into a PCR-4 vector and cloned into *E. coli* using a TA-TOPO kit (Life Technologies Grand Isle, NY) and the plasmid was extracted (QIAquick Spin Miniprep kit; Qiagen). The cloned region was sequenced to verify the correct insert and linearized

with NotI (Roche, Indianapolis, IN) after cleanup (QIAquick PCR purification kit; Qiagen). Linearized standards for the *Vibrio*-specific qPCR assay were quantified using a Qubit fluorometer and serially diluted in Qiagen AE buffer and run with each *Vibrio*-specific qPCR assay.

Calculation of *Vibrio* relative abundance. The *Vibrio* relative abundance index (VAI) was calculated as the ratio of *Vibrio* spp. cell equivalents to total bacterial cell equivalents. *Vibrio* spp. cellular equivalents were determined by dividing the sample copy number in *Vibrio*-specific qPCR assays by the average per-genome copy of the 16S gene in *Vibrio* (n = 9.1), published in the ribosomal RNA operon copy number database (rrnDB) v.5.0 . To determine total bacterial cell equivalents, we acquired publically available 16S community data from apparently healthy *A. palmata* in the Florida Keys (Kemp *et al.*, 2015). The mean per-genome copy number for the entire community (n = 2.65) was calculated by weighting the published rrnDB 16S gene copy number for all bacterial taxa present in the *A. palmata* samples by their mean relative abundance (Appendix A, Table S3.2). Total bacteria cellular equivalents were then determined by dividing the sample copy number in the general bacterial qPCR assays by 2.65. The arcsine square root transformation for proportional data was used on all VAI data preceding one-way ANOVA analysis and Tukey's multiple comparisons tests.

Multilocus sequence analysis. To investigate the diversity of *Vibrio* associated diseased and healthy *A. palmata, Vibrio* spp. were isolated from TCBS agar in August 2012 and July 2013. Colonies were transferred and stored in deep-agar stabs of Zobell marine agar (Difco™ 2216) and were later purified by streak-isolation on TCBS media for a minimum of three times. To obtain genomic DNA, the purified bacterial isolates

were grown overnight in Zobell marine broth (Difco™ 2216) at 29 °C. Then, 750 µl of overnight growth was pelleted (3500 rpm for 5 min), washed twice with phosphate buffered saline, and re-suspended in 180 µl Qiagen ATL buffer. We proceeded with DNeasy blood and tissue kit (Qiagen, Valencia, CA) extractions according to the manufacturer's protocol for Gram-negative bacteria.

Whole genome sequences (WGS) for 69 isolates that grew on TCBS selective media (*seawater*, n = 17; *H mucus*, n = 15; *DH mucus*, n = 19; *D mucus*, n=18) were obtained using the Illumina NextSeq platform in the mid output mode (150 cycles with 150 bp paired-end reads). The sequence reads were subsampled for Bayesian error correction and *de novo* assembled using SPAdes v.3.6.2 with the careful mode turned on (Bankevich *et al.*, 2012). The resulting contigs were further scaffolded using with SSPACE v.2.0 (Boetzer *et al.*, 2011) and then gap-closed with GapFiller v.1.11 (Boetzer and Pirovano, 2012).

Multilocus sequencing analysis (MLSA) was performed using regions of the eight housekeeping genes *gapA*, *gyrB*, *ftsZ*, *mreB*, *pryH*, *recA*, *rpoA*, and *topA*, suggested by Sawabe and colleagues (2013; 2007) for inferring the evolutionary history of vibrios. Nucleotide sequences of the housekeeping genes were retrieved from the full genomes following auto-annotation by the online server for Rapid Annotation of Microbial Genomes using Subsystems Technology (RAST) (Overbeek *et al.*, 2013). We obtained partial housekeeping gene sequences for reference *Vibrio* used in previous phylogenetic studies (Sawabe *et al.*, 2013; 2007) from the NCBI GenBank nucleotide sequence database. Additional reference sequences were retrieved from full *Vibrio* genomes available on the Pathosystems Resource Integration Center (PATRIC) online database

v.3.2.76 (Wattam *et al.*, 2013). All references sequences are listed with NCBI GenBank accession numbers in Appendix A, Table S3.1.

Multiple sequence alignments for each gene were created using muscle v.3.8.31 (Edgar, 2004) and trimmed, allowing no gaps, with trimAl v.1.3 (Capella-Gutierrez *et al.*, 2009). Concatenations of the eight loci (4203 bp) were used for maximum likelihood (ML) phylogenetic analysis with RAxML v.8.2.4 (Stamatakis, 2014), using the GTR plus gamma model and 20 randomized starting trees. Concatenated loci were partitioned and the shape of the gamma distribution, nucleotide frequencies, and nucleotide substitution rates were estimated individually for each partition. Tree topology was checked by 500 bootstrap replicates. The average nucleotide identity (ANI) for the 8-gene loci concatenation was calculated for the *Vibrio* spp. isolates and reference strains they clustered with using Jspecies v.1.2.1 (Richter and Rosselló-Móra, 2009) and is reported in Table 3.1.

Results

Abundance of cultivable *Vibrio* spp. White pox disease (WPX) signs were noted at Looe Key Reef during late summer sampling events in August 2012, July 2013, and August 2014. No WPX occurred during winter and early summer sampling events. We enumerated colony-forming units (CFU) of *Vibrio* spp. that grew on *Vibrio*-selective thiosulfate citrate bile sucrose agar media (TCBS). During periods of active WPX, the mean *Vibrio* CFU ml^{-1} was ~19 times higher in mucus from WPX lesions (*D mucus*) compared to adjacent asymptomatic areas on the same *A. palmata* colonies (*DH mucus*; $P_{Tukey} \leq 0.001$ in all cases) and apparently healthy colonies with no WPX signs (*H mucus*;

$P_{Tukey} < 0.0001$ in all cases) (Figure 3.1). There was no difference between mean CFU ml^{-1} in *H mucus* and *DH mucus* ($P_{Tukey} \geq 0.31$ in all cases). When comparing the mean *Vibrio* CFU ml^{-1} in late summer across the three years, *Vibrio* concentrations in all sample types were one to two orders of magnitude higher in 2013 ($P_{Tukey} \leq 0.024$ in all cases). Additionally, in 2013 *Vibrio* concentrations in apparently healthy samples (*H mucus*, 7,289 ± 1,351; *DH mucus,* 13,524 ± 8,335) reached levels measured in disease samples during other years (*D mucus* 2012 8,885± 4,196; *D mucus* 2014 24,572 ± 19,857) (df = 55, $q \leq 2.15$, $P_{Tukey} \geq 0.913$ in all cases).

Quantitative PCR. We examined the *Vibrio* relative abundance index (VAI) of coral mucus samples collected during August 2014 as the ratio of *Vibrio* spp. cell equivalents to total bacterial cell equivalents assessed by quantitative PCR. *Vibrio* spp. densities were ~18.4 times higher in *D mucus* compared to *H mucus* (df = 9, q = 4.7, $P_{Tukey} = 0.02$) and *DH mucus* (df = 9, q = 6.0, $P_{Tukey} = 0.0054$, Figure 3.2), corroborating trends documented by enumerating cultivable *Vibrio* spp. on TCBS media. Total bacteria densities were also ~6.4 times higher in *D mucus* compared to *H mucus* (df = 9, q = 5.0, $P_{Tukey} = 0.016$) and *DH mucus* (df = 9, q = 6.1, $P_{Tukey} = 0.0048$, Figure 3.2). The VAI of *D mucus* (0.24 ± 0.082) was ~ 4.2 times higher than that of adjacent *DH mucus* on the same *A. palmata* colonies (0.058 ± 0.0095, df = 9, q = 4.1, $P_{Tukey} = 0.041$, Figure 3.2). There was no difference in the VAI of *H mucus* and *DH mucus* (df = 9, q = 0.73, $P_{Tukey} = 0.86$).

Isolate diversity assessed by multilocus sequence analysis. We analyzed the phylogenetic relatedness and diversity of 69 bacterial isolates that grew on *Vibrio*-selective TCBS media via multilocus sequence analysis (MLSA) using eight previously defined housekeeping genes (Sawabe *et al.*, 2007). The isolates clustered within 5 of the

17 defined *Vibrio* clades (Sawabe *et al.*, 2013), with the majority, 54% (37/69), belonging to the *Harveyi* clade (Figure 3.3 and 3.4). There was no evidence of phylogenetic clustering by sample type (*seawater*, *H mucus*, *DH mucus*, and *D mucus*). However, 86% (59/69) of the isolates clustered (bootstrap = 100%) among six of the ten *Vibrio* species with known pathogenicity to corals (Figure 3.3 and 3.4). The average nucleotide identity (ANI) of the 8-gene loci concatenation confirmed the species identity of isolates clustering with reference strains: *V. alginolyticus* (n = 3, 99.5%), *V. coralliilyticus* (n = 2, 98.3%), *V. harveyi* (n = 14, 99.5%), *V. mediterranei* (n = 2, 99.0%), *V. owensii* (n = 37, 98.2%), and *V. tubiashii* (n = 1, 94.2%).

Discussion

Vibrio can be characterized as conditionally rare taxa (CRT) (Shade *et al.*, 2014) in coastal seawater because they typically make up a minor portion of the total microbial assemblage, but are capable of blooming in response to nutrient availability and other environmental factors (Westrich *et al.*, 2016). Likewise, *Vibrio* are often rare members in the microbiome of apparently healthy corals (Alves *et al.*, 2010; Pollock *et al.*, 2016; Rubio-Portillo *et al.*, 2014). However, *Vibrio* relative abundance can increase significantly in the coral microbiome during disease (Ushijima *et al.*, 2012; Sussman *et al.*, 2008; Pantos and Bythell, 2006), temperature stress (Ziegler *et al.*, 2017; Tout *et al.*, 2015; Lee *et al.*, 2015), and low water flow (Lee *et al.*, 2017). It is not fully understood how these abundance transitions affect microbiome homeostasis and host health. *Vibrio alginolyticus, V. harveyi, V. campbellii,* and *V. parahaemolyticus* isolates from coral mucus are capable of fixing N_2, and in doing so may function as coral mutualists during

non-stressful conditions (Chimetto *et al.*, 2008; Benavides *et al.*, 2017). However, with environmental stress or when hosts are immunosuppressed, *Vibrio* may shift along the symbiotic spectrum from functioning as commensals or mutualists to functioning as potential pathogens. These symbiotic shifts may be driven by an increase in *Vibrio* relative abundance, a transition of *Vibrio* from the coral mucus into coral tissue, and/or activation and expression of *Vibrio* virulence mechanisms. In this study, concentrations of both total bacteria and *Vibrio* bacteria were significantly elevated in disease lesions compared with mucus from healthy tissue. An increase in bacterial load has been noted in other disease studies, including those that examined the role of *Vibrio* (Luna *et al.*, 2009; Sussman *et al.*, 2008; Ushijima *et al.*, 2012). In the present study, the relative abundance of *Vibrio* spp. increased from ~5% of total bacteria in healthy samples to ~25% in diseased samples. To date, ten *Vibrio* species have been shown to cause disease in coral through infection trials, with partial or complete fulfillment of Koch's postulates (Table 3.1). Multilocus sequencing analysis (MLSA) revealed that 86% (59/69) of isolates in this study clustered with six of these ten species (*V. alginolyticus*, *V. coralliilyticus*, *V. harveyi*, *V. mediterranei*, *V. owensii*, and *V. tubiashii*), but there was no strong association between health status and the presence of particular *Vibrio* species in the *A. palmata* SML.

The lack of association between particular *Vibrio* spp. and disease status while overall relative abundance of *Vibrio* increased, suggested that *Vibrio* may be a part of an opportunistic non-specific infection. In such a scenario, heterotrophic *Vibrio* blooms may contribute to tissue loss through inducing localized hypoxia. Microgradients of O_2, driven by microbial activity, are known to be important in the progression of other coral diseases

such as black band disease (Glas *et al.*, 2012). However, to determine the course of the WPX disease process, it is critical to know the age of lesions sampled, which can be difficult to determine in the field without very high resolution monitoring (e.g., at least daily). The lesions sampled here were active (tissue was sloughing and skeleton was bright white), but we did not know when disease signs started with respect to when we collected our samples. It is likely that our results reflect secondary disease stages while missing initial pathogenesis. Future studies, with higher temporal resolution, are needed to understand whether certain *Vibrio* spp. are directly involved in WPX onset and progression.

It is important to note that corals harbor different microbial communities in their SML compared to their tissue and skeleton (Sweet *et al.*, 2010). Due to sampling restrictions, we were only able to analyze coral mucus and may have missed species-specific trends in other compartments. *Vibrio* have been shown to migrate from the coral SML into coral tissue under temperature stress (Lee *et al.*, 2015). It is likely that some *Vibrio* species are able to make this transition (due to traits such as chemotactic motility, attachment mechanisms, and oxidative stress defense systems (Santos *et al.*, 2011; Munn *et al.*, 2008)), while other *Vibrio* species cannot. For instance, Lee and colleagues (Lee *et al.*, 2015) found that under thermal stress, the relative abundance of *Vibrio* spp. increased first in coral mucus and then in coral tissue. The majority of the *Vibrio* sequences recovered from coral tissues under thermal stress belonged to *V. coralliilyticus* (Lee *et al.*, 2015). Our data, showing an increase in the relative abundance of *Vibrio* spp. in mucus, suggest that it would be valuable to examine possible transitions of *Vibrio* populations between the *A. palmata* SML and tissue during late summer WPX outbreaks.

Seawater temperature and irradiance are two well-described environmental factors that are known to influence coral disease dynamics (Thurber *et al.*, 2009; Tout *et al.*, 2015; Bourne *et al.*, 2007; Bourne and Munn, 2005); however, other stressors such as increased nutrients and sedimentation are less studied (Zaneveld *et al.*, 2016). For example, we measured 1–2 orders of magnitude more *Vibrio* in all sample types during late summer 2013 compared to other years. Late summer sea temperatures were no warmer in 2013 compared to 2012 and 2014 ($df = 9$, $q > 3.9$, $P_{Tukey} > 0.05$, Appendix A, Table S3.3). However, our sampling event on July 25th, 2013 coincided with the significant influx of Saharan dust aerosols, which deposited iron and other nutrients into the oligotrophic coastal waters of the Florida Keys (Westrich *et al.*, 2016). Westrich et al. (2016) demonstrated that within 24 h of the arrival and deposition of Saharan dust, *Vibrio* spp. increased from less than 1% to 20% of the total microbial community in coastal waters. Our data show that during the 2013 sampling event, *Vibrio* concentrations from apparently healthy *A. palmata* reached levels typically measured in disease samples (Figure 3.1, *H mucus* in 2013 compared to *D mucus* in 2012 and 2014). It is unknown how long-lived this dust-induced *Vibrio* bloom was and whether it had lasting effects on the *A. palmata* microbiome. However, this suggests that Saharan dust deposition may serve to tip iron and nutrient availability above certain thresholds, thus promoting *Vibrio* growth in the coral microbiome and potentially disrupting microbial community dynamics. Further studies are warranted to investigate whether African dust storms influence disease dynamics in *A. palmata* and other Caribbean corals by promoting the expansion of pathobionts and/or the colonization of opportunistic infectious agents.

Sweet and Bulling (2017) recently proposed that considering the coral 'pathobiome' (members within the microbiome that are directly involved in pathogenesis) offers a new framework for advancing coral disease research beyond the 'one pathogen, one disease' paradigm. Given that *Vibrio* spp. are often found in low abundance in apparently healthy coral hosts, it may be useful to examine conditionally rare *Vibrio* spp. as potential 'pathobionts' in WPX and other tissue loss diseases. The term 'pathobiont' was developed to distinguish resident microbes with pathogenic potential from opportunistic infectious agents that are typically acquired from the environment (Round and Mazmanian, 2009). Pathobionts are defined as regularly occurring microbiome members that are normally innocuous and promote pathology only under conditions of disrupted homeostasis (Chow *et al.*, 2011). The concept is based, in part, on evidence that several gastrointestinal inflammatory disorders in humans are caused by bacterial species found in most healthy hosts (Chow *et al.*, 2011; Round and Mazmanian, 2009). Several well-described examples from human microbiome studies include the bacteria *Clostridium difficile* and *Heliobacter pylori*, which can cause severe gastrointestinal inflammation and lead to colon cancer (Moyat, 2014; Kamada *et al.*, 2013). Fifty percent of the human population is colonized by *H. pylori*, but only a small percentage actually develops gastric disorders (Moyat, 2014). *Clostridium difficile* can be detected in low abundance in 5% of healthy adults; however, in some patients toxigenic *C. difficile* are able to bloom and cause severe colitis, diarrhea, and even death (Kamada *et al.*, 2013). While the pathobiont/pathobiome concept has not yet been widely applied to the study of coral disease (Sweet and Bulling, 2017), studies have begun to described such observations. For example, Muller and van Woesik (2014) concluded that a normal

member of the *A. palmata* microbiome was the likely agent of WPX signs in *A. palmata*, but only under certain environmental conditions. The authors found that WPX did not display properties of a contagious disease *in situ*. Instead high seawater temperatures, colony size, and host genetics were important predictors of WPX (Muller and van Woesik, 2014), consistent with the pathobiome model.

Coral diseases have traditionally been viewed and studied through the lens of contagion models, focusing on: transmission of pathogens directly from colony to colony, indirectly through the water column, or by biological vectors (Muller and van Woesik, 2012). However, in addition to WPX, several other common Caribbean diseases (yellow-band, dark-spot, and white plague) do not display contagious properties *in situ* (Muller and van Woesik, 2012). If this is true of many coral diseases, adopting non-contagion frameworks developed in other fields, such as the pathobiome model, could advance coral disease research. A non-contagion approach should emphasize environmental thresholds that are important tipping points for disease induction, disruption of microbiome homeostasis, and host organismal traits that affect susceptibility to biotic and abiotic stressors (Muller and van Woesik, 2012; Sweet and Bulling, 2017).

We detected both a higher concentration and an increased relative abundance of *Vibrio* spp. in WPX lesions and many of these *Vibrio* were closely related species with known pathogenicity to coral. We argue that some *Vibrio* spp. may exist as 'pathobionts' in the coral microbiome, capable of eliciting disease under certain environmental conditions. *Vibrio* have a relatively large two-chromosomal genome encoding an expansive metabolic repertoire that enables a competitive, quick response to new resources (Polz *et al.*, 2006). Several *Vibrio* spp. display some of the fastest known

bacterial growth rates at 8–9 doublings per minute (Aiyar *et al.*, 2002), particularly at temperatures higher than 25°C and in carbon-rich environments such as coral mucus (Sharon and Rosenberg, 2008). Thus, *Vibrio* may exist as CRT in the healthy coral microbiome, primed to respond rapidly to changing environmental conditions. Many diseases caused by *Vibrio* are temperature-dependent, with higher rates of tissue lysis and disease progression when seawater temperatures rise above 29–30°C (Séré *et al.*, 2013). This further suggests that many *Vibrio* spp. may operate as opportunistic pathogens in many marine organisms. Examining *Vibrio* from a pathobiome/pathobiont framework, emphasizing environmental thresholds that trigger changes in *Vibrio* population growth and virulence expression with potential consequences for microbiome and immune homeostasis can advance our understanding of the role *Vibrio* play in coral disease.

Acknowledgements

This work was supported by the NSF grant EF1015342 (to E.K.L) as part of the joint NSF-NIH Ecology of Infectious Disease program. Jeff Turner provided helpful suggestions and feedback for the phylogenetic analyses. The authors thank Dustin Kemp, Katie Sutherland, and James Porter assisted in field surveys and sample collection. The authors would also like to acknowledge Erich Bartels and the staff at the Mote Tropical Research Lab on Summerland Key for their logistical support. Mucus and other specimens were obtained under permit FKNMS-2010-131-A.

References

Ainsworth TD, Thurber R, Gates R. (2010). The future of coral reefs: a microbial perspective. *Trends Ecol Evol* **25**: 233–240.

Aiyar SE, Gaal T, Gourse RL. (2002). rRNA promoter activity in the fast-growing bacterium *Vibrio natriegens*. *J Bacteriol* **184**: 1349–1358.

Alvarez-Filip L, Dulvy NK, Gill JA, Cote IM, Watkinson AR. (2009). Flattening of Caribbean coral reefs: region-wide declines in architectural complexity. *Proc R Soc B Biol Sci* **276**: 3019–3025.

Alves N, Neto OSM, Silva BSO, De Moura RL, Francini-Filho RB, Barreira e Castro C, *et al.* (2010). Diversity and pathogenic potential of vibrios isolated from Abrolhos Bank corals. **2**: 90–95.

Arboleda M, Reichardt WT. (2010). *Vibrio* sp. causing *Porites* ulcerative white spot disease. *Dis Aquat Org* **90**: 93–104.

Bankevich A, Nurk S, Antipov D, Gurevich AA, Dvorkin M, Kulikov AS, *et al.* (2012). SPAdes: a new genome assembly algorithm and its applications to single-cell sequencing. *J Comput Biol* **19**: 455–477.

Ben-Haim Y, Rosenberg E. (2002). A novel *Vibrio* sp. pathogen of the coral *Pocillopora damicornis*. *Mar Biol* **141**: 47–55.

Ben-Haim Y, Zicherman-Keren M, Rosenberg E. (2003). Temperature-regulated bleaching and lysis of the coral *Pocillopora damicornis* by the novel pathogen *Vibrio coralliilyticus*. *Appl Environ Microbiol* **69**: 4236–4242.

Benavides M, Bednarz VN, Ferrier-Pagès C. (2017). Diazotrophs: overlooked key players within the coral symbiosis and tropical reef ecosystems? *Front Mar Sci* **4**: 2261–17.

Boetzer M, Henkel CV, Jansen HJ, Butler D, Pirovano W. (2011). Scaffolding pre-assembled contigs using SSPACE. *Bioinformatics* **27**: 578–579.

Boetzer M, Pirovano W. (2012). Toward almost closed genomes with GapFiller. *Genome Biol* **13**: R56.

Bourne D, Iida Y, Uthicke S, Smith-Keune C. (2007). Changes in coral-associated microbial communities during a bleaching event. *ISME J* **2**: 350–363.

Bourne DG, Morrow KM, Webster NS. (2016). Insights into the coral microbiome: underpinning the health and resilience of reef ecosystems. *Annu Rev Microbiol* **70**: 317–340.

Bourne DG, Munn CB. (2005). Diversity of bacteria associated with the coral *Pocillopora damicornis* from the Great Barrier Reef. *Environ Microbiol* **7**: 1162–1174.

Bruno JF, Petes LE, Drew Harvell C, Hettinger A. (2003). Nutrient enrichment can increase the severity of coral diseases. *Ecol Lett* **6**: 1056–1061.

Capella-Gutierrez S, Silla-Martinez JM, Gabaldon T. (2009). trimAl: a tool for automated alignment trimming in large-scale phylogenetic analyses. *Bioinformatics* **25**: 1972–1973.

Ceccarelli D, Colwell RR. (2014). *Vibrio* ecology, pathogenesis, and evolution. *Front Microbiol* **5**: 256.

Cervino JM, Thompson FL, Gomez-Gil B, Lorence EA, Goreau TJ, Hayes RL, *et al.* (2008). The *Vibrio* core group induces yellow band disease in Caribbean and Indo-Pacific reef-building corals. *J Appl Microbiol* **105**: 1658–1671.

Chimetto LA, Brocchi M, Thompson CC, Martins RCR, Ramos HR, Thompson FL. (2008). Vibrios dominate as culturable nitrogen-fixing bacteria of the Brazilian coral *Mussismilia hispida*. *Syst Appl Microbiol* **31**: 312–319.

Chow J, Tang H, Mazmanian SK. (2011). Pathobionts of the gastrointestinal microbiota and inflammatory disease. *Curr Opin Immunol* **23**: 473–480.

Edgar RC. (2004). MUSCLE: multiple sequence alignment with high accuracy and high throughput. *Nucl Acids Res* **32**: 1792–1797.

Gil-Agudelo DL, Smith GW, Weil E. (2006). The white band disease type II pathogen in Puerto Rico. *Rev Biol Trop* **54**: 59–67.

Glas MS, Sato Y, Ulstrup KE, Bourne DG. (2012). Biogeochemical conditions determine virulence of black band disease in corals. *ISME J* **6**: 1526–1534.

Gomez-Gil B, Thompson CC, Matsumura Y, Sawabe T, Iida T, Christen R, *et al.* (2014). The Famlily *Vibrionaceae*. In: Rosenberg E, Delong EF, Lory S, Stackebrandt E, Thompson F (eds) Gammaproteobacteria. *The Prokaryotes*. Springer Berlin Heidelberg: Berlin, Heidelberg, pp 659–747.

Joyner J, Wanless D, Sinigalliano CD, Lipp EK. (2014). Use of quantitative real-time PCR for direct detection of *Serratia marcescens* in marine and other aquatic environments. *Appl Environ Microbiol* **80**: 1679–1683.

Kamada N, Chen GY, Inohara N, Núñez G. (2013). Control of pathogens and pathobionts by the gut microbiota. *Nat Immunol* **14**: 685–690.

Kemp DW, Rivers AR, Kemp KM, Lipp EK, Porter JW, Wares JP. (2015). Spatial homogeneity of bacterial communities associated with the surface mucus layer of the reef-building coral *Acropora palmata*. *PLoS One* **10**: e0143790.

Kushmaro A, Banin E, Loya Y, Stackebrandt E, Rosenberg E. (2001). *Vibrio shiloi* sp. nov., the causative agent of bleaching of the coral *Oculina patagonica*. *Int J Syst Evol Microbiol* **51**: 1383–1388.

Lee STM, Davy SK, Tang S-L, Fan T-Y, Kench PS. (2015). Successive shifts in the microbial community of the surface mucus layer and tissues of the coral *Acropora muricata* under thermal stress. *FEMS Microbiol Ecol* **91**: fiv142.

Lee STM, Davy SK, Tang S-L, Kench PS. (2017). Water flow buffers shifts in bacterial community structure in heat-stressed *Acropora muricata*. *Sci Rep* **7**: 43600.

Lesser MP, Jarett JK. (2014). Culture-dependent and culture-independent analyses reveal no prokaryotic community shifts or recovery of *Serratia marcescens* in *Acropora palmata* with white pox disease. *FEMS Microbiol Ecol* **88**: 457–467.

Luna GM, Bongiorni L, Gili C, Biavasco F, Danovaro R. (2009). *Vibrio harveyi* as a causative agent of the White Syndrome in tropical stony corals. *Environ Microbiol Rep* **2**: 120–127.

May LA, Avadanei AR, Rogers CS, Miller J, Woodley CM. (2011). Microbial community analysis of *Acropora palmata* mucus swabs, water and sediment samples from Hawksnest Bay, St. John, U.S. Virgin Islands. NOAA Technical Memorandum NOS NCCOS 123 and CRCP 14.

Moyat M. (2014). Immune responses to *Helicobacter pyloriinfection*. *WJG* **20**: 5583–12.

Muller EM, van Woesik R. (2012). Caribbean coral diseases: primary transmission or secondary infection? *Global Change Biol* **18**: 3529–3535.

Muller EM, van Woesik R. (2014). Genetic susceptibility, colony size, and water temperature drive white-pox disease on the coral *Acropora palmata*. *PLoS One* **9**: e110759–5.

Munn CB, Marchant HK, Moody AJ. (2008). Defences against oxidative stress in vibrios associated with corals. *FEMS Microbiol Lett* **281**: 58–63.

Nelson A, De Soyza A, Perry JD, Sutcliffe IC, Cummings SP. (2012). Polymicrobial challenges to Koch's postulates: ecological lessons from the bacterial vaginosis and cystic fibrosis microbiomes. *Innate Immunity* **18**: 774–783.

Overbeek R, Olson R, Pusch GD, Olsen GJ, Davis JJ, Disz T, *et al.* (2013). The SEED and the rapid annotation of microbial genomes using subsystems technology (RAST). *Nucl Acids Res* **42**: D206–D214.

Pantos O, Bythell JC. (2006). Bacterial community structure associated with white band disease in the elkhorn coral *Acropora palmata* determined using culture-independent 16S rRNA techniques. *Dis Aquat Org* **69**: 79–88.

Patterson KL, Porter JW, Ritchie KB, Polson SW, Mueller E, Peters EC, *et al.* (2002). The etiology of white pox, a lethal disease of the Caribbean elkhorn coral, *Acropora palmata*. *Proc Natl Acad Sci* **99**: 8725–8730.

Pollock FJ, Wada N, Torda G, Willis BL, Bourne DG. (2016). White syndrome-affected corals have a distinct microbiome at disease lesion fronts. *Appl Environ Microbiol* **83**: e02799–16–16–15.

Polz MF, Hunt DE, Preheim SP, Weinreich DM. (2006). Patterns and mechanisms of genetic and phenotypic differentiation in marine microbes. *Philos Trans R Soc Lond B Biol Sci* **361**: 2009–2021.

Precht WF, Gintert BE, Robbart ML, Fura R, van Woesik R. (2016a). Unprecedented disease-related coral mortality in Southeastern Florida. *Sci Rep* **6**: 31374–31311.

Precht WF, Gintert BE, Robbart ML, Fura R, van Woesik R. (2016b). Unprecedented disease-related coral mortality in Southeastern Florida. *Sci Rep* **6**: 31374–38.

Randall CJ, van Woesik R. (2015). Contemporary white-band disease in Caribbean corals driven by climate change. *Nat Clim Chang* **5**: 375–379.

Richter M, Rosselló-Móra R. (2009). Shifting the genomic gold standard for the prokaryotic species definition. *Proc Natl Acad Sci* **106**: 19126–19131.

Ritchie KB, Smith GW. (1998). Type II white-band disease. **46**: 199–203.

Round JL, Mazmanian SK. (2009). The gut microbiota shapes intestinal immune responses during health and disease. *Nat Rev Immunol* **9**: 313–323.

Rubio-Portillo E, Yarza P, alver CPN, aacute AAR-E, n JAO. (2014). New insights into *Oculina patagonica* coral diseases and their associated *Vibrio* spp. communities. *ISME J* **8**: 1794–1807.

Ruiz-Moreno D, Willis BL, Page AC, Weil E, Croquer A, Vargas-Angel B, *et al.* (2012). Global coral disease prevalence associated with sea temperature anomalies and local factors. *Dis Aquat Org* **100**: 249–261.

Santos E de O, Alves N, Dias GM, Mazotto AM, Vermelho A, Vora GJ, *et al.* (2011). Genomic and proteomic analyses of the coral pathogen *Vibrio coralliilyticus* reveal a diverse virulence repertoire. *ISME J* **5**: 1471–1483.

Sawabe T, Kita-Tsukamoto K, Thompson FL. (2007). Inferring the evolutionary history of vibrios by means of multilocus sequence analysis. *J Bacteriol* **189**: 7932–7936.

Sawabe T, Ogura Y, Matsumura Y, Gao F, Amin AR, Mino S, *et al.* (2013). Updating the *Vibrio* clades defined by multilocus sequence phylogeny: proposal of eight new clades, and the description of *Vibrio tritonius* sp. nov. *Front Microbiol* **4**: 1–14.

Séré MG, Tortosa P, Chabanet P, Quod J-P, Sweet MJ, Schleyer MH. (2015). Identification of a bacterial pathogen associated with *Porites* white patch syndrome in the Western Indian Ocean. *Mol Ecol* **24**: 4570–4581.

Séré MG, Tortosa P, Chabanet P, Turquet J, Quod J-P, Schleyer MH. (2013). Bacterial Communities Associated with Porites White Patch Syndrome (PWPS) on Three Western Indian Ocean (WIO) Coral Reefs. *PLoS One* **8**: e83746–10.

Shade A, Jones SE, Caporaso JG, Handelsman J, Knight R, Fierer N, *et al.* (2014). Conditionally rare taxa disproportionately contribute to temporal changes in microbial diversity. *mBio* **5**: e01371–14–e01371–14.

Sharon G, Rosenberg E. (2008). Bacterial growth on coral mucus. *Curr Microbiol* **56**: 481–488.

Stamatakis A. (2014). RAxML version 8: a tool for phylogenetic analysis and post-analysis of large phylogenies. *Bioinformatics* **30**: 1312–1313.

Stoddard SF, Smith BJ, Hein R, Roller BRK, Schmidt TM. (2015). rrnDB: improved tools for interpreting rRNA gene abundance in bacteria and archaea and a new foundation for future development. *Nucl Acids Res* **43**: D593–D598.

Sussman M, Willis BL, Victor S, Bourne DG. (2008). Coral pathogens identified for White Syndrome (WS) epizootics in the Indo-Pacific. *PLoS One* **3**: e2393–14.

Sutherland KP, Berry B, Park A, Kemp DW, Kemp KM, Lipp EK, *et al.* (2016). Shifting white pox aetiologies affecting *Acropora palmata* in the Florida Keys, 1994-2014. *Philos Trans R Soc Lond B Biol Sci* **371**: 20150205.

Sweet M, Bythell J. (2015). White syndrome in *Acropora muricata*: nonspecific bacterial infection and ciliate histophagy. *Mol Ecol* **24**: 1150–1159.

Sweet MJ, Brown BE. (2016). Coral responses to anthropogenic stress in the twenty-first century: an ecophysiological perspective. *Oceanogr Mar Bio Ann Rev* **54**: 271–314.

Sweet MJ, Bulling MT. (2017). On the importance of the microbiome and pathobiome in coral health and disease. *Front Mar Sci* **4**: 2261–11.

Sweet MJ, Croquer A, Bythell JC. (2010). Bacterial assemblages differ between compartments within the coral holobiont. *Coral Reefs* **30**: 39–52.

Thompson JR, Randa MA, Marcelino LA, Tomita-Mitchell A, Lim E, Polz MF. (2004). Diversity and dynamics of a North Atlantic coastal *Vibrio* community. *Appl Environ Microbiol* **70**: 4103–4110.

Thurber RV, Willner-Hall D, Rodriguez-Mueller B, Desnues C, Edwards RA, Angly F, *et al.* (2009). Metagenomic analysis of stressed coral holobionts. *Environ Microbiol* **11**: 2148–2163.

Tout J, Siboni N, Messer LF, Garren M, Stocker R, Webster NS, *et al.* (2015). Increased seawater temperature increases the abundance and alters the structure of natural *Vibrio*

populations associated with the coral *Pocillopora damicornis*. *Front Microbiol* **6**: 403–12.

Ushijima B, Smith A, Aeby GS, Callahan SM. (2012). *Vibrio owensii* Induces the tissue loss disease *Montipora* white syndrome in the Hawaiian reef coral *Montipora capitata*. *PLoS One* **7**: e46717–10.

Ushijima B, Videau P, Burger AH, Shore-Maggio A, Runyon CM, Sudek M, *et al.* (2014). *Vibrio coralliilyticus* strain ocn008 is an etiological agent of acute *Montipora* white syndrome. *Appl Environ Microbiol* **80**: 2102–2109.

Vayssier-Taussat M. (2014). Shifting the paradigm from pathogens to pathobiome: new concepts in the light of meta-omics. *Front Cell Infect Microbiol* **4**: 1–7.

Vega Thurber RL, Burkepile DE, Fuchs C, Shantz AA, McMinds R, Zaneveld JR. (2014). Chronic nutrient enrichment increases prevalence and severity of coral disease and bleaching. *Global Change Biol* **20**: 544–554.

Wattam AR, Abraham D, Dalay O, Disz TL, Driscoll T, Gabbard JL, *et al.* (2013). PATRIC, the bacterial bioinformatics database and analysis resource. *Nucl Acids Res* **42**: D581–D591.

Westrich JR, Ebling AM, Landing WM, Joyner JL, Kemp KM, Griffin DW, *et al.* (2016). Saharan dust nutrients promote *Vibrio* bloom formation in marine surface waters. *Proc Natl Acad Sci* **113**: 5964–5969.

Williams DE, Miller MW. (2011). Attributing mortality among drivers of population decline in *Acropora palmata* in the Florida Keys (USA). *Coral Reefs* **31**: 369–382.

Zaneveld JR, Shantz AA, Pritchard CE, McMinds R, Payet JEROMP, Welsh R, *et al.* (2016). Overfishing and nutrient pollution interact with temperature to disrupt coral reefs down to microbial scales. *Nat Commun* **7**: 1–12.

Ziegler M, Seneca FO, Yum LK, Palumbi SR, Voolstra CR. (2017). Bacterial community dynamics are linked to patterns of coral heat tolerance. *Nat Commun* **8**: 14213.

Tables

Table 3.1. Isolate distribution among *Vibrio* spp. previously shown to cause disease in coral through infection trials, with partial or complete fulfillment of Koch's postulates.

Species	ANI (%)[a]	no. of isolates[b]				% of total isolates	Coral disease or syndrome (reference)
		H2O	CH	CDH	CDPX		
Clade *Corallilyticus*							
V. coralliilyticus	98.3	—	—	—	2	2.8	bacterial bleaching disease, *Pocillopora damicornis* and *Oculina patagonia* (Ben-Haim *et al.*, 2003; Rubio-Portillo *et al.*, 2014); *Montipora* white syndrome, acute, *M. capitata* (Ushijima *et al.*, 2014)*; white syndrome, *Acropora cytherea*, *Montipora aequituberculata*, and *Pachyseris speciosa* (Sussman *et al.*, 2008)*
Clade *Harveyi*							
V. alginolyticus	99.5	1	1	1	—	4.3	yellow band disease, *Orbicella faveolata* (Cervino *et al.*, 2008)**; *Porites* white patch syndrome, *P. andrewsi* (Zhenyu *et al.*, 2013)
V. harveyi (synonym of *V. charachariae*)	99.5	2	2	4	6	20.3	white syndrome, *Acropora* spp. (Luna *et al.*, 2009)*; white band disease, *Acropora cervicornis* (Ritchie and Smith, 1998; Gil-Agudelo *et al.*, 2006)*; yellow band disease, *O. faveolata* (Cervino *et al.*, 2008)**
V. natriegens	—	—	—	—	—	—	*Porites* ulcerative white spot disease, *P. cylindrical* (Arboleda and Reichardt, 2010)

V. owensii	98.2	10	10	11	6	53.6	*Montipora* white syndrome, chronic, *M. capitata* (Ushijima *et al.*, 2012)*
V. parahaemolyticus	—	—	—	—	—	—	*Porites* ulcerative white spot disease, *P. cylindrical* (Arboleda and Reichardt, 2010)
V. rotiferianus	—	—	—	—	—	—	yellow band disease, *O. faveolata* (Cervino *et al.*, 2008)**
V. mediterranei (synonym of *V. shiloi*)	99.0	1	—	—	1	2.9	bacterial bleaching disease, *O. patagonia* (Kushmaro *et al.*, 2001)
Clade *Orientalis*							
V. tubiashii	94.2	—	—	1	—	1.4	white syndrome, *Acropora muricata* (Sweet and Bythell, 2015)*
Clade *Proteolyticus*							
V. proteolyticus	—	—	—	—	—	—	yellow band disease, *O. faveolata* (Cervino *et al.*, 2008)**

[a]Average nucleotide identity (ANI) of the 8-gene concatenation of isolates and reference strains

[b]H2O, seawater; H, mucus from apparently healthy coral; DH, mucus from an asymptomatic region of a diseased coral; DPX, mucus from white pox lesions

*Diseases in which additional, non-*Vibrio* pathogens have been detected or are suspected

**Diseases caused by a consortium of *Vibrio* species

Figures

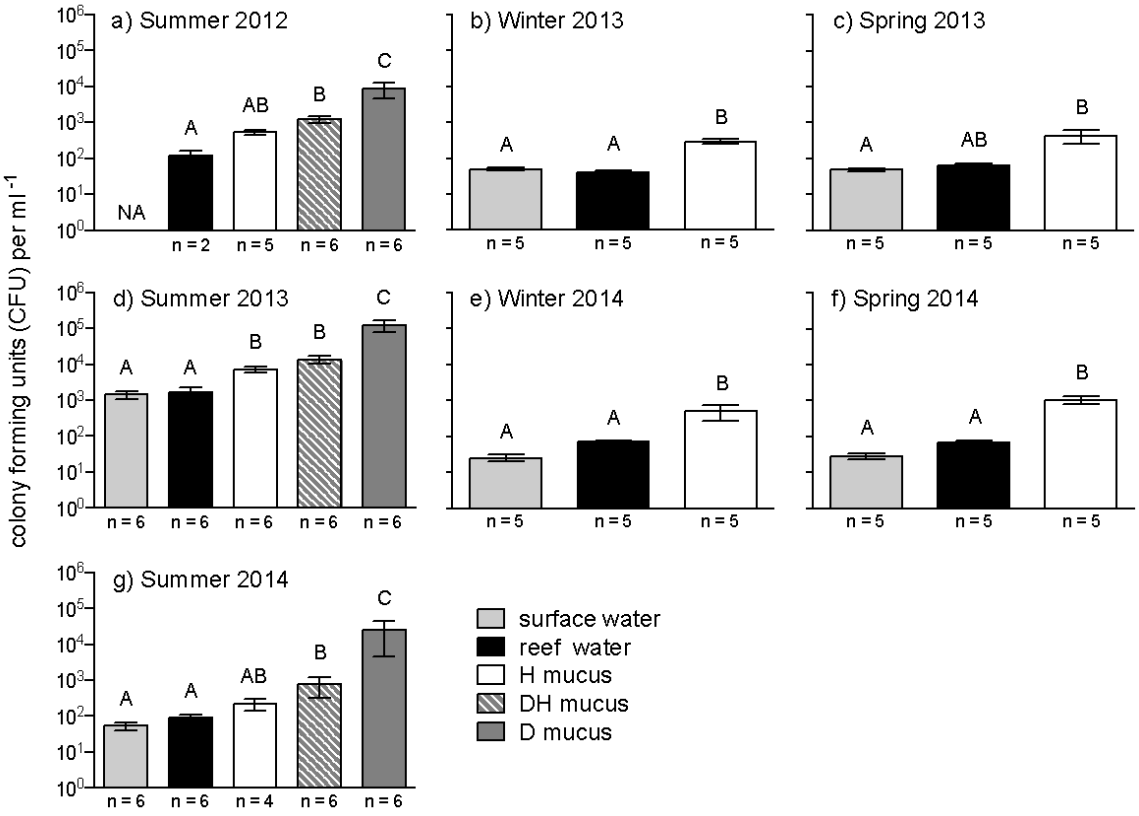

Figure 3.1. The abundance of TCBS cultivable *Vibrio* spp. (mean CFU ml^{-1} ± SEM) for *A. palmata* mucus samples and seawater collected from Looe Key Reef, FL. Letters designate significant groupings based on Tukey's multiple comparisons tests following one-way ANOVA for each sampling period. Abbreviations: H, mucus from apparently healthy colonies with no white pox disease (WPX) signs; D, mucus from WPX lesions; DH, mucus from asymptomatic areas colonies with WPX lesions.

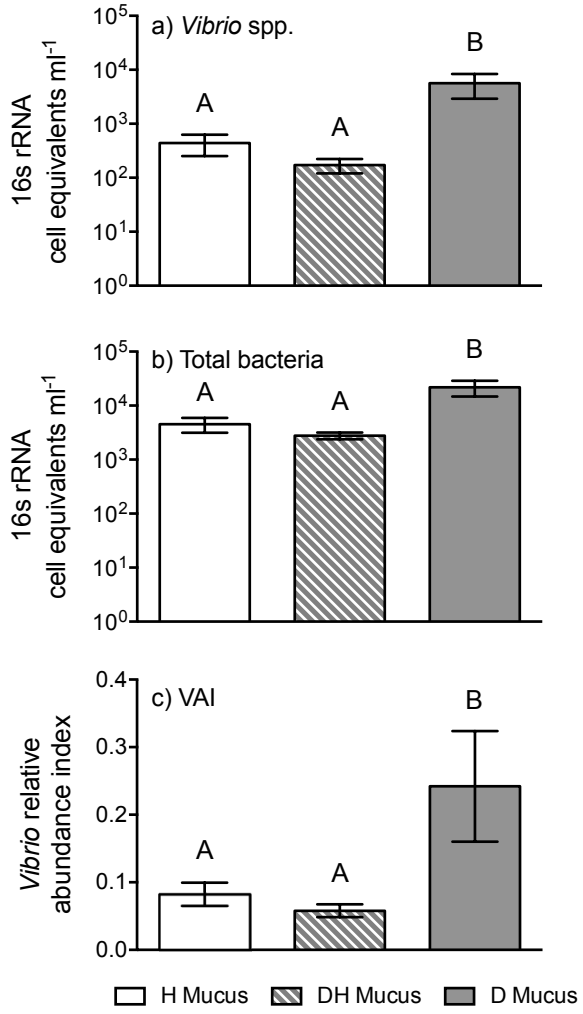

Figure 3.2. Quantitative real-time PCR data for *A. palmata* mucus samples collected from Looe Key Reef, FL during August 2014. Concentration of (a) *Vibrio* spp. and (b) total bacteria estimated by cell equivalents ml^{-1} of the 16S rRNA gene (mean ± SEM). *Vibrio* relative abundance index (VAI; mean ± SEM) (c) calculated as the ratio of *Vibrio* spp. cell equivalents to total bacteria cell equivalents. Letters designate significant groupings assessed by Tukey's multiple comparisons tests following one-way ANOVA. Abbreviations: H, mucus from apparently healthy colonies with no white pox disease (WPX) signs; D, mucus from WPX lesions; DH, mucus from asymptomatic areas colonies with WPX lesions.

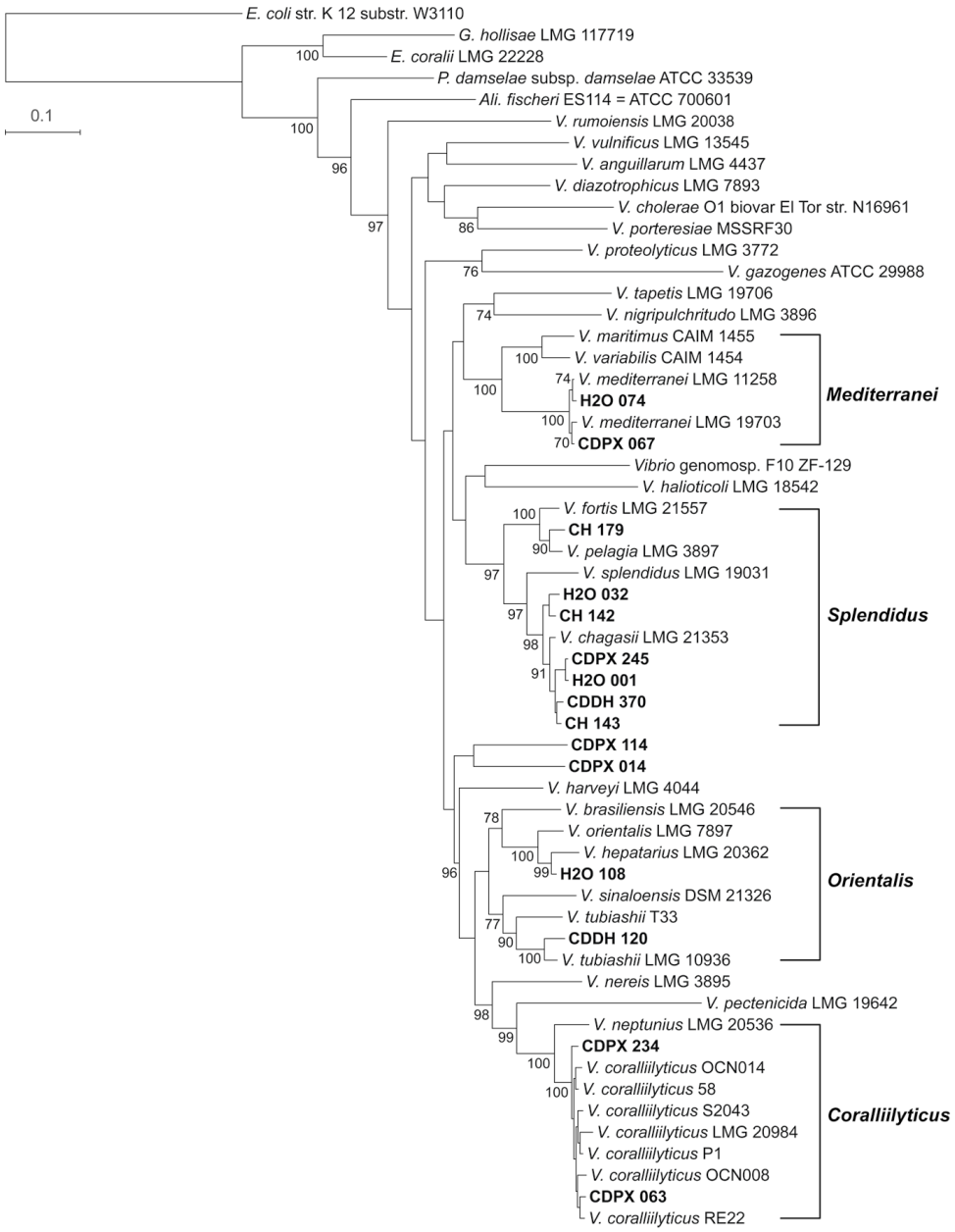

Figure 3.3. Maximum likelihood phylogenetic analysis based on eight gene loci. Bootstrap values for 500 iterations (≥ 70) are shown. Brackets indicate clades containing A. palmata isolates. Boldface type indicates study isolates. Abbreviations for isolation source: CH, mucus from apparently healthy colonies with no white pox disease (WPX) signs; CDPX, mucus from WPX lesions; CDDH, mucus from asymptomatic areas colonies with WPX lesions; H2O, reef water.

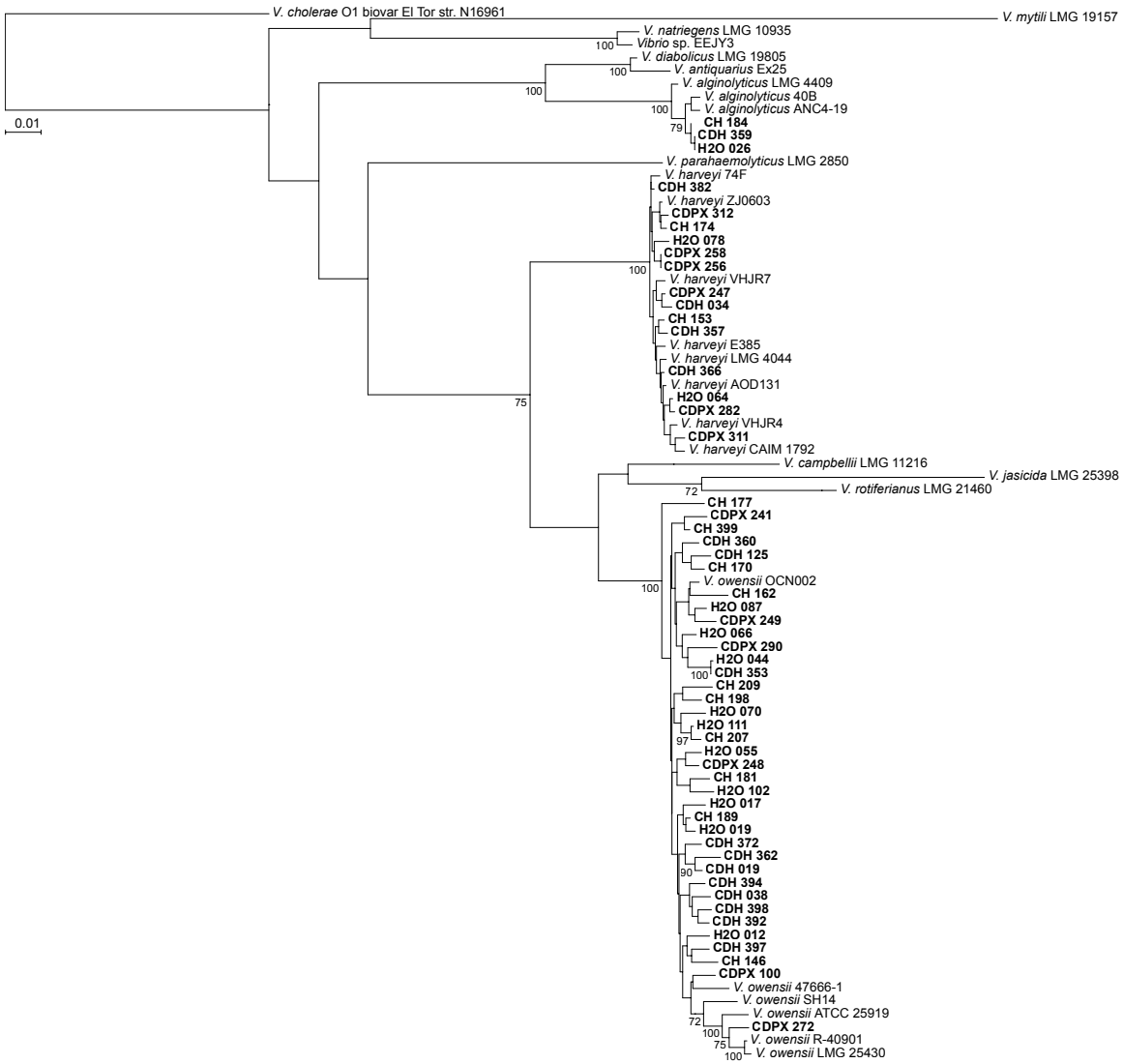

Figure 3.4. Maximum likelihood phylogenetic analysis based on eight gene loci for the *Harveyi* clade. Bootstrap values for 500 iterations (≥ 70) are shown. Boldface type indicates study isolates. Abbreviations for isolation source: CH, mucus from apparently healthy colonies with no white pox disease (WPX) signs; CDPX, mucus from WPX lesions; CDDH, mucus from asymptomatic areas colonies with WPX lesions; H2O, reef water.

CHAPTER 4

TEMPORAL SAMPLING OF CORAL DISEASE REAVEALS DISTINCT SPATIOTEMPORAL PATTERNS IN MICROBIAL COMMUNITY DIVERSITY AND STRUCTURE

Despite the region-wide ecological impacts posed by coral disease, few etiologic agents have been identified and our understanding of coral disease epidemiology remains limited. Corals are most frequently sampled after classic disease signs are already apparent while the onset of disease is missed. In this study, we aimed to document white pox disease onset and progression in *A. palmata* in the Florida Keys, USA through high resolution monitoring 2–3 times per week. This approach revealed unique spatiotemporal dynamics in microbial communities in lesions ≤ 24 h old compared to aging lesions. Alpha diversity was lower while sample-to-sample variation (beta-diversity) was higher in new lesions ≤ 24 h old compared to apparently healthy samples and aging lesions. Increased microbiome variability during stress is thought to reflect decreased ability of the host and/or the commensal microbiota to regulate microbial community composition. *Vibrio* bacteria bloomed from < 1% to ~33% relative abundance within the first 24 h of lesion formation. However, this bloom had subsided by 3–5 d and microbiome destabilization in new WPX appeared to be ephemeral. Moreover, WPX lesions healed rapidly in this study and decreased in size by ~29% after just 8–13 d. This suggests that although *A. palmata* in the Florida Keys continue to develop WPX signs, they may now be resilient to tissue-loss progression due to WPX. Alternatively, additional factors such

as history of thermal stress may affect the susceptibility of *A. palmata* to WPX. Future studies should investigate environmental thresholds that may serve as tipping points, inducing WPX signs and destabilization in *A. palmata* immune function or microbiome homeostasis.

Introduction

Coral disease is recognized as an increasing threat to coral populations worldwide, and has fundamentally altered Caribbean reef ecosystems (Aeby *et al.*, 2011; Maynard *et al.*, 2015; Weil and Rogers, 2010). The once dominant Caribbean shallow-water species, *Acropora palmata* and *A. cervicornis*, have suffered substantial losses due to disease (Patterson *et al.*, 2002; Precht *et al.*, 2016). These framework building species are considered ecologically irreplaceable in terms of their structural complexity, and their precipitous decline has lead to a "flattening" of Caribbean reefs (Alvarez-Filip *et al.*, 2009). The widespread loss of reef architecture in the Caribbean has serious consequences for reef fish assemblages, benthic biodiversity, and coastal protection.

Despite the region-wide ecological impacts posed by coral disease, our understanding of coral disease epidemiology is limited and, to date, few etiologic agents have been identified (Sutherland *et al.*, 2016). Establishing disease causation is complicated by the intimate interaction between framework building corals and their microbiome, which includes a diverse array of archaea, bacteria, fungi, viruses, protists, and photosynthetic microalgae (Bourne *et al.*, 2016; Ainsworth *et al.*, 2010). These microbial communities found in the coral surface mucus layer (SML), tissue, and skeleton (Sweet *et al.*, 2010) play an important role in nutrient cycling and host

immunity. Because the health and function of reef-building corals is intricately intertwined with their microbial symbionts, this association has been termed the coral 'holobiont' (Rohwer *et al.*, 2002).

Coral disease studies have historically focused on describing the relationship between specific microbial taxa and the disease state, in keeping with the 'one pathogen, one disease' paradigm (Sutherland *et al.*, 2016; Sweet and Bulling, 2017). The goal has been to identify taxa that are (1) present in disease samples while absent in healthy samples or (2) have increased abundance in disease samples compared to healthy samples. However, most of these investigations have failed to produce an inviolable association between a single microbial agent and the disease state (Sutherland *et al.*, 2016).

Sampling in coral disease has often been conducted in a cross-sectional manner, in which collections for microbiological investigation are made at a single time point during a disease outbreak to compare healthy versus diseased samples. Studies that have included temporal sampling have done so in a seasonal manner, comparing samples collected at single time point within a given season (*i.e.*, summer, winter, spring, fall) (Joyner *et al.*, 2015; Pollock *et al.*, 2016; Sussman *et al.*, 2008; Séré *et al.*, 2015). While these sampling schemes have yielded important information on seasonal shifts in the coral microbiome (Pollock *et al.*, 2016) and have led to the identification of several disease agents (Sussman *et al.*, 2008; Séré *et al.*, 2015; Patterson *et al.*, 2002), they often lack the resolution needed to distinguish initial pathogenesis from secondary disease stages. Since corals are most frequently sampled after classic disease signs are already apparent and disease onset in often missed, many described microbial patterns typical of

the disease state, such as increased abundance of Rhodobacteraceae (Sunagawa *et al.*, 2009; Cárdenas *et al.*, 2011; Roder *et al.*, 2014; Pollock *et al.*, 2016), may reflect secondary opportunistic stages rather than primary pathogenesis.

In this study, we aimed to document disease onset and progression in *A. palmata* in the Florida Keys, USA through high resolution monitoring 2–3 times per week. Living cover of *A. palmata* in the upper Florida Keys declined by 50% from 2004–2010 (Williams and Miller, 2011) and 30% of this loss was attributable to partial mortality caused by white pox (WPX) and other tissue loss diseases. The established WPX pathogen *Serratia marcescens* is not consistently associated with contemporary WPX outbreaks (Joyner *et al.*, 2014; Lesser and Jarett, 2014), and it has been suggested that contemporary WPX signs are likely caused by multiple pathogens or a member of the *A. palmata* microbiome that is able to cause disease under certain conditions (Sutherland *et al.*, 2016; Muller and van Woesik, 2014). We have previously shown that the relative abundance of *Vibrio* bacteria is higher in mucus from WPX lesions compared to mucus from apparently healthy tissue (Chapter 3). We have also shown that potentially pathogenic *Vibrio* spp. are found in low abundance in apparently healthy *A. palmata*. However, it remains unknown whether *Vibrio* are involved in WPX lesion onset and progression.

The highly resolved sampling in this study revealed unique spatiotemporal dynamics in microbial communities at the front (or margins) of lesions ≤ 24 h old, as well as blooming of potential *Vibrio* pathobionts and a reduction of presumed beneficial taxa.

Methods

Field surveys. White pox disease (WPX) outbreaks typically occur in middle to late summer months and subside in the winter and spring (Sutherland *et al.*, 2016). Therefore**,** we monitored *Acropora palmata* for the development of WPX 2–3 times weekly between June 25th and July 24th 2015 at Looe Key Reef (3 m depth; N 24°32.724' W 81°24.360') in the Florida Keys National Marine Sanctuary. Trips to the reef were conducted through commercial dive operations and dives were limited to 1 h; therefore, due to these time restraints disease surveys and sample collection often occurred on different dates (Table 4.1). To conduct disease surveys, individual *A. palmata* colonies (n = 19) were mapped, photographed, catalogued, and tracked throughout the study. Colonies were examined visually and records were made of active WPX, defined by irregularly shaped lesions (at least 1 cm^2) with sloughing tissue and exposure of bright white skeleton (Patterson *et al.*, 2002). *A. palmata* colonies were digitally photographed from directly overhead with a standard scale for reference. WPX prevalence was determined by calculating the percentage of the monitored colonies with WPX lesions. WPX severity was calculated as the average number of active WPX lesions per diseased colony. Additionally, we mapped the location of lesions on each colony to discriminate new verses old lesions and estimate lesion age.

Sample collection. To minimize the affects of repeated sampling, non-destructive methods were utilized to collect the surface mucus layer (SML) of *A. palmata* for microbial community analysis with sterile, needleless syringes (20-ml, luer-lock) (Kemp *et al.*, 2015; Zaneveld *et al.*, 2016). Colony health status, lesion location, and lesion age were recorded for each sample collected. A single location was sampled on apparently

healthy colonies, displaying no visual signs of active WPX lesions (denoted as *H*). Three locations were sampled on WPX-affected colonies: the lesion front (denoted as *WPX*), apparently healthy regions ~2 cm and ~10 cm away from the lesion (denoted as DH_2 and DH_{10}). Samples were collected from colonies with WPX lesions ≤ 24 h old (n = 6) on July 13th and July 14th, 2015. Thereafter, newly developed lesions were noted and allowed to age, undisturbed, until they were sampled at 3–5 d (n = 6) or 8–10 d (n = 4). Thus, no lesions in this study were re-sampled, minimizing potential sampling artifacts. When possible, we prioritized sampling lesions of the three age classes from the same coral colony.

At the end of the dive, SML samples were processed immediately shipboard by connecting the luer-lock syringes to a 5-µm Acrodisc® syringe pre-filter (Supor® membrane, Paul Co. Ltd., Ann Arbor, MI, USA) inline with a 0.22-µm Sterivex-GV cartridge (EMD Millipore, Bedford, MA, USA). After filtering, Sterivex were pumped dry, placed in individual sterile Whirl-Pak™ bags, immediately frozen in dry ice, and then transferred to -80°C within 1 h of collection. Additionally, two to three seawater samples were collected in sterile, 1 L Nalgene bottles approximately 1 m above the *A. palmata* colonies on each sampling date. Seawater samples were transported in a cooler filled with ice to the laboratory and processed within 1 h of collection. Each liter sample was filtered, with the aid of a peristaltic pump, through a 5-µm pre-filter inline with a 0.22-µm Sterivex and immediately frozen at -80°C.

DNA extraction. DNA was extracted from Sterivex cartridges using a protocol modified from that of Boström and colleagues (Boström *et al.*, 2004). After Sterivex were thawed, 1600 µl of lysis buffer (400 mM NaCl, 750 mM sucrose, 20 mM EDTA, 50 mM

Tris-HCL) and 100 µl of lysozyme solution (125 mg in 1000 µl lysis buffer) were added and the ends were capped. Cartridges were vortexed gently and incubated at 37°C for 30 min, while rotating on a Boekel carousel. Proteins were digested by adding 100 µl of proteinase K and 200 µl of 10% sodium dodecyl sulfate (1% v/v final), followed by gently vortexing and incubation with rotation at 55°C for 3 h. Using a 5-cc syringe, the lysate was withdrawn from the Sterivex filter and transferred equally among two 2-ml centrifuge tubes (~1000 µl in each). Then, 4 µl of RNase A (10 mg ml^{-1}) were added to each tube and the samples were vortexed and incubated at 37°C for 10 min. DNA was recovered with GenElute™-LPA (Sigma-Aldrich, St. Louis, MO, USA) as a co-precipitate with 1⁄25th volume 5M NaCl and 0.7 × volume of isopropanol. DNA was precipitated overnight at -20°C, followed by centrifugation at 4°C and for 20 min (17,000 × g). Supernatant fluids were discarded and the pellets were resuspended in 100 µl of 10 mM Tris-Cl, pH 8.5. The two DNA aliquots for each sample were combined and purified using the Zymo Genomic DNA Clean and Concentrator kit (Zymo Research Corp., Irvine, CA, USA). DNA concentration was measured using a Qubit fluorometer (Invitrogen, Carlsbad, CA, USA) and 2 ng $µl^{-1}$ dilutions were prepared for each sample.

16S rRNA amplicon sequencing. Libraries for 84 samples (Appendix B, Table S4.2) were prepared in two-step PCR method (Tinker and Ottesen, 2016), amplifying the V4 region of the 16S rRNA with the primers 515F (GTGCCAGCMGCCGCGGTAA) and 806R (GGACTACHVGGGTWTCTAAT) established by Caporaso et al. (Caporaso *et al.*, 2011). The two-step process required a total of 25 amplification cycles, detailed below. The first reaction mixture contained 2 µl 5× Q5 buffer (New England Biolabs, Ipswich, MA, USA), 0.1µl Q5 polymerase, 200 µM dNTPs, 0.5 µM primers, and 2 µl of

DNA template with molecular grade water added for a total reaction volume of 10 µl. The V4 region was first amplified with following conditions: 98°C for 30 s, then 15 cycles at 98°C for 10 s, 52°C for 30 s, and 72°C for 30 s, with a final extension at 72°C for 2 min. The second amplification step utilized 515F and 806R primers that contained Hamady barcodes for multiplexing (Hamady *et al.*, 2008). Upon completion of the first reaction, 9 µl of amplicon product were immediately added to a PCR mixture containing 6 µl 5× Q5 buffer, 0.3 µl Q5 polymerase, 200 µM dNTPs, 0.5 µM primers, and molecular grade water added to a volume of 21 µl. The 30 µl reaction was then amplified with the following conditions: 98°C for 30 s, then 4 cycles at 98°C for 10 s, 52°C for 10 s, and 72°C for 30 s, followed by 6 cycles at 98°C for 10 s and 72°C for 1 min, and a final extension at 72°C for 2 min. Two replicate PCR amplifications were prepared for each sample and purified by adding 1:1 Agencourt AMPure XP magnetic beads (Beckman Coulter, Brea, CA, USA) followed by a 15-min incubation at room temperature. Bead-bound DNA was then magnet captured, washed twice with 80 µl of 80% molecular grade EtOH, and eluted in 25 µl of 10 mM Tris-Cl, pH 8.5. Purified libraries were quantified using a Qubit fluorometer (Invitrogen, Carlsbad, CA, USA) and pooled in equimolar ratios. The pooled library was submitted for sequencing at the Georgia Genomics Facility at the University of Georgia, Athens, GA, USA (Illumina MiSeq 250 × 250 bp; Illumina, Inc., San Diego, CA).

Sequence processing and OTU selection. Sequence reads were processed using USEARCH ver.5.2.236 (Edgar, 2010) and QIIME ver.1.9.1 (Bushman *et al.*, 2010). In USEARCH, forward and reverse reads were merged with the *fastq_mergepairs* command and then quality filtered by an expected error rate of 1.0 (Edgar and Flyvbjerg, 2015)

with the *fastq_maxee E* command. Merged sequences greater than 275 bp were removed (19 sequences in total), resulting in ~6.19 million high quality reads. *De novo* based chimera detection and *de novo* operational taxonomic unit (OTU) picking were preformed via USEARCH ver.5.2.236 within the QIIME platform. OTUs were clustered with UCLUST (Edgar, 2010) at 97% similarity and a representative sequence for each OTU was classified taxonomically according to the Greengenes ribosomal database ver.13.9 (McDonald *et al.*, 2011) with the Ribosomal Database Project (RDP) naïve Bayesian classifier (Wang *et al.*, 2007). Prior to downstream analysis, sequences classified as "unknown" (*i.e.*, sequences not classified at the kingdom level), chloroplasts, and mitochondria were removed. OTUs that occurred only once across the entire dataset were removed, while OTUs that occurred singly in multiple samples (*e.g.*, occurred once in *sample A* and once in *sample B*) were retained.

Sequence statistical analyses. Alpha diversity metrics including richness, evenness, and phylogenetic diversity (PD) were calculated in QIIME v.1.9.1 using the multiple_rarefactions.py, collate_alpha.py and compare_alpha.ph scripts. Values for chao1, Shannon Entropy, and Faith's PD were calculated by rarefaction to 20,000 reads per sample with 10 iterations. Alpha diversity values were averaged across the 10 iterations and compared across categories. Student's *t*-tests were used to evaluate significant differences between comparisons of all sample types to *H* samples. Beta-diversity was calculated based on the weighted UniFrac distance matrix, a phylogenetic measure of community similarity that takes into account organismal abundance and phylogeny (Lozupone and Knight, 2005). Phylogenetic trees used to calculate this metric were constructed in QIIME v.1.9.1 by aligning representative

sequence for each OTU with PyNAST (Caporaso *et al.*, 2010) against the Greengenes ribosomal database ver.13.9 (McDonald *et al.*, 2011). The alignment was filtered, allowing no gaps, and a phylogenetic tree was constructed with the FastTree method (Price *et al.*, 2009). UniFrac distances were calculated based on the multiple OTU tables resulting from the rarefaction step described above. Beta diversity was visualized using non-metric multi-dimensional scaling (NMDS) of the weighted UniFrac distance. Significance of the differences in overall microbial community composition across sample types was tested with permutational multivariate analysis of variance (PERMANOVA) implemented using the Adonis method in the vegan R package ver.2.4.2 with 999 permutations (Oksanen *et al.*, 2017). Distances between samples within each category (Table 4.2) were pooled using the QIIME script make_distance_boxplots.py. Significance was assessed by non-parametric *t*-tests, each with 1,000 Monte Carlo permutations (permutation is important in this instance to account for the non-independence of distances).

A linear discriminant analysis (LDA) effect size (LEfSe) method (Segata *et al.*, 2011) was used to explore the potential presence of taxonomic groups that could serve as biomarkers for different metadata classes, in this case health status (*H* versus $WPX \leq 24$ h). OTUs were pooled to family level with the QIIME script summarize_taxa.py, which served as an input for LEfSe analysis. LEfSe utilizes the non-parametric factorial Kruskal-Wallis (KW) sum-rank test to detect taxa with significant differential abundance among sample groups. LEfSe then identifies a taxonomic group as a biomarker only if it is consistently abundant across a group of samples. Effect size is quantified by averaging the differences between sample group means with the differences between metadata class

means along the first linear discriminant axis in the LDA model, which equally weights a taxon's variability and discriminatory power (Segata *et al.*, 2011). The LDA effect size is then reported in logarithm (base 10).

Lesion size change. Individual lesions (n = 18) were photographed over time with a scale in view to calculate changes in lesion surface area (mm^2) with IMAGEJ ver.1.51f software (Schneider *et al.*, 2012). Because disease surveys could not be conducted every day, it was impossible to estimate the absolute age for most lesions. Instead, size change was estimated from the initial day-of-discovery. Percent change was calculated for three discrete time periods: 3–5 days since discovery (DSD), 8–13 DSD, and 15–27 DSD. Lesion regeneration rates have been shown to depend on initial lesion size in *A. palmata* and other corals (Lirman, 2000; van Woesik, 1998); therefore, WPX lesions were grouped into three size classes (10-100 mm^2, 101-300 mm^2, and 301-1200 mm^2) to visualize changes in surface area (mm^2) with DSD.

Results

Disease survey data. During the 5-week observation period in Summer 2015, 15 of 18 (78.6%) *Acropora palmata* colonies observed developed white pox disease (WPX) lesions (Appendix B, Table S4.1). WPX severity increased from zero active lesions per colony on June 25th to seven active lesions per colony on July 24th. Lesions were observed to move from the active state (sloughing tissue at margins and bright white exposed skeleton in the center) to the inactive state (no sloughing tissue at the margins and new turf algal colonization of bare skeleton) within 8–10 d. Within the first 3–5 days since discovery (DSD), 7 of 18 lesions observed increased in size (Appendix B Figure

S4.1). After 8–13 DSD, only 3 of 18 lesions increased in size. All lesions observed for more than 14 DSD (n = 6) decreased in size. Overall, lesions decreased in size by 3.5% (± 3.1% SEM) within 3–5 DSD, 29.4% (± 7.4% SEM) within 8–13 DSD, and 38.9% (± 14.3% SEM) within 15–27 DSD (Figure 4.1).

Microbial community beta diversity. Samples of the surface mucus layer (SML) of corals and the surrounding reef water resulted in 5.86 million classifiable, nonchimeric reads, with an average of 65,160 ± 2,864 (SEM) reads per sample. Beta diversity considered as community composition was significantly different among sample types (*H*, DH_2, DH_{10}, *WPX*, and seawater) based on permutational multivariate analysis of variance (PERMANOVA) of weighted UniFrac dissimilarity matrix of phylogenetic distance (df = 4, $R^2 = 0.24$, $P_{perm} > 0.001$). *WPX* ≤ 24 h samples separated from all other coral mucus samples (*H*, DH_2, DH_{10}, and aging *WPX*) in non-metric multi-dimensional scaling (NMDS) analysis based on weighted UniFrac distances (Figure 4.3).

Beta diversity considered as sample-to-sample variability (calculated as the mean weighted UniFrac distance between samples within a sample category), was significantly higher in *WPX* ≤ 24 h samples compared to *H* samples (Figure 4.2).

Microbial community alpha diversity. Compared to *H* samples, bacterial communities in *WPX* ≤ 24 h samples had significantly lower phylogenetic diversity (Faith's PD, *P = 0.003*) and evenness (Shannon Entropy, using a base 2 logarithm, *P* < 0.001) (Figure 4.3). There was no difference in choa1 operational taxonomic unit (OTU) richness (*P* = 0.10, Figure 4.3a).

Significant indicator taxa. A total of 35 bacterial families displayed significant differential abundance ($P_{KW} < 0.05$), between *H* and *WPX* ≤ 24 h samples based on

LEfSe linear discriminant analysis (LDA) (Figure 4.6a). The indicator families with the highest relative abundance in *WPX* ≤ 24 h samples were *Vibrionaceae*, *Campylobacteraceae*, and *Ferrimonadaceae*, while *H* samples had the highest relative abundance of *Halomonadaceae*, *Flavobacteriaceae*, and *Pelagibacteraceae* (Figure 4.6b). *Endozoicimonaceae*, proposed as important endosymbionts of reef-building coral species (Neave *et al.*, 2016), were significantly enriched in *H* samples (Fig 4.6a, P_{KW} = 0.0039). *H* samples were also enriched in predatory bacteria in two families within the order *Myxococcales* ($P_{KW} \leq 0.039$) and the family *Bdellovibrionaceae* ($P_{KW} = 0.026$). LEfSe analysis among all sample types identified indicator families significantly enriched in aging lesions and apparently healthy regions on diseased coral colonies (Appendix B, Table S4.3); however, the majority of these indicator families comprised less than <1% of the total sample community (Appendix B, Figure S4.3).

Vibrionaceae had the highest LDA_{log10} score (5.26, $P_{KW} = 0.007$) out of all indicator families (Appendix B, Table S4.3) and exhibited the most dramatic change in relative abundance between *H* and *WPX* ≤ 24 h samples, increasing from 0.39% (± 0.07% SEM) to 34.24% (± 8.04% SEM) (Figure 4.6b). The genus *Vibrio* drove this trend, with a relative abundance of 33.5% (± 8.1% SEM) in *WPX* ≤ 24 h samples was compared to <1% in all other sample types (Table 4.2, Figure 4.5).

Discussion

It is becoming increasingly clear that many infections in corals and other hosts have a polymicrobial etiology, in which several microorganisms are involved in disease origin and/or manifestation. In humans for example, bacterial vaginosis (Machado *et al.*,

2016), cystic fibrosis lung infections (Sibley *et al.*, 2008), inflammatory bowel diseases (Kamada *et al.*, 2013), and periodontal diseases (Lamont and Hajishengallis, 2015) all display polymicrobial etiology. Well-defined polymicrobial diseases in coral include black band disease (Sato *et al.*, 2017; Glas *et al.*, 2012), yellow band disease (Cervino *et al.*, 2008), and white syndrome (Sweet and Bythell, 2015; Sussman *et al.*, 2008).

The term 'dysbiosis' has been utilized extensively in human disease to describe a state of imbalance, in which immune homeostasis is disrupted by shifts in the relative abundance or influence of species within a microbial community (Lamont and Hajishengallis, 2015; Round and Mazmanian, 2009; Hajishengallis *et al.*, 2012). Only recently, has it been suggested that many marine diseases, including coral disease, may manifest as microbial dysbiosis (Egan and Gardiner, 2016). Multiple mechanisms may contribute to microbial dysbiosis including a reduction of alpha diversity, the loss of beneficial taxa, colonization of opportunistic pathogens, and/or expansion of 'pathobionts' (Petersen and Round, 2014; Stecher *et al.*, 2013). Pathobionts are defined as normally innocuous community members that promote pathology under certain environmental pressures and/or host stress (Chow *et al.*, 2011). The pathobiont concept is exemplified by intestinal inflammatory diseases that are caused by commensal bacteria, which become virulent (via mechanisms such as horizontal gene transfer (HGT) of virulence genes) or shift in relative abundance following a disturbance (*e.g.*, antibiotic usage) (Stecher *et al.*, 2013).

Thus, disease dynamics are influenced by a complex interplay between beneficial species, opportunistic pathogens, environmental factors, and the host immune system (Kamada *et al.*, 2013; Hooper *et al.*, 2012; Lamont and Hajishengallis, 2015). There is a

growing recognition that polymicrobial infections represent functional communities, referred to as the 'pathobiome' (Vayssier-Taussat, 2014), in which pathogens live and interact with other microorganisms and these complex interactions influence or drive disease dynamics. The pathobiome framework places a new emphasis on elucidating ecological interactions and spatiotemporal dynamics of these communities, drawing on ecological theory in community assembly and succession (Vayssier-Taussat, 2014; Nelson *et al.*, 2012; Byrd and Segre, 2016; Sweet and Bulling, 2017).

To capture these dynamic microbial interactions during polymicrobial diseases, an appropriate sampling resolution must be applied. The approach utilized in this study, high resolution sampling of *Acropora palmata* during the typical WPX outbreak period in summer (Sutherland *et al.*, 2016), revealed unique spatiotemporal dynamics in microbial communities at the front (or margins) of lesions ≤ 24 h old, as well as blooming of potential pathobionts and a reduction of beneficial taxa.

Spatiotemporal dynamics in diversity. Alpha diversity metrics of evenness (Shannon Entropy) and phylogenetic diversity (PD) were significantly lower in samples taken from lesion fronts (W*PX*) at ≤ 24 h compared to apparently healthy coral colonies (*H*) (Fig 4.4, $P < 0.001$ and $P = 0.003$, respectively). Phylogenetic diversity is believed to represent trait diversity (Vellend *et al.*, 2011), and this reduction in PD may represent the loss of ecological functions from microbial communities in *WPX* ≤ 24 h old. Higher beta diversity was detected in *WPX* ≤ 24 h samples compared to *H* samples (Fig 4.3, $P = 0.006$, 1,000 Monte Carlo permutations). This suggests destabilization of the coral microbiome, manifested as increased sample-to-sample variation, when lesions are ≤ 24 h old. Traditionally, sample-to-sample variation has been thought to arise from high rates

of species turnover, or species replacement (Whittaker, 1972). In this sense, each sample of a diseased community may represent a different point along the trajectory of change towards the diseased state. Alternatively, sample-to-sample variation may arise when the microbiome of each individual shifts from the healthy to the disease state in a different manner as seen in inflammatory bowl disease (Halfvarson *et al.*, 2017). Thus, the microbiome of the diseased state may manifest as alternative stable states among individuals, each individual microbiome changing in its own way (Costello *et al.*, 2012).

Blooming of *Vibrio* bacteria. We documented a dramatic bloom of *Vibrio* bacteria in new WPX lesions, which increased from < 1% in all other samples to ~33% in *WPX* ≤ 24 h samples (Table 4.2, Figure 4.5). Many *Vibrio* species are pathogenic to humans and a variety of marine organisms (Gomez-Gil *et al.*, 2014). Vibrios have received a great deal of attention in coral disease for their role in pathogenesis in white syndromes (Ushijima *et al.*, 2014; 2012; Sussman *et al.*, 2008), white band disease (Ritchie and Smith, 1998; Gil-Agudelo *et al.*, 2006), *Porites* white patch and white spot diseases (Arboleda and Reichardt, 2010; Zhenyu *et al.*, 2013), and Caribbean yellow band disease (Cervino *et al.*, 2008). However, *Vibrio* spp. are also found in low abundance in apparently healthy coral hosts (Alves *et al.*, 2010; Pollock *et al.*, 2016; Rubio-Portillo *et al.*, 2014). Several coral-associated *Vibrio* are capable of fixing N_2, and may function as coral mutualists during non-stressful conditions (Chimetto *et al.*, 2008; Benavides *et al.*, 2017). Our data suggest that *Vibrio* may be considered conditionally rare taxa (CRT) (Shade *et al.*, 2014) in the *A. palmata* coral microbiome, and are capable of blooming under certain environmental conditions or when hosts are

immunosuppressed. Thus, *Vibrio* spp. may shift along the symbiotic spectrum from functioning as commensals or mutualists to functioning as potential pathobionts.

Blooming of CRT that have pathogenic potential (*i.e*., pathobionts) has been proposed as an important mechanism for the evolution of virulence in host-microbiome systems (Stecher *et al.*, 2013). Blooming may promote horizontal gene transfer (HGT) of fitness factors, virulence factors, and antibiotic resistance among members of the microbiome. *Vibrio*, in particular, have a very high flux of mobile genes owing to multiple plasmids, bacteriophages, and their super integron region comprised of mobile gene cassettes. Moreover, there is evidence that rates of HGT may be higher in *Vibrio* found in coral mucus compared to free-living vibrios (Koenig *et al.*, 2011). Thus, ephemeral *Vibrio* blooms may promote the spread of virulence and fitness factors, affecting the overall functioning of the microbiome even after the bloom has subsided.

At least one *Vibrio*, *V. coryalliilyticus*, has been shown to suppress coral innate immune pathways (Vidal-Dupiol *et al.*, 2014). Thus, *V. coryalliilyticus*, may prove to be a keystone coral pathogen (Hajishengallis *et al.*, 2012), capable of remodeling normally benign microbiota into a dysbiotic role by interrupting normal coral immune function. In the mouse model of periodontitis, the keystone pathogen *Porphyromonas gingivalis* initiates an uncontrolled inflammatory response and impairs leukocyte killing cells, resulting in overgrowth of commensals (Hajishengallis *et al.*, 2012). A key point is that no one microorganism (including *P. gingivalis*) is sufficient alone to cause disease in this system. It is likely that similar mechanisms, involving polymicrobial synergy (Lamont and Hajishengallis, 2015), give rise to disease and dysbiosis in corals. However, it is unclear whether *Vibrio* blooming documented in this study was cause or consequence of

microbiome disruption. Experimental studies are needed to further examine the interaction between *Vibrio* spp. and other potential coral pathogens, the host immune system, and coral microbiome.

Reduction of presumed beneficial taxa. The loss of beneficial taxa and keystone stabilizers has been suggested as one important mechanism leading to microbial dysbiosis (Kamada *et al.*, 2013). The term beneficial microorganisms for corals (BMCs) has been proposed to define (specific) symbionts that promote coral health (Peixoto *et al.*, 2017). One BMC that has received a great deal of attention is the endosymbiont *Endozoicimonaceae*, which has consistently been detected in multiple coral species in multiple geographic regions (Neave *et al.*, 2016; Ding and Schloss, 2014). *Endozoicomonas* strains produce antimicrobial compounds that have the potential to regulate the commensal community (Ritchie, 2006). The relative abundance of this group has been shown to decrease in disease corals (Meyer *et al.*, 2014; Vezzulli *et al.*, 2013) and heat-stressed corals (Ziegler *et al.*, 2017). Likewise, we found that the relative abundance of *Endozoicimonaceae* was significantly reduced in *WPX* ≤ 24 h samples compared to *H* samples (Figure 4.6a).

Predatory bacteria have been suggested to play a significant role in controlling pathogenic bacterial populations in coral and plant microbiome systems, and in doing so may act as keystone stabilizers (Sweet and Bulling, 2017; Welsh and Thurber, 2016). There was a significant reduction in the relative abundance of the deltaproteobacteria orders *Myxococcales* and *Bdellovibrionales* in *WPX* ≤ 24 h samples compared to *H* samples (Figure 4.6a). These taxa represent the best-characterized facultative and obligate predatory bacteria, respectively (Jurkevitch, 2007) and are capable of exerting

significant top-down control even when they account for just 1–10% of the total microbiome community (Welsh *et al.*, 2015). Deltaproteobacteria *Bdellovibrio* and like organisms (BALOs) in particular are obligate predators of Gram-negative bacteria (Jurkevitch, 2007). Predatory bacteria isolated from coral microbiomes have been shown to attack and consume the coral pathogens *V. coralliilyticus* and *V. harveyi* (Welsh *et al.*, 2015). Thus a loss of the keystone stabilizers from the coral microbiome may promote the condition for *Vibrio* bloom formations.

Evidence for resilience to WPX. Increased microbiome variability during stress is thought to reflect decreased ability of the host and/or the commensal microbiota to regulate microbial community composition (Kamada *et al.*, 2013; Halfvarson *et al.*, 2017). It is presently unclear what is driving destabilization in new WPX lesions (though *Vibrio* may be involved); however, this disruption appears to be ephemeral as beta diversity is no higher in aging *WPX* samples compared to *H* samples (Fig 4.2). Moreover, as lesions age they form a cluster with healthy samples in ordination space that is discrete from *WPX* ≤ 24 h old (Figure 4.2). This suggests either the coral host and/or the commensal microbiota are resilient to the biotic or abiotic stress causing WPX, and that the microbiome may return to the original "healthy" state within days of lesion formation. As further evidence, WPX lesions healed rapidly in this study, decreasing in size by ~29% after just 8–13 d (Figure 4.1). A recent study by Sutherland and colleagues (2015) found that lesion size, disease severity, and whole colony mortality were greater in historical WPX outbreaks (1994–2004) compared to contemporary WPX outbreaks (2008–2014). Taken together, with results of the present study, this suggests that although *A. palmata* in the Florida Keys develop WPX signs, they may now be resilient

to tissue-loss progression due to WPX. Alternatively, additional factors such as history of thermal stress (Precht *et al.*, 2016), may affect the susceptibility of *A. palmata* to WPX.

We observed that WPX occurs in cyclic outbreaks during middle to late summer months; however, we were only able to sample during a single outbreak event at the beginning of the disease season. Disease dynamics may change after multiple rounds of new WPX lesion formation. A ratcheting-down affect may occur in which coral health an immunity are reduced with each WPX outbreak round, while the microbiome becomes less resilient to opportunistic blooms of potentially pathogenic bacteria (*via* mechanisms like horizontal gene transfer (HGT) of virulence genes and/or the loss of keystone stabilizers). Alternatively, the coral host and its microbiome may be robust to repeated disease outbreaks, even gaining resistance with exposure. Further field and manipulative studies are needed to examine these scenarios.

Benefits of longitudinal studies. Longitudinal studies are expensive, logistically difficult to implement and have been sparse in host-microbiome disease studies both in coral and human hosts (Halfvarson *et al.*, 2017). However, we argue that longitudinal studies have the potential yield a greater understanding of the disease process in corals. Many of the dynamics that we documented— including reduced alpha diversity, increased beta diversity, and *Vibrio* bloom formation— would have been missed without a highly resolved temporal sampling scheme. The temporal scale of disease dynamics is likely to differ between disease types and coral hosts, and it will be necessary to determine and apply the appropriate sampling resolution for each situation. The combination of appropriately scaled longitudinal studies and examination of biotic and

abiotic thresholds that may serve as tipping points for disruption of microbiome and coral immune homeostasis will advance coral disease research.

Acknowledgements

This work was supported by the NSF grant EF1015342 (to E.K.L and J.W.P) as part of the joint NSF-NIH Ecology of Infectious Disease program and travel grant from the Association of Marine Laboratories of the Caribbean (to K.M.K). We would like to acknowledge Erich Bartels, Mark Knowels, and the entire staff at the Mote Tropical Research Lab on Summerland Key for their logistical support. Finally, this work would not have been possible without the generous support of Looe Key Reef Resort & Dive Center in Ramrod Key, Florida and captain Ronald Stein. Coral mucus and seawater samples were obtained under permit FKNMS-2010-131-A.

References

Aeby GS, Williams GJ, Franklin EC, Kenyon J, Cox EF, Coles S, *et al.* (2011). Patterns of coral disease across the Hawaiian archipelago: relating disease to environment. *PLoS One* **6**: e20370.

Ainsworth TD, Thurber R, Gates R. (2010). The future of coral reefs: a microbial perspective. *Trends Ecol Evol* **25**: 233–240.

Alvarez-Filip L, Dulvy NK, Gill JA, Cote IM, Watkinson AR. (2009). Flattening of Caribbean coral reefs: region-wide declines in architectural complexity. *Proc R Soc B Biol Sci* **276**: 3019–3025.

Alves N, Neto OSM, Silva BSO, De Moura RL, Francini-Filho RB, Barreira e Castro C, *et al.* (2010). Diversity and pathogenic potential of vibrios isolated from Abrolhos Bank corals. *Environ Microbiol Rep* **2**: 90–95.

Arboleda M, Reichardt WT. (2010). *Vibrio* sp. causing *Porites* ulcerative white spot disease. *Dis Aquat Org* **90**: 93–104.

Benavides M, Bednarz VN, Ferrier-Pagès C. (2017). Diazotrophs: overlooked key players within the coral symbiosis and tropical reef ecosystems? *Front Mar Sci* **4**: 2261–17.

Boström KH, Simu K, Hagström Å, Riemann L. (2004). Optimization of DNA extraction for quantitative marine bacterioplankton community analysis. *Limnol Oceanogr Methods* **2**: 365–373.

Bourne D, Iida Y, Uthicke S, Smith-Keune C. (2007). Changes in coral-associated microbial communities during a bleaching event. *ISME J* **2**: 350–363.

Bourne DG, Morrow KM, Webster NS. (2016). Insights into the coral microbiome: underpinning the health and resilience of reef ecosystems. *Annu Rev Microbiol* **70**: 317–340.

Bourne DG, Munn CB. (2005). Diversity of bacteria associated with the coral *Pocillopora damicornis* from the Great Barrier Reef. *Environ Microbiol* **7**: 1162–1174.

Bushman FD, Fierer N, Goodrich JK, Kelley ST, Koenig JE, Ley RE, *et al.* (2010). QIIME allows analysis of high-throughput community sequencing data. *Nat Meth* **7**: 335–336.

Byrd AL, Segre JA. (2016). Adapting Koch's postulates. *Science* **351**: 224–226.

Caporaso JG, Bittinger K, Bushman FD, DeSantis TZ, Andersen GL, Knight R. (2010). PyNAST: a flexible tool for aligning sequences to a template alignment. *Bioinformatics* **26**: 266–267.

Caporaso JG, Lauber CL, Walters WA. (2011). Global patterns of 16S rRNA diversity at a depth of millions of sequences per sample. *Proc Natl Acad Sci* **108**: 4516–4522.

Cárdenas A, Rodriguez-R LM, Pizarro V, Cadavid LF, Arévalo-Ferro C. (2011). Shifts in bacterial communities of two caribbean reef-building coral species affected by white plague disease. *ISME J* **6**: 502–512.

Cervino JM, Thompson FL, Gomez-Gil B, Lorence EA, Goreau TJ, Hayes RL, *et al.* (2008). The *Vibrio* core group induces yellow band disease in Caribbean and Indo-Pacific reef-building corals. *J Appl Microbiol* **105**: 1658–1671.

Chimetto LA, Brocchi M, Thompson CC, Martins RCR, Ramos HR, Thompson FL. (2008). Vibrios dominate as culturable nitrogen-fixing bacteria of the Brazilian coral *Mussismilia hispida*. *Syst Appl Microbiol* **31**: 312–319.

Chow J, Tang H, Mazmanian SK. (2011). Pathobionts of the gastrointestinal microbiota and inflammatory disease. *Curr Opin Immunol* **23**: 473–480.

Costello EK, Stagaman K, Dethlefsen L, Bohannan BJM, Relman DA. (2012). The application of ecological theory toward an understanding of the human microbiome. *Science* **336**: 1255–1262.

Ding T, Schloss PD. (2014). Dynamics and associations of microbial community types across the human body. *Nature* **509**: 357–360.

Eakin CM, Lough JM, Heron SF. (2009). Climate variability and change: monitoring data and evidence for increased coral bleaching stress. In: Van Oppen MJH, Lough JM (eds) Ecological Studies Vol. 205. *Coral Bleaching*. Springer Berlin Heidelberg: Berlin, Heidelberg, pp 41–67.

Edgar RC. (2010). Search and clustering orders of magnitude faster than BLAST. *Bioinformatics* **26**: 2460–2461.

Edgar RC, Flyvbjerg H. (2015). Error filtering, pair assembly and error correction for next-generation sequencing reads. *Bioinformatics* **31**: 3476–3482.

Egan S, Gardiner M. (2016). Microbial Dysbiosis: Rethinking Disease in Marine Ecosystems. *Front Microbiol* **7**: 842–8.

Gil-Agudelo DL, Smith GW, Weil E. (2006). The white band disease type II pathogen in Puerto Rico. *Rev Biol Trop* **54**: 59–67.

Glas MS, Sato Y, Ulstrup KE, Bourne DG. (2012). Biogeochemical conditions determine virulence of black band disease in corals. *ISME J* **6**: 1526–1534.

Gomez-Gil B, Thompson CC, Matsumura Y, Sawabe T, Iida T, Christen R, *et al.* (2014). The Famlily *Vibrionaceae*. In: Rosenberg E, Delong EF, Lory S, Stackebrandt E, Thompson F (eds) Gammaproteobacteria. *The Prokaryotes*. Springer Berlin Heidelberg: Berlin, Heidelberg, pp 659–747.

Hajishengallis G, Darveau RP, Curtis MA. (2012). The keystone-pathogen hypothesis. *Nat Rev Micro* **10**: 717–725.

Halfvarson J, Brislawn CJ, Lamendella R, Vázquez-Baeza Y, Walters WA, Bramer LM, *et al.* (2017). Dynamics of the human gut microbiome in inflammatory bowel disease. *Nat Microbiol* **2**: 1–7.

Hamady M, Walker JJ, Harris JK, Gold NJ, Knight R. (2008). Error-correcting barcoded primers for pyrosequencing hundreds of samples in multiplex. *Nat Meth* **5**: 235–237.

Hooper LV, Littman DR, Macpherson AJ. (2012). Interactions between the microbiota and the immune system. *Science* **336**: 1268–1273.

Joyner J, Wanless D, Sinigalliano CD, Lipp EK. (2014). Use of quantitative real-time PCR for direct detection of *Serratia marcescens* in marine and other aquatic environments. *Appl Environ Microbiol* **80**: 1679–1683.

Joyner JL, Sutherland KP, Kemp D, Berry B, Griffin A, Porter J, *et al.* (2015). Systematic analysis of white pox disease in *Acropora palmata* of the Florida Keys and the role of *Serratia marcescens*. *Appl Environ Microbiol* AEM.00116–15.

Jurkevitch E. (2007). Predatory behaviors in bacteria-diversity and transitions. *Microbe* **2**: 67–73.

Kamada N, Chen GY, Inohara N, Núñez G. (2013). Control of pathogens and pathobionts by the gut microbiota. *Nat Immunol* **14**: 685–690.

Kemp DW, Rivers AR, Kemp KM, Lipp EK, Porter JW, Wares JP. (2015). Spatial homogeneity of bacterial communities associated with the surface mucus layer of the reef-building coral *Acropora palmata*. *PLoS One* **10**: e0143790.

Koenig JE, Bourne DG, Curtis B, Dlutek M, Stokes HW, Doolittle WF, *et al.* (2011). Coral-mucus-associated Vibrio integrons in the Great Barrier Reef: genomic hotspots for environmental adaptation. *ISME J* **5**: 962–972.

Lamont RJ, Hajishengallis G. (2015). Polymicrobial synergy and dysbiosis in inflammatory disease. *Trends Mol Med* **21**: 172–183.

Lee STM, Davy SK, Tang S-L, Kench PS. (2017). Water flow buffers shifts in bacterial community structure in heat-stressed *Acropora muricata*. *Sci Rep* **7**: 43600.

Lesser MP, Jarett JK. (2014). Culture-dependent and culture-independent analyses reveal no prokaryotic community shifts or recovery of *Serratia marcescens* in *Acropora palmata* with white pox disease. *FEMS Microbiol Ecol* **88**: 457–467.

Lirman D. (2000). Lesion regeneration in the branching coral *Acropora palmata*: effects of colonization, colony size, lesion size, and lesion shape. *Mar Ecol Prog Ser* **197**: 209–215.

Lozupone C, Knight R. (2005). UniFrac: a new phylogenetic method for comparing microbial communities. *Appl Environ Microbiol* **71**: 8228–8235.

Machado D, Castro J, Palmeira-de-Oliveira A, Martinez-de-Oliveira J, Cerca N. (2016). Bacterial vaginosis biofilms: challenges to current therapies and emerging Solutions. *Front Microbiol* **6**: 683640–13.

Maynard J, van Hooidonk R, Eakin CM, Puotinen M, Garren M, Williams G, *et al.* (2015). Projections of climate conditions that increase coral disease susceptibility and pathogen abundance and virulence. *Nat Clim Chang* **5**: 688–694.

McDonald D, Price MN, Goodrich J, Nawrocki EP, DeSantis TZ, Probst A, *et al.* (2011). An improved Greengenes taxonomy with explicit ranks for ecological and evolutionary analyses of bacteria and archaea. *ISME J* **6**: 610–618.

Meyer JL, Paul VJ, Teplitski M. (2014). Community shifts in the surface microbiomes of the coral *Porites astreoides* with unusual lesions. *PLoS One* **9**: e100316–9.

Muller EM, van Woesik R. (2012). Caribbean coral diseases: primary transmission or secondary infection? *Global Change Biol* **18**: 3529–3535.

Muller EM, van Woesik R. (2014). Genetic susceptibility, colony size, and water temperature drive white-pox disease on the coral *Acropora palmata*. *PLoS One* **9**: e110759–5.

Neave MJ, Rachmawati R, Xun L, Michell CT, Bourne DG, Apprill A, *et al.* (2016). Differential specificity between closely related corals and abundant *Endozoicomonas* endosymbionts across global scales. *ISME J* **11**: 186–200.

Nelson A, De Soyza A, Perry JD, Sutcliffe IC, Cummings SP. (2012). Polymicrobial challenges to Koch's postulates: ecological lessons from the bacterial vaginosis and cystic fibrosis microbiomes. *Innate Immun* **18**: 774–783.

Oksanen J, Blanchet FG, Friendly M, Kindt R, Legendre P, McGlinn D, *et al.* (2017). vegan: Community Ecology Package. R package version 2.4-2. https://CRAN.R-project.org/package=vegan.

Patterson KL, Porter JW, Ritchie KB, Polson SW, Mueller E, Peters EC, *et al.* (2002). The etiology of white pox, a lethal disease of the Caribbean elkhorn coral, *Acropora palmata*. *Proc Natl Acad Sci* **99**: 8725–8730.

Peixoto RS, Rosado PM, Leite DC de A, Rosado AS, Bourne DG. (2017). Beneficial microorganisms for corals (bmc): proposed mechanisms for coral health and resilience. *Front Microbiol* **8**: 100–16.

Petersen C, Round JL. (2014). Defining dysbiosis and its influence on host immunity and disease. *Cell Microbiol* **16**: 1024–1033.

Pollock FJ, Wada N, Torda G, Willis BL, Bourne DG. (2016). White syndrome-affected corals have a distinct microbiome at disease lesion fronts. *Appl Environ Microbiol* **83**: e02799–16–16–15.

Precht WF, Gintert BE, Robbart ML, Fura R, van Woesik R. (2016). Unprecedented disease-related coral mortality in Southeastern Florida. *Sci Rep* **6**: 31374–38.

Price MN, Dehal PS, Arkin AP. (2009). FastTree: computing large minimum evolution trees with profiles instead of a distance matrix. *Mol Biol Evol* **26**: 1641–1650.

Ritchie KB. (2006). Regulation of microbial populations by coral surface mucus and mucus-associated bacteria. *Mar Ecol Prog Ser* **322**: 1–14.

Ritchie KB, Smith GW. (1998). Type II white-band disease. *Rev Biol Trop* **46**: 199–203.

Roder C, Arif C, Bayer T, Aranda M, Daniels C, Shibl A, *et al.* (2014). Bacterial profiling of White Plague Disease in a comparative coral species framework. *ISME J* **8**: 31–39.

Rohwer F, Seguritan V, Azam F, Knowlton N. (2002). Diversity and distribution of coral-associated bacteria. *Mar Ecol Prog Ser* **243**: 1–10.

Round JL, Mazmanian SK. (2009). The gut microbiota shapes intestinal immune responses during health and disease. *Nat Rev Immunol* **9**: 313–323.

Rubio-Portillo E, Yarza P, alver CPN, aacute AAR-E, n JAO. (2014). New insights into *Oculina patagonica* coral diseases and their associated *Vibrio* spp. communities. *ISME J* **8**: 1794–1807.

Sato Y, Ling EYS, Turaev D, Laffy P, Weynberg KD, Rattei T, *et al.* (2017). Unraveling the microbial processes of black band disease in corals through integrated genomics. *Sci Rep* **7**: 40455–54.

Schneider CA, Rasband WS, Eliceiri KW. (2012). NIH Image to ImageJ: 25 years of image analysis. *Nat Meth* **9**: 671–675.

Segata N, Izard J, Waldron L, Gevers D, Miropolsky L, Garrett WS, *et al.* (2011). Metagenomic biomarker discovery and explanation. *Genome Biol* **12**: R60.

Séré MG, Tortosa P, Chabanet P, Quod J-P, Sweet MJ, Schleyer MH. (2015). Identification of a bacterial pathogen associated with *Porites* white patch syndrome in the Western Indian Ocean. *Mol Ecol* **24**: 4570–4581.

Shade A, Jones SE, Caporaso JG, Handelsman J, Knight R, Fierer N, *et al.* (2014). Conditionally rare taxa disproportionately contribute to temporal changes in microbial diversity. *mBio* **5**: e01371–14–e01371–14.

Sibley CD, Parkins MD, Rabin HR, Duan K, Norgaard JC, Surette MG. (2008). A polymicrobial perspective of pulmonary infections exposes an enigmatic pathogen in cystic fibrosis patients. *Proc Natl Acad Sci* **105**: 15070–15075.

Stecher B, Maier L, Hardt W-D. (2013). 'Blooming' in the gut: how dysbiosis might contribute to pathogen evolution. *Nat Rev Micro* **11**: 277–284.

Sunagawa S, DeSantis TZ, Piceno YM, Brodie EL, DeSalvo MK, Voolstra CR, *et al.* (2009). Bacterial diversity and White Plague Disease-associated community changes in the Caribbean coral Montastraea faveolata. *ISME J* **3**: 512–521.

Sussman M, Willis BL, Victor S, Bourne DG. (2008). Coral pathogens identified for White Syndrome (WS) epizootics in the Indo-Pacific. *PLoS One* **3**: e2393–14.

Sutherland KP, Berry B, Park A, Kemp DW, Kemp KM, Lipp EK, *et al.* (2016). Shifting white pox aetiologies affecting *Acropora palmata* in the Florida Keys, 1994-2014. *Philos Trans R Soc Lond B Biol Sci* **371**: 20150205.

Sweet M, Bythell J. (2015). White syndrome in *Acropora muricata*: nonspecific bacterial infection and ciliate histophagy. *Mol Ecol* **24**: 1150–1159.

Sweet MJ, Bulling MT. (2017). On the importance of the microbiome and pathobiome in coral health and disease. *Front Mar Sci* **4**: 2261–11.

Sweet MJ, Croquer A, Bythell JC. (2010). Bacterial assemblages differ between compartments within the coral holobiont. *Coral Reefs* **30**: 39–52.

Thurber RV, Willner-Hall D, Rodriguez-Mueller B, Desnues C, Edwards RA, Angly F, *et al.* (2009). Metagenomic analysis of stressed coral holobionts. *Environ Microbiol* **11**: 2148–2163.

Tinker KA, Ottesen EA. (2016). The core gut microbiome of the american cockroach, *Periplaneta americana*, is stable and resilient to dietary shifts. *Appl Environ Microbiol* **82**: 6603–6610.

Tout J, Siboni N, Messer LF, Garren M, Stocker R, Webster NS, *et al.* (2015). Increased seawater temperature increases the abundance and alters the structure of natural *Vibrio* populations associated with the coral *Pocillopora damicornis*. *Front Microbiol* **6**: 403–12.

Ushijima B, Smith A, Aeby GS, Callahan SM. (2012). *Vibrio owensii* Induces the tissue loss disease *Montipora* white syndrome in the Hawaiian reef coral *Montipora capitata*. *PLoS One* **7**: e46717–10.

Ushijima B, Videau P, Burger AH, Shore-Maggio A, Runyon CM, Sudek M, *et al.* (2014). *Vibrio coralliilyticus* strain ocn008 is an etiological agent of acute *Montipora* white syndrome. *Appl Environ Microbiol* **80**: 2102–2109.

van Woesik R. (1998). Lesion healing on massive *Porites* spp. corals. *Mar Ecol Prog Ser* **164**: 213–220.

Vayssier-Taussat M. (2014). Shifting the paradigm from pathogens to pathobiome: new concepts in the light of meta-omics. *Front Cell Infect Microbiol* **4**: 1–7.

Vellend M, Cornwell WK, Magnuson-Ford K, Mooers A. (2011). Measuring phylogenetic biodiversity. In: *Biological diversity frontiers in measurement and assessment.* Oxford, pp 194–207.

Vezzulli L, Pezzati E, Huete-Stauffer C, Pruzzo C, Cerrano C. (2013). 16s rDNA pyrosequencing of the mediterranean gorgonian *Paramuricea clavata* reveals a link among alterations in bacterial holobiont members, anthropogenic influence and disease outbreaks. *PLoS One* **8**: e67745–10.

Vidal-Dupiol J, Dheilly NM, Rondon R, Grunau C, Cosseau C, Smith KM, *et al.* (2014). Thermal stress triggers broad *Pocillopora damicornis* transcriptomic remodeling, while *Vibrio coralliilyticus* infection induces a more targeted immuno-suppression response. *PLoS One* **9**: e107672.

Wang Q, Garrity GM, Tiedje JM, Cole JR. (2007). Naïve Bayesian classifier for rapid assignment of rRNA sequences into the new bacterial taxonomy. *Appl Environ Microbiol* **73**: 5261–5267.

Weil E, Rogers CS. (2010). Coral Reef Diseases in the Atlantic-Caribbean. In: Coral Reefs: An Ecosystem in Transition. *Coral Reefs: An Ecosystem in Transition*. Springer Netherlands: Dordrecht, pp 465–491.

Welsh RM, Thurber RV. (2016). Bacterial predators in host microbiomes. *Microbe Magazine* **11**: 61–67.

Welsh RM, Zaneveld JR, Rosales SM, Payet JP, Burkepile DE, Thurber RV. (2015). Bacterial predation in a marine host-associated microbiome. *ISME J* **10**: 1–5.

Whittaker RH. (1972). Evolution and measurement of species diversity. *Taxon* **21**: 213–251.

Williams DE, Miller MW. (2011). Attributing mortality among drivers of population decline in *Acropora palmata* in the Florida Keys (USA). *Coral Reefs* **31**: 369–382.

Zaneveld JR, Shantz AA, Pritchard CE, McMinds R, Payet JP, Welsh R, *et al.* (2016). Overfishing and nutrient pollution interact with temperature to disrupt coral reefs down to microbial scales. *Nat Commun* **7**: 1–12.

Zhenyu X, Shaowen K, Chaoqun H, Zhixiong Z, Shifeng W, Yongcan Z. (2013). First characterization of bacterial pathogen, *Vibrio alginolyticus*, for *Porites andrewsi* white syndrome in the South China Sea. *PLoS One* **8**: e75425–8.

Ziegler M, Seneca FO, Yum LK, Palumbi SR, Voolstra CR. (2017). Bacterial community dynamics are linked to patterns of coral heat tolerance. *Nat Commun* **8**: 14213.

Tables

Table 4.1. Date, health status, and lesion age of samples collected from *A. palmata* at Looe Key.

	Date											
Colony	6/25*	6/27	7/3*	7/7	7/12*	7/13*	7/14	7/19	7/20	7/22*	7/24*	7/29
LK-Apl-21	—	H	H	—	—	H	—	—	—	—	—	—
LK-Apl-24	—	—	—	—	—	—	D ≤ 24 h	—	—	—	—	—
LK-Apl-29	—	H	—	—	—	—	—	—	—	—	—	—
LK-Apl-30	—	—	—	—	—	—	D ≤ 24 h	—	D 3–5 d	—	—	—
LK-Apl-62	—	—	H	H	H	—	D ≤ 24 h	D 3–5 d	D 3–5 d	—	—	—
LK-Apl-64	—	—	—	H	H	—	—	—	—	—	—	—
LK-Apl-65	—	—	—	—	—	D ≤ 24 h	—	D 3–5 d	—	—	—	—
LK-Apl-66	—	H	—	—	H	D ≤ 24 h	—	D 3–5 d	—	—	—	D 8–10 d
LK-Apl-68	—	—	—	—	—	D ≤ 24 h	—	D 3–5 d	—	—	—	D 8–10 d
LK-Apl-71	—	—	—	—	—	D ≤ 24 h	—	D 3–5 d	—	—	—	D 8–10 d
LK-Apl-72	—	H	H	H	H	—	—	—	—	—	—	—
LK-Apl-73	—	H	—	—	H	—	D ≤ 24 h	—	—	—	—	D 8–10 d

* Indicates a disease survey was conducted; *H*, apparently healthy colonies; *D*, colonies displaying active white pox lesions; —, no sample collected

Table 4.2. Relative abundance of the genus *Vibrio*.

Sample	Relative abundance (%)	SEM	*n*
H	0.29	0.06	14
≤ 24 h			
WPX	33.49	8.12	6
DH_2	0.32	0.12	7
DH_{10}	1.09	0.98	5
3–5 d			
WPX	0.21	0.04	6
DH_2	0.19	0.05	6
DH_{10}	0.16	0.02	6
8–10 d			
WPX	0.82	0.60	4
DH_2	0.08	0.04	4
DH_{10}	0.15	0.10	4

Abbreviations: *H*, mucus from apparently healthy *Acropora palmata* colonies with no white pox disease (WPX) signs; *WPX*, mucus from the active margin of disease lesions; DH_2, mucus from apparently healthy regions two cm from an active WPX lesion; DH_{10}, mucus from apparently healthy regions ten cm from an active WPX lesion.

Figures

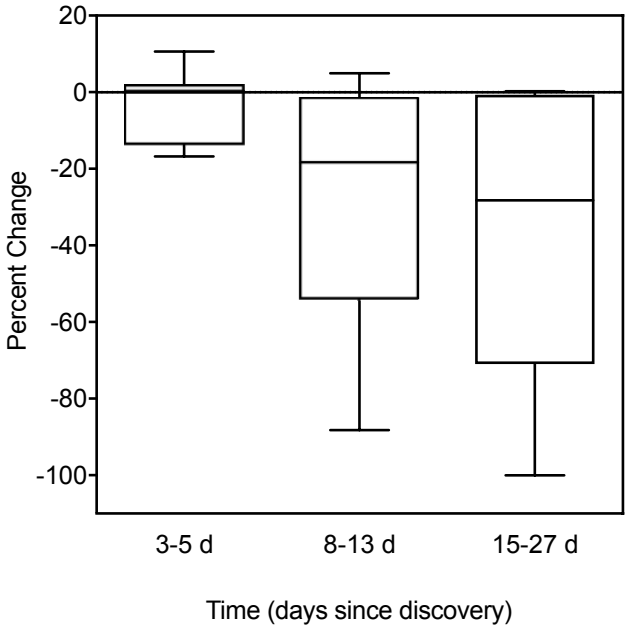

Figure 4.1. Percent size change of white pox lesions (n = 18) since day of discovery.

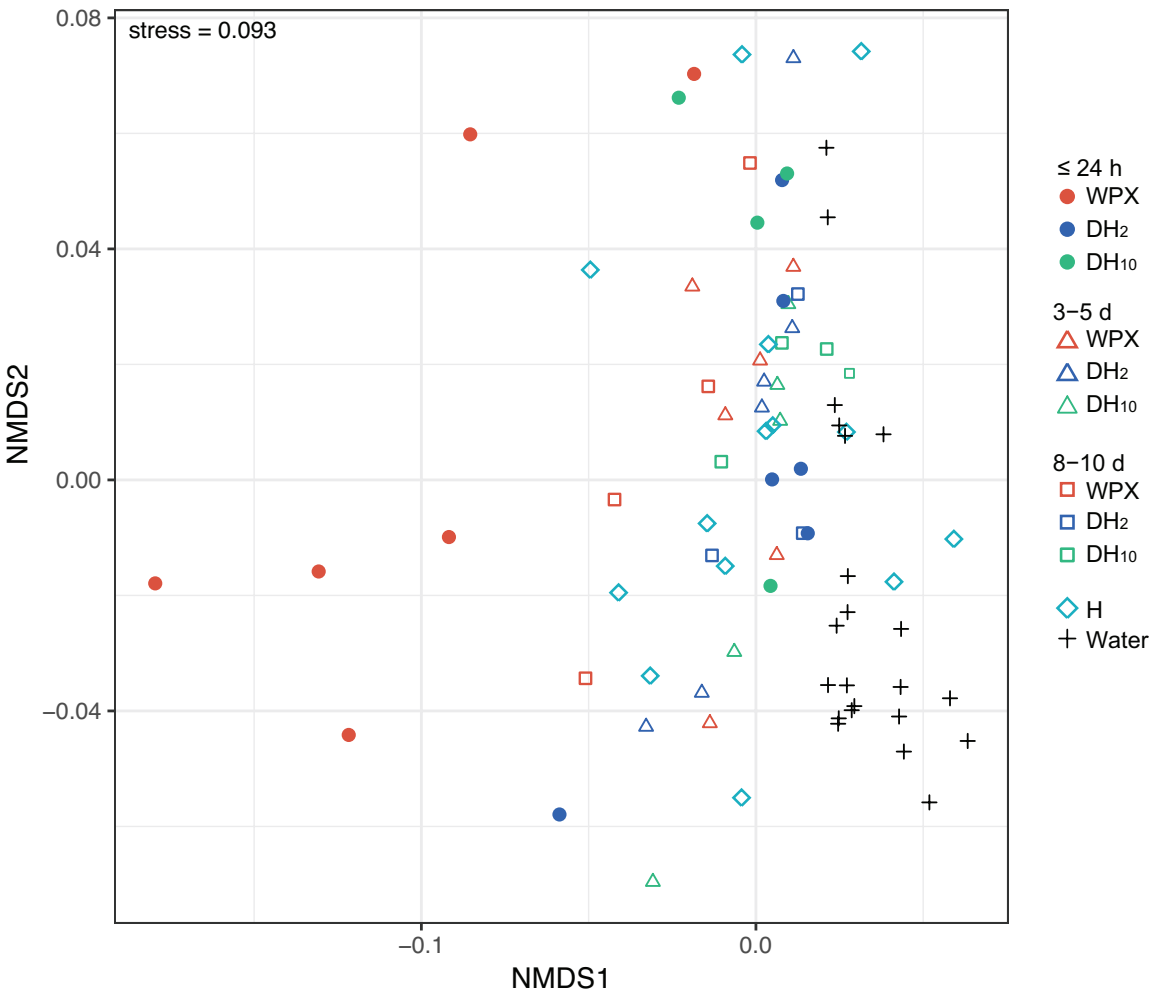

Figure 4.2. Non-metric multi-dimensional scaling (NMDS) plot summarizing weighted UniFrac distances. Proximity of samples on the NMDS plot illustrates similarity of bacterial communities. Abbreviations: *H*, mucus from apparently healthy *Acropora palmata* colonies with no white pox disease (WPX) signs; *WPX*, mucus from the active margin of disease lesions; DH_2, mucus from apparently healthy regions two cm from an active WPX lesion; DH_{10}, mucus from apparently healthy regions ten cm from an active WPX lesion; *Water*, seawater 1 m above *A. palmata* colonies.

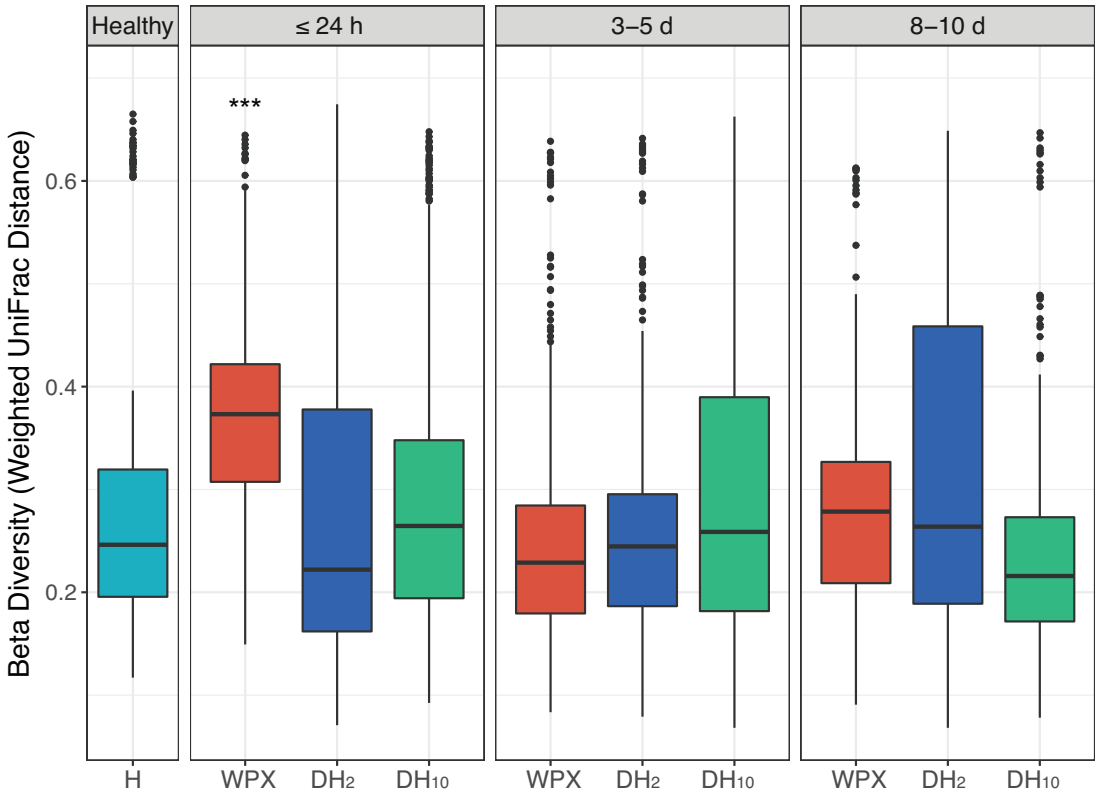

Figure 4.3. Beta diversity (sample-to-sample) variation, based on weighted UniFrac distances, for samples taken from apparently healthy *Acropora palmata* colonies (*H*), the active margin of white pox disease lesions (*WPX*), and apparently healthy regions two and 10 cm from an active lesion (DH_2 and DH_{10}). Boxes represent the mean, first and 3 quartiles and whiskers represent 1.5 * the inter-quartile range (IQR) and outliers plotted as points. *P*-values significant differences from healthy samples based on non-parametric *t*-tests with 1000 replications (***$P < 0.001$).

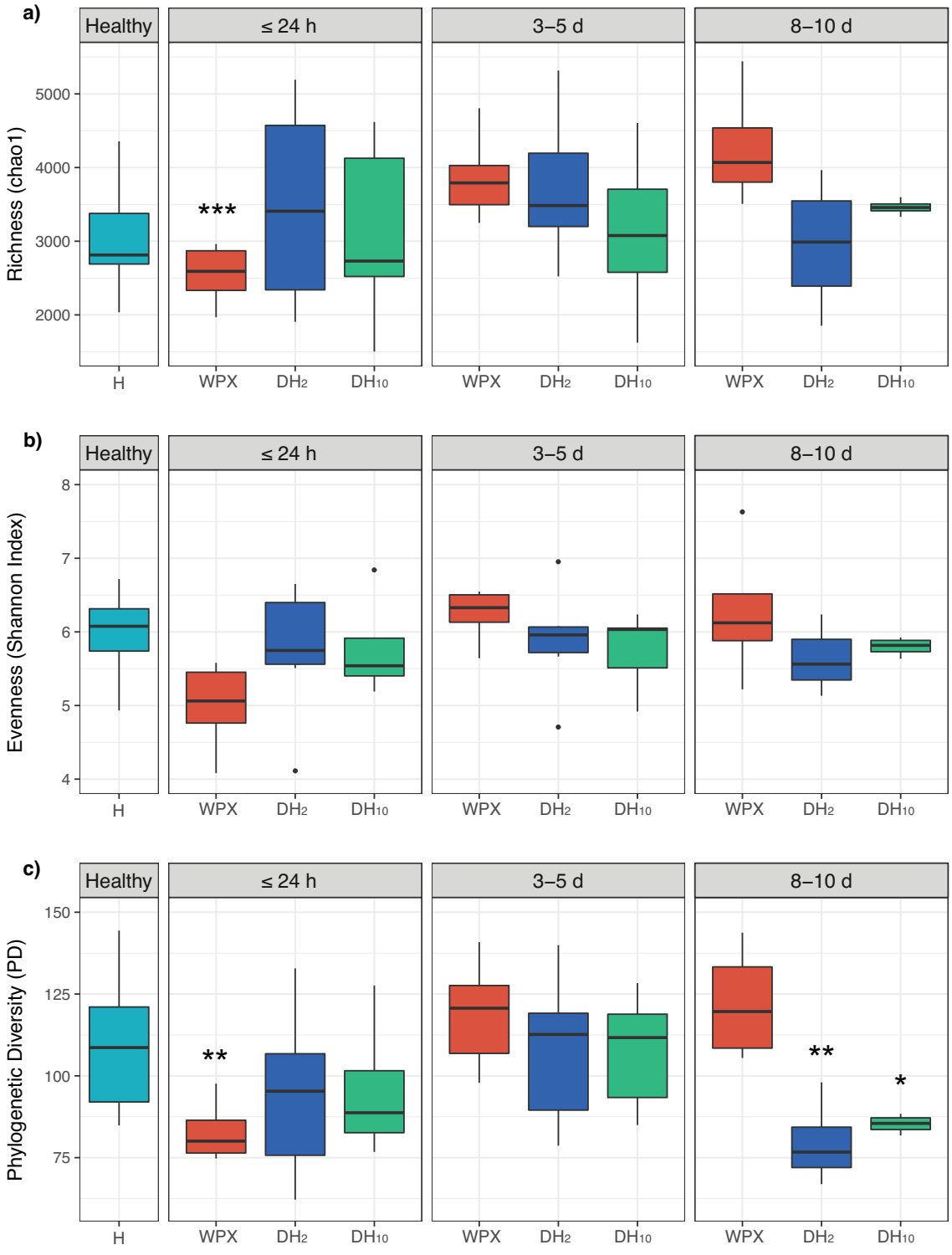

Figure 4.4. Alpha diversity metrics for samples taken from apparently healthy *Acropora palmata* colonies (*H*), the active margin of white pox disease lesions (*WPX*), and apparently healthy regions two and 10 cm from an active lesion (DH_2 and DH_{10}). Boxes

represent the mean, first and 3 quartiles and whiskers represent 1.5 * the inter-quartile range (IQR) with outliers plotted as points. Asterisks denote a significant difference compared to healthy samples based on *t*-tests (*, $P < 0.05$; **, $P < 0.01$; ***$P < 0.001$).

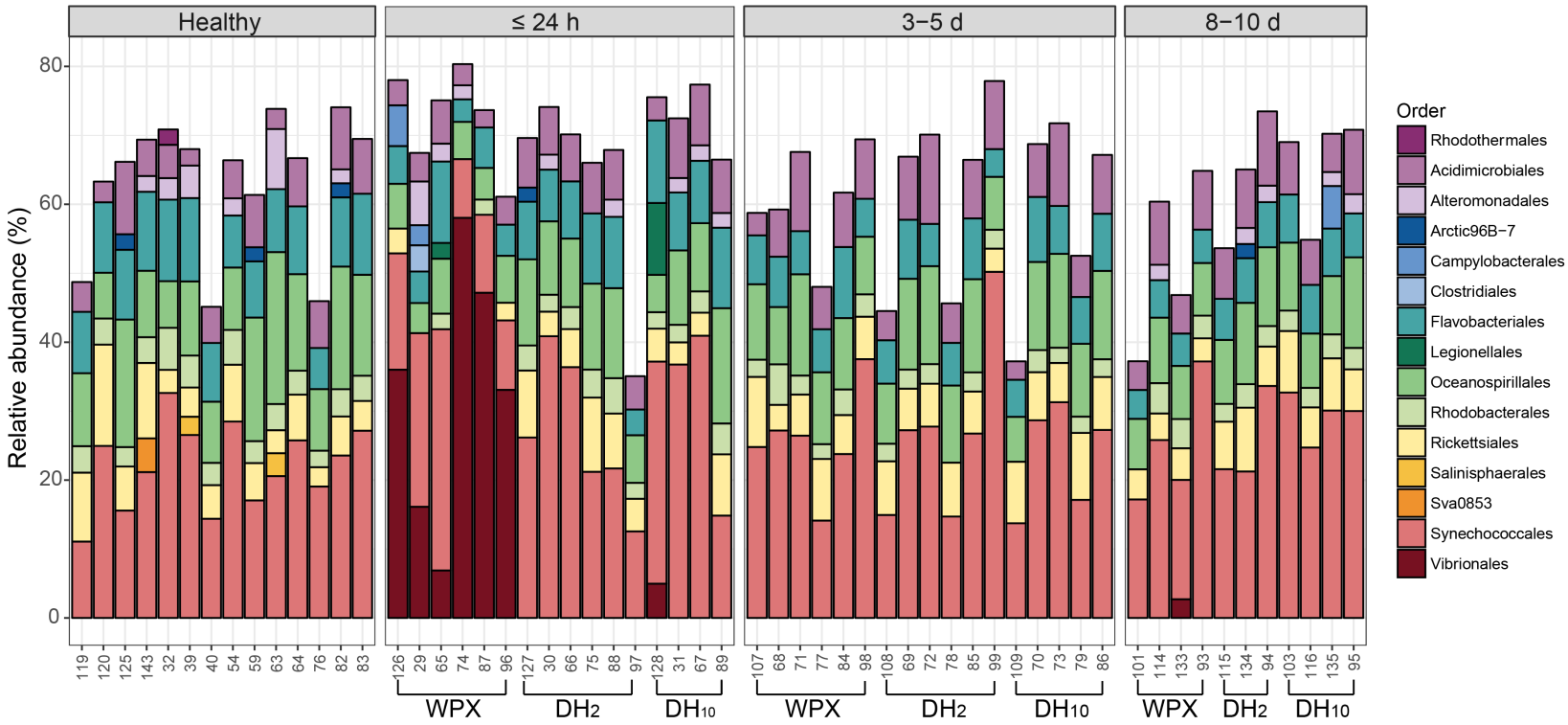

Figure 4.5. Community composition based on all orders representing > 2% relative abundance. The unique numerical identifier for each sample is depicted below its respective bar. Abbreviations: apparently healthy *Acropora palmata* colonies (*Healthy*), the active margin of white pox disease lesions (*WPX*), and apparently healthy regions two and 10

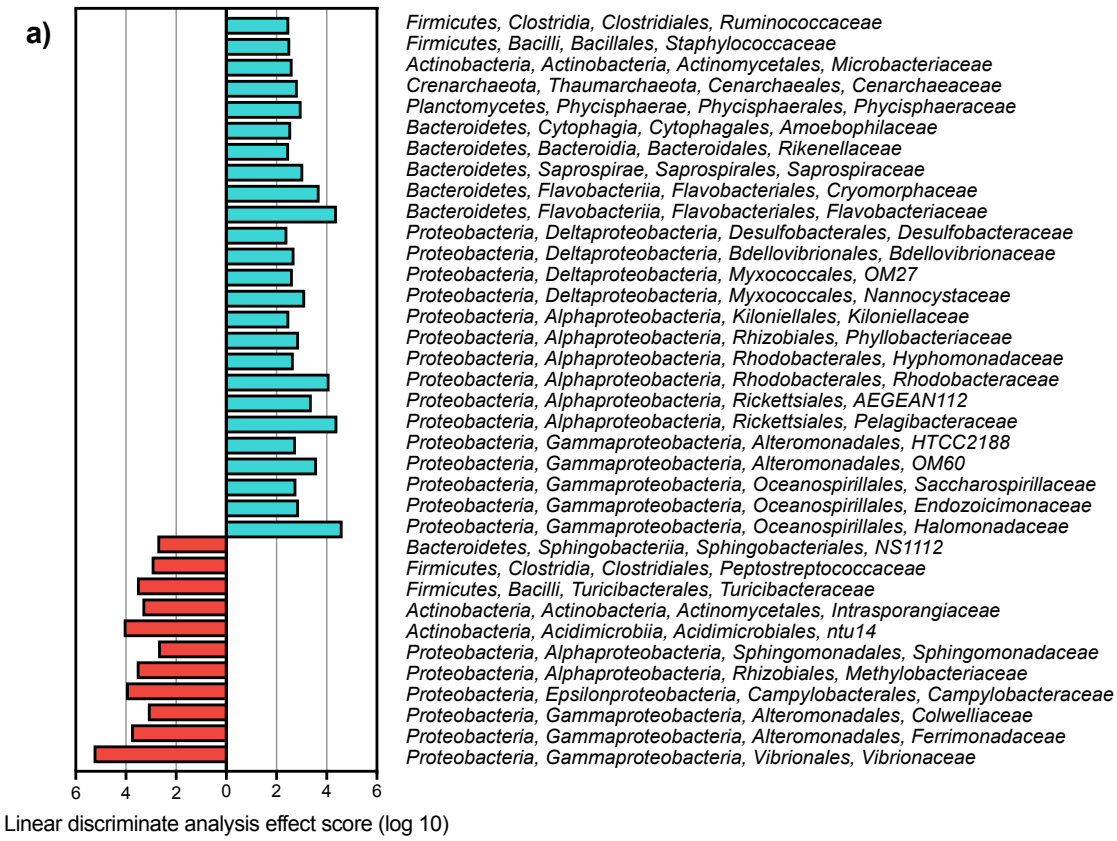

Figure 4.6. LEfSe indicator families for samples taken from apparently healthy *Acropora palmata* colonies (*Healthy*) and the active margin of white pox disease lesions (*WPX*) at ≤ 24 h. (A) all families with significant ($P < 0.05$) linear discriminate analysis (LDA) effect scores and (B) differential relative abundance (± SEM) for indicator families greater than 1% of the total microbial community.

CHAPTER 5

PANGENEOME ANALYSIS OF CORAL ASSOCIATED *VIBRIO*

We present 69 draft genome sequences of *Vibrio* spp. isolated from the critically endangered Caribbean elkhorn coral, *Acropora palmata*, and its surrounding environment to advance our understanding of the genetic features underlying coral reef associated vibrios.

Introduction

Vibrio is one of the most diverse marine bacterial genera with more than 110 described species and is globally distributed in the coastal environment (Gomez-Gil *et al.*, 2014). *Vibrio* have been extensively studied because of their pathogenicity to humans and many commercially important marine aquaculture species. Ten *Vibrio* species are also capable of causing disease in ecologically important reef-building coral (reviewed in Chapter 3). To advance our understanding of the genetic features of coral-associated *Vibrio* spp., we assembled 69 draft genomes of *Vibrio* isolated from the critically endangered Caribbean elkhorn coral, *A. palmata*, and the surrounding seawater. *Vibrio* cultivars were obtained from the surface mucus layer of *A. palmata* colonies afflicted with white pox disease (WPX) (Sutherland *et al.*, 2016) and apparently healthy colonies showing no disease signs.

Methods

Cultivar collection. We sequenced 69 *Vibrio* cultivars isolated from *Acropora palmata* and seawater samples collected at Looe Key Reef, Florida (N 24°32.724' W81°24.360') in August 2012 and August 2013. Coral colonies were examined visually for signs of white pox disease (WPX), defined as irregularly shaped lesions with necrotic, sloughing tissue and exposure of bright white skeleton (Sutherland *et al.*, 2016). Sterile, needless syringes (12 ml) were used to sample mucus from apparently healthy *A. palmata* colonies and diseased *A. palmata* colonies (from the active margin of WPX lesions and an adjacent coral branch displaying no disease signs). Seawater samples were collected in the same manner from the sea surface, 1 m above the benthos, and 10 cm from the coral surface. Samples were transferred into sterile 15 ml conical vials and brought back to the laboratory for bacterial isolation using the *Vibrionaceae* selective media thiosulfate-citrate-bile salts sucrose agar (TCBS; Oxoid). Following incubation at 29°C for 24 h, cultivars were transferred to deep-agar stabs of Zobell marine agar (Difco™ 2216) and later purified by streak-isolation on TCBS media for a minimum of three times. Cultivars chosen for full-genome sequencing were distributed across sample types: WPX lesions (n=18) and asymptomatic tissue (n=19) of diseased *A. palmata*, apparently healthy *A. palmata* (n=15), and surrounding seawater (n=17).

Genomic purification and library preparation. To obtain genomic DNA, the purified bacterial isolates were grown overnight in Zobell marine broth (Difco 2216) at 29 °C. Then, 750 µl of overnight growth was pelleted (3500 rpm for 5 min), washed twice with phosphate buffered saline, and re-suspended in 180 µl Qiagen ATL buffer. We proceded with DNeasy blood and tissue kit (Qiagen, Valencia, CA) extractions according

to the manufacturer's protocol for Gram-negative bacteria with a two min RNase A (Qiagen, Valencia, CA) treatment preceding column purification. DNA quality was assessed using a Nanodrop spectrophotometer.

High quality genomic DNA (50 µl) was sheared to 450-500 bp by focused ultrasonication in single use Covaris™ snap-cap microTUBEs on a Covaris™ E220 system (10% duty cycle, 2.0 intensity, 200 cycles per burst, 45 s duration). After shearing the DNA size distribution was checked on a Fragment Analyzer™ CE system. Illumina® compatible libraries were prepared using the KAPA LTP Library Preparation kit (#KR0452, KAPA Biosystems, Boston, MA), adjusting the manufacturer's protocol in the following ways. Briefly, 25 µl of sheared DNA was incubated in 10 µl of End Repair master mix and incubated at 20 °C for 30 min in a thermocycler. DNA was incubated with 100 µl of Agencourt AMPure XP beads (Beckman Coulter) at room temperature for 15 min, magnet captured, and washed twice with 80 µl of 80% molecular grade EtOH. Bead-bound DNA was eluted in 25 µl of the A-Tailing master mix and incubated at 30 °C for 30 min. Then 45 µl of PEG/NaCl were added, the samples were vortexed briefly, incubated at room temperature for 15 min, followed by an AMPure bead cleanup as previously described. Bead-bound DNA was eluted in 22.5 µl of Ligation master mix and 2.5 µl of 5 µM Y-yoke adapters and incubated at 20 °C for 15 min.

Post-ligation library size selection was preformed with a two-step AMPure bead cleanup. First libraries were mixed with 25 µl of PEG/NaCl followed by an AMPure bead cleanup. Bead-bound DNA was eluted in 100 µl of Qiagen EB buffer and mixed with 55 µl of PEG/NaCl, followed by a 15-min incubation at room temperature to release DNA from the magnetic beads. Beads were magnet captured and 150 µl of the supernatant

were transferred to new tubes. Then, 25 µl AMPure beads were added and a second AMPure bead cleanup was preformed. Size-selected library DNA was eluted in 25 µl of Qiagen EB buffer.

In new PCR reaction tubes, 25 µl of KAPA Hotstart ReadyMix (2X), 2.5 µl each of the i5 and i7 primers were mixed with 20 µl of size-selected library DNA. Library amplification conditions were as follows: initial denaturation at 98 °C for 45 s, followed by six cycles of 98 °C for 15 s, 60 °C for 30 s, 72 °C for 30 s, and a final extension at 72 °C for 60 s. Amplified libraries were purified with a 2:1 AMPure bead cleanup (50 µl amplified library: 25 µl AMPure beads). Final library size (mean range 400-500 bp) was spot-checked on a Fragment Analyzer™ CE system. Libraries were quantified by a Qubit fluorometer (Life Technologies), normalized to 10 ng μl^{-1}, and evenly pooled.

Sequencing and assembly. Genomic libraries were sequenced on an Illumina NextSeq using the mid output mode (150 cycles with 150 bp paired-end reads). The sequence reads were subsampled for error correction and de novo assembled using SPAdes v.3.6.2 (Bankevich *et al.*, 2012) in the careful mode. The resulting contigs were used for scaffolding with SSPACE v.2.0 (Boetzer *et al.*, 2011) and then gap-closed with GapFiller v.1.11 (Boetzer and Pirovano, 2012). Genome assemblies were evaluated with Quast v.3.1 (Gurevich *et al.*, 2013).

Phylogenetic analysis. We used Phylosift v1.0.1 (Darling *et al.*, 2014) to analyze the phylogenetic relationship between the 69 genomes. Briefly, Phylosift uses 37 'elite' marker gene families that have largely congruent phylogenetic histories, are nearly universal, and are present in single copy (Wu *et al.*, 2013). Homologs were identified in the 69 *Vibrio* genomes and aligned to the profile hidden Markov models (HMM) for

these 37 marker genes. Aligned maker genes were then concatenated into a single codon-aligned nucleotide sequence, and FastTree (Price *et al.*, 2009) was utilized to infer the approximately-maximum-likelihood phylogenetic tree with the general time reversal (GTR) nucleotide substitution model. Bootstrap values reported by FastTree analysis indicate local support values for 1,000 resamplings. We used FigTree v1.4.3 (http://tree.bio.ed.ac.uk/software/figtree/) to visualize and annotate the phylogenetic tree.

Pangenomic analysis. Anvi'o v.2.1.0 (available from http://merenlab.org/software/anvio) was used to organize amino acid sequences and gene functional annotation into a genome storage bin for each of the 69 *Vibrio* genomes with the workflow outlined by Eren *et al.* (2015). Genes were organized into protein clusters (PCs) based on amino acid sequence similarities. We then used the anvi'o script 'anvi-pan-genome', calling upon blastp (with the flag '--use-ncbi-blast') to calculate amino acid sequence similarity of each genome against each other. Weak hits (maxbit < 0.5) were removed using 'maxbit heuristic', and then the Markov CLuster algorithm (MCL) (van Dongen and Abreu-Goodger, 2011) identified protein clusters (PCs) in the remaining blastp search results with the parameter '--mcl-inflation 2.0'. We visualized the distribution of PCs across the genomes, and binned PCs based on their clade affiliation determined through Phylosift phylogenetic analysis.

Results

Genomes assembled into 20–156 scaffolds ≥ 1000 bp (mean = 48 ± 3 SEM) with half of the assembled genome length (L50) contained in 2–13 scaffolds (mean = 5, Table

5.1). The mean genome size (of contigs ≥ 1000 bp) was 5,705,770 ± 42,551 bp long, with a mean G+C content of 45.2% ± 0.6%.

Phylogenetic analysis based on 37 housekeeping genes (Figure 5.1), revealed that the 69 *Vibrio* genomes clustered into five of the seventeen described clades within the *Vibrio* genus (Sawabe *et al.*, 2013). These clades were assigned taxonomy based on previous classifications of the isolates (Chapter 3) and the *Harveyi* clade was further broken into three groups based on the species level (Table 5.2). Two isolates (C_D_PX_014 and C_D_PX_114) did not fall within any of the presently described *Vibrio* clades (Sawabe *et al.*, 2013).

The pangenome totaled 22,718 protein clusters (PCs) derived from sequencing 353,038 genes (Figure 5.2). The core genome (*i.e.*, PCs present in all genomes) consisted of 1,998 orthologous PCs (8.8% of the total PCs). Clade-specific PCs, defined as present in 100% of the clade members and absent from all other sequenced genomes included: *Harveyi* clade; *owensii* (n = 82), *Harveyi* clade; *harveyi* (n = 80), *Harveyi* clade; *alginolyticus* (n = 223), *Mediterranei* clade (n = 899), *Corallilyticus* clade (n = 507), *Orientalis* clade (n = 89) and *Splendidus* clade (n = 114).

Discussion

This study compared the genomes of *Vibrio* spp. associated with the critically threatened reef-building coral *Acropora palmata* and the surrounding seawater. The sequencing and availability of these genomes, representing five of the seventeen described *Vibrio* clades (Sawabe *et al.*, 2013), provides a foundation for understanding the potential functional role of these taxa in the coral microbiome. *Vibrio* can be characterized as conditionally

rare taxa (CRT) (Shade *et al.*, 2014) in coastal seawater because they typically make up a minor portion of the total microbial assemblage, but are capable of blooming in response to nutrient availability and other environmental factors (Westrich *et al.*, 2016). Likewise, *Vibrio* are often rare members in the microbiome of apparently healthy corals (Alves *et al.*, 2010; Pollock *et al.*, 2016; Rubio-Portillo *et al.*, 2014), but can increase significantly during disease (Ushijima *et al.*, 2012; Sussman *et al.*, 2008; Pantos and Bythell, 2006) and environmental pressures including temperature stress (Ziegler *et al.*, 2017) and low water flow (Lee *et al.*, 2017). We have previously shown that *Vibrio* are capable of blooming in disease lesions on *A. palmata*, increasing from <1 to ~34% of the total microbial community in the surface mucus layer (SML) (Chapter 4). Thus, *Vibrio* spp. may exist as CRT in the healthy coral microbiome, primed to respond to rapidly changing biotic and abiotic factors with consequences for coral health.

There has been recent interest in examining the genomic content, life history strategies, and ecological roles of CRT within seawater microbial communities in the coastal environments (Lauro *et al.*, 2009; Shade *et al.*, 2014). CRT capable of bloom formation, such as *Vibrio*, have been less explored in marine host-microbiome systems. The availability of the genomes presented in this study will provide an important foundation for understanding *Vibrio* blooming in the coral microbiome.

Acknowledgements

This work was supported by the NSF grant EF1015342 (to E.K.L and J.W.P) as part of the joint NSF-NIH Ecology of Infectious Disease program. Magdy Alabady assisted with genome assembly and Sonny Lee conducted pangenome binning. I would

also like to acknowledge the entire staff at the Summerland Key Mote Marine Tropical Research Laboratory, with species thanks to Erich Bartels and Mark Knowles for their advice and logistical support. Mucus and other specimens were obtained under permit FKNMS-2010-131-A.

References

Alves N, Neto OSM, Silva BSO, De Moura RL, Francini-Filho RB, Barreira e Castro C, *et al.* (2010). Diversity and pathogenic potential of vibrios isolated from Abrolhos Bank corals. *Environ Microbiol Rep* **2**: 90–95.

Bankevich A, Nurk S, Antipov D, Gurevich AA, Dvorkin M, Kulikov AS, *et al.* (2012). SPAdes: a new genome assembly algorithm and its applications to single-cell sequencing. *J Comput Biol* **19**: 455–477.

Boetzer M, Henkel CV, Jansen HJ, Butler D, Pirovano W. (2011). Scaffolding pre-assembled contigs using SSPACE. *Bioinformatics* **27**: 578–579.

Boetzer M, Pirovano W. (2012). Toward almost closed genomes with GapFiller. *Genome Biol* **13**: R56.

Darling AE, Jospin G, Lowe E, Matsen FA IV, Bik HM, Eisen JA. (2014). PhyloSift: phylogenetic analysis of genomes and metagenomes. *PeerJ* **2**: e243–28.

Eren AM, Esen ÖC, Quince C, Vineis JH, Morrison HG, Sogin ML, *et al.* (2015). Anvi'o: an advanced analysis and visualization platform for 'omics data. *PeerJ* **3**: e1319–29.

Gomez-Gil B, Thompson CC, Matsumura Y, Sawabe T, Iida T, Christen R, *et al.* (2014). The Famlily *Vibrionaceae*. In: Rosenberg E, Delong EF, Lory S, Stackebrandt E, Thompson F (eds) Gammaproteobacteria. *The Prokaryotes*. Springer Berlin Heidelberg: Berlin, Heidelberg, pp 659–747.

Gurevich A, Saveliev V, Vyahhi N, Tesler G. (2013). QUAST: quality assessment tool for genome assemblies. *Bioinformatics* **29**: 1072–1075.

Lauro FM, McDougald D, Thomas T, Williams TJ, Egan S, Rice S, *et al.* (2009). The genomic basis of trophic strategy in marine bacteria. *Proc Natl Acad Sci* **106**: 15527–15533.

Lee STM, Davy SK, Tang S-L, Kench PS. (2017). Water flow buffers shifts in bacterial community structure in heat-stressed *Acropora muricata*. *Sci Rep* **7**: 43600.

Pantos O, Bythell JC. (2006). Bacterial community structure associated with white band disease in the elkhorn coral *Acropora palmata* determined using culture-independent 16S rRNA techniques. *Dis Aquat Org* **69**: 79–88.

Pollock FJ, Wada N, Torda G, Willis BL, Bourne DG. (2016). White syndrome-affected corals have a distinct microbiome at disease lesion fronts. *Appl Environ Microbiol* **83**: e02799–16–16–15.

Price MN, Dehal PS, Arkin AP. (2009). FastTree: computing large minimum evolution trees with profiles instead of a distance matrix. *Mol Biol Evol* **26**: 1641–1650.

Rubio-Portillo E, Yarza P, alver CPN, aacute AAR-E, n JAO. (2014). New insights into *Oculina patagonica* coral diseases and their associated *Vibrio* spp. communities. *ISME J* **8**: 1794–1807.

Sawabe T, Ogura Y, Matsumura Y, Gao F, Amin AR, Mino S, *et al.* (2013). Updating the *Vibrio* clades defined by multilocus sequence phylogeny: proposal of eight new clades, and the description of *Vibrio tritonius* sp. nov. *Front Microbiol* **4**: 1–14.

Shade A, Jones SE, Caporaso JG, Handelsman J, Knight R, Fierer N, *et al.* (2014). Conditionally rare taxa disproportionately contribute to temporal changes in microbial diversity. *mBio* **5**: e01371–14–e01371–14.

Sussman M, Willis BL, Victor S, Bourne DG. (2008). Coral pathogens identified for White Syndrome (WS) epizootics in the Indo-Pacific. *PLoS One* **3**: e2393–14.

Sutherland KP, Berry B, Park A, Kemp DW, Kemp KM, Lipp EK, *et al.* (2016). Shifting white pox aetiologies affecting *Acropora palmata* in the Florida Keys, 1994-2014. *Philos Trans R Soc Lond B Biol Sci* **371**: 20150205.

Ushijima B, Smith A, Aeby GS, Callahan SM. (2012). *Vibrio owensii* Induces the tissue loss disease *Montipora* white syndrome in the Hawaiian reef coral *Montipora capitata*. *PLoS One* **7**: e46717–10.

van Dongen S, Abreu-Goodger C. (2011). Using MCL to extract clusters from networks. In: Methods in Molecular Biology Vol. 804. *Bacterial Molecular Networks*. Springer New York: New York, NY, pp 281–295.

Westrich JR, Ebling AM, Landing WM, Joyner JL, Kemp KM, Griffin DW, *et al.* (2016). Saharan dust nutrients promote *Vibrio* bloom formation in marine surface waters. *Proc Natl Acad Sci* **113**: 5964–5969.

Wu D, Jospin G, Eisen JA. (2013). Systematic identification of gene families for use as 'markers' for phylogenetic and phylogeny-driven ecological studies of Bacteria and Archaea and their major subgroups. *PLoS One* **8**: e77033–11.

Ziegler M, Seneca FO, Yum LK, Palumbi SR, Voolstra CR. (2017). Bacterial community dynamics are linked to patterns of coral heat tolerance. *Nat Commun* **8**: 14213.

Tables

Table 5.1. Assembly statistics.

Anvio Name*	GC (%)	Total length (≥ 0 bp)	Total length (≥1000 bp)	no. contigs ≥ 0 bp	no. contigs ≥ 1000 bp	Largest contig length (bp)	N50[a]	N75[b]	L50[c]	L75[d]	# N's per 100 kbp[e]
C_D_DH_019	45.6	5864097	5852759	51	36	1129958	1005529	319678	3	6	**0.0**
C_D_DH_034	45.0	5757784	5741781	72	48	836794	341837	172740	5	11	2.7
C_D_DH_038	45.6	5944983	5938703	49	40	1155963	983936	203110	3	8	0.0
C_D_DH_120	44.9	5070696	5067298	34	29	1692156	608740	230103	3	7	5.5
C_D_DH_125	45.6	5861927	5858032	40	34	1017130	791334	243336	4	7	6.7
C_D_DH_353	45.3	6046788	6039722	63	51	1095435	400833	161668	4	10	0.0
C_D_DH_357	44.9	5823933	5811096	69	50	808951	387132	173935	5	11	2.3
C_D_DH_359	44.6	5081015	5067770	84	65	657937	259534	158646	7	13	1.8
C_D_DH_360	45.6	5798619	5795786	34	30	1100517	858321	398510	3	6	0.0
C_D_DH_362	45.5	6050016	6045417	62	55	748009	382826	178660	6	12	0.0
C_D_DH_366	45.0	5666379	5657129	63	50	996768	296176	137085	6	12	0.0
C_D_DH_370	44.5	5188508	5187147	24	22	1176443	484336	288413	4	7	1.4
C_D_DH_372	45.6	5896379	5886885	67	53	777643	386135	254134	6	10	0.0
C_D_DH_382	45.0	6299413	6295178	49	43	660775	463894	206174	6	11	1.2
C_D_DH_390	44.6	5964404	5925525	185	130	512790	150505	81203	12	26	0.5
C_D_DH_392	45.6	5846863	5840520	47	38	1139731	380836	267727	5	10	0.0
C_D_DH_394	45.6	5801511	5795575	51	42	768045	304388	214239	6	11	0.0
C_D_DH_397	45.5	5887727	5882905	47	39	894406	665718	395294	4	7	0.0
C_D_DH_398	45.4	6271539	6267534	46	40	1042289	517710	187593	4	9	0.0
C_D_DH_399	45.5	5922546	5914970	46	36	1105767	523652	315102	5	8	0.0
C_D_PX_014	45.3	5177648	5174003	30	24	1089380	801027	295577	3	6	3.8
C_D_PX_063	45.5	5291062	5287390	25	20	1891276	1619317	363350	2	4	9.5
C_D_PX_067	44.0	5922761	5917240	63	56	1567038	576770	174807	3	9	2.5
C_D_PX_100	45.6	5832616	5822945	51	37	1091903	515857	189209	4	9	3.8
C_D_PX_114	45.4	4953841	4949610	33	26	1422037	1114283	325624	2	5	0.0
C_D_PX_234	45.4	5445429	5425572	120	93	303729	157770	77968	13	26	2.8
C_D_PX_241	45.7	5891067	5885096	41	32	2315970	853818	379661	2	5	1.3
C_D_PX_245	44.1	5000655	4990680	71	55	805726	293421	145954	6	11	2.8
C_D_PX_247	44.9	5639926	5634717	45	37	892004	390620	287016	5	9	0.0
C_D_PX_248	45.6	5842599	5835101	47	35	1163165	510836	377720	4	7	0.0
C_D_PX_249	45.6	5864895	5854256	59	42	951564	424199	206296	4	9	9.2
C_D_PX_256	45.0	5664293	5650771	66	47	576631	339910	179933	7	12	0.0

C_D_PX_258	45.0	5662676	5650574	61	43	696197	338385	179933	7	12	0.0
C_D_PX_272	45.6	5945402	5940354	48	41	642146	449277	261581	6	10	0.0
C_D_PX_282	44.9	5845577	5831022	96	75	540645	227845	99860	9	18	1.9
C_D_PX_290	45.8	6062032	6058320	40	34	1135590	990264	323833	3	6	3.5
C_D_PX_311	44.8	5796282	5786452	76	62	942284	387982	153452	6	12	23.1
C_D_PX_312	45.0	5610141	5599421	58	41	948955	526587	148623	4	10	2.4
C_H_142	44.4	5417097	5407082	51	36	775196	424491	244829	5	9	0.6
C_H_143	44.4	5233346	5230304	28	23	1292660	439488	247337	3	7	4.9
C_H_146	45.6	5830048	5826307	45	39	859838	400809	231499	5	9	0.0
C_H_153	44.9	5757253	5750016	55	44	816641	422172	185892	5	11	0.0
C_H_162	45.6	5893257	5885005	53	41	985595	558120	362105	4	7	1.4
C_H_170	45.6	5709182	5701865	63	51	645992	308422	204205	7	12	0.0
C_H_174	45.0	5769959	5762017	66	55	945346	288650	168891	6	12	0.0
C_H_177	45.5	5745129	5738610	55	47	939570	410140	318326	5	9	2.2
C_H_179	45.0	5361348	5360266	26	24	983775	444569	224754	4	8	0.0
C_H_181	45.7	5743274	5739293	36	31	1201371	912769	304339	3	6	0.0
C_H_184	44.7	5048667	5031508	68	44	799803	402427	171456	5	9	0.0
C_H_189	45.6	5880127	5867286	67	46	1266716	867739	255075	3	6	0.0
C_H_198	45.5	6015169	6010916	42	36	1085514	592552	220156	4	8	4.4
C_H_207	45.6	5852167	5840563	68	51	887091	322772	214608	7	12	0.5
C_H_209	45.4	6087395	6079183	56	43	874614	379511	230117	5	10	2.5
H2O_10cm_070	45.5	5942404	5934925	50	38	748133	517246	178675	5	9	0.0
H2O_10cm_074	44.0	5854618	5822359	106	55	707682	357501	177063	6	11	3.1
H2O_10cm_078	44.9	5752105	5737432	70	48	917333	467620	232177	5	9	0.0
H2O_10cm_087	45.5	5928518	5920736	55	43	979986	466276	287698	5	9	0.0
H2O_10cm_102	45.6	5885458	5881644	41	35	954934	497964	202579	4	9	0.0
H2O_10cm_108	44.7	4670841	4667424	29	24	1144049	637589	233111	3	6	0.0
H2O_10cm_111	45.6	5874723	5865220	54	39	1127998	831130	269426	3	7	0.0
H2O_1m_044	45.6	6246909	6191463	238	156	1121626	379798	128677	4	11	2.2
H2O_1m_055	45.6	5904543	5901722	52	48	1132503	413109	212642	5	10	0.0
H2O_1m_064	44.9	5716998	5708880	64	52	677315	264855	108114	7	15	0.0
H2O_1m_066	45.6	5815277	5812282	38	33	1313437	771351	301665	3	7	0.0
H2O_S_001	44.1	4966846	4958440	78	66	505103	139312	90115	11	22	0.0
H2O_S_012	45.6	5810015	5806201	45	39	892254	460819	235131	5	10	0.0
H2O_S_017	45.6	6329440	6228385	273	127	527819	143762	78029	12	26	0.0
H2O_S_019	45.6	6311704	6169677	327	104	433066	186977	91224	11	22	20.2
H2O_S_026	44.6	5082828	5070228	80	62	657937	289118	167916	6	12	1.8
H2O_S_032	44.4	5482690	5478375	65	58	1007036	195926	94471	8	19	0.0

*Abbreviations for isolation sources: C_H, apparently healthy *Acropora palmata* colonies; C_D_PX, white pox disease lesions on *A. palmata* colonies; C_D_DH,

apparently healthy regions on diseased *A. palmata* colonies; H2O_S, surface seawater; H2O_1m, seawater 1 m above *A. palmata* colonies; H2O_10cm, seawater with 10 cm of the *A. palmata* surface.

[a] N50, length of the genome contained in 50% of the contigs

[b] N75, length of the genome contained in 75% of the contigs

[c] L50, number of contigs which contain 50% of the total genome length

[d] L75, number of contigs which contain 75% of the genome length

[e] N's, number of ambiguous bases

Table 5.2 Distribution of genomes among *Vibrio* clades

	no. of genomes	Mean G+C (%)	Mean Length (bp)*
Coralliilyticus clade	2	45.5 ± 0.05	5,356,481 ± 69,091
Harveyi clade	54	45.3 ± 0.05	5,813,173 ± 36,492
alginolyticus	3	44.7 ± 0.05	5,050,868 ± 19,360
harveyi	14	44.9 ± 0.02	5,768,766 ± 45,022
owensii	37	45.5 ± 0.03	5,907,645 ± 33,493
Mediterranei clade	2	44.0 ± 0.00	5,888,699 ± 34,072
Orientalis clade	2	44.8 ± 0.10	4,870,769 ± 1,999,927
Splendidus clade	7	44.5 ± 0.15	5,228,517 ± 65,794

* based on contigs ≥ 1,000 bp

Figures

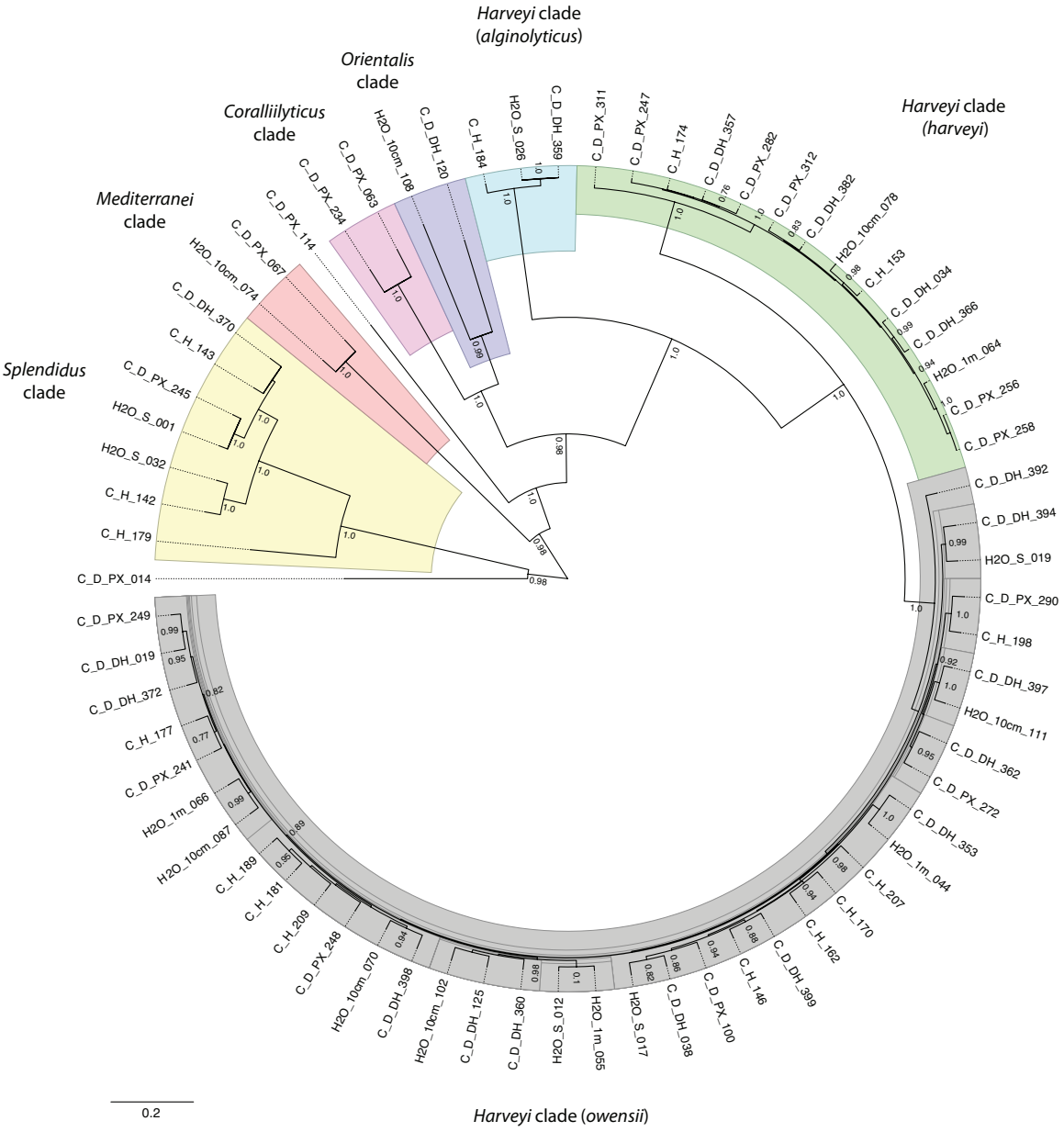

Figure 5.1 Maximum likelihood phylogenetic analysis based on 37 gene loci, for *Vibrio* cultivars isolated from *Acropora palmata* and seawater at Looe Key Reef, Florida. Local support values for 1,000 resamplings are shown. Abbreviations for isolation source: C_H, mucus from apparently healthy colonies with no white pox disease (WPX) signs; C_D_PX, mucus from WPX lesions; C_D_DH, mucus from asymptomatic areas colonies

with WPX lesions; H2O_10cm, seawater 10 cm from the surface of *A. palmata*; H2O_1m, seawater 1 m above *A. palmata* colonies; H2O_sur, surface seawater.

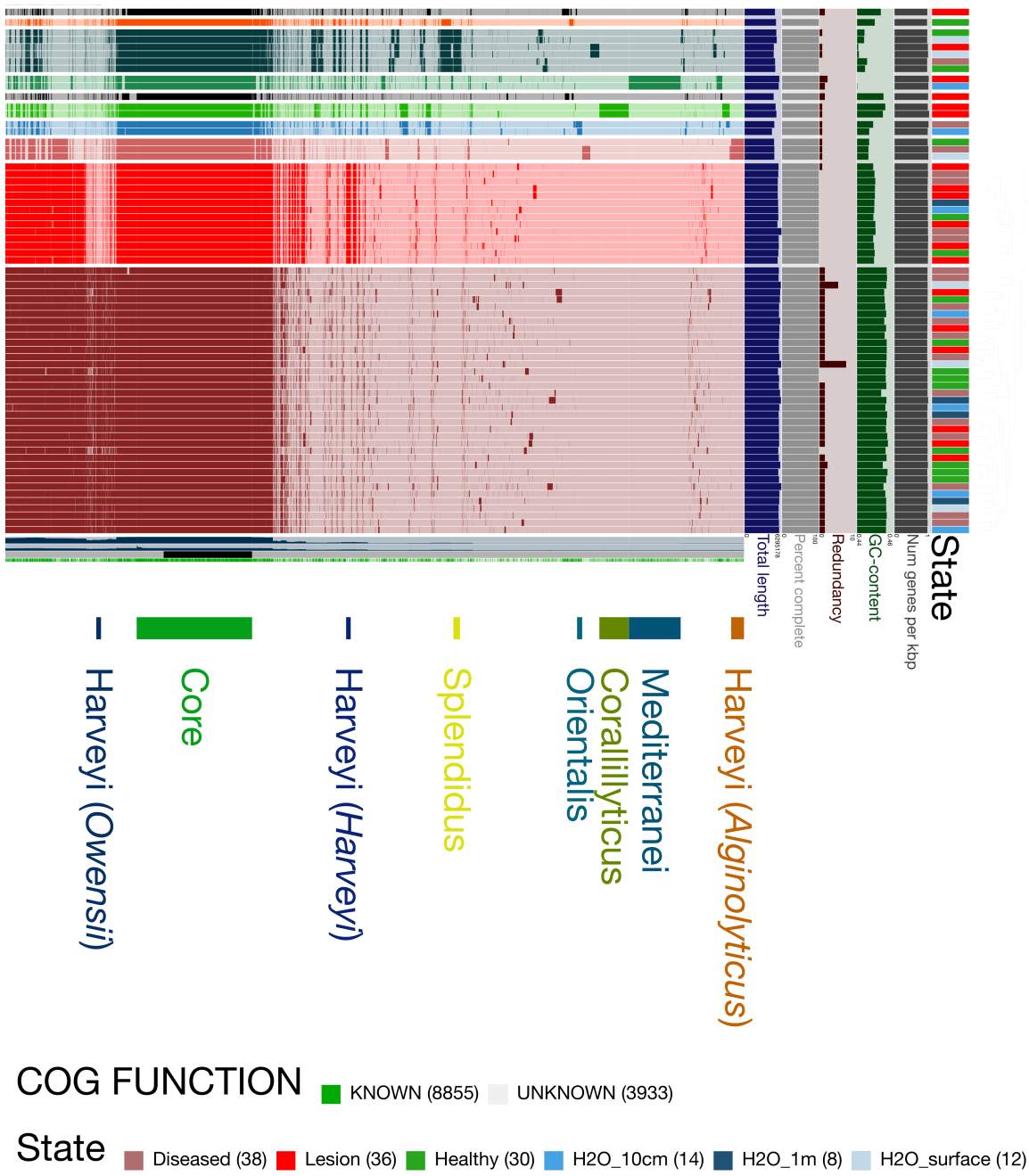

Figure 5.2. The pangenome of 69 *Acropora palmata* and seawater *Vibrio* cultivars isolated from Looe Key Reef, Florida. Core protein clusters (PCs) present in all genomes and clade-specific PCs are depicted by bars below the phylogram. Isolation source (or State) are depicted by colored coded bars. State Abbreviations: Healthy, mucus from apparently healthy colonies with no disease signs; Lesion, mucus from disease lesions;

Diseased, mucus from asymptomatic areas colonies with lesions; H2O_10cm, seawater 10 cm from the surface of *A. palmata*; H2O_1m, seawater 1 m above *A. palmata* colonies; H2O_sur, surface seawater.

CHAPTER 6

CONCLUSION

Coral diseases are increasing worldwide and are now considered a major contributor to coral reef decline. The Caribbean, in particular, has been noted as a coral disease hotspot owing to the dramatic decline of framework-building acroporid corals to tissue loss diseases (Weil and Rogers, 2011). The critically endangered elkhorn coral, *Acropora palmata*, is affected by white pox disease (WPX) throughout the Florida Reef Tract and wider Caribbean. Living cover of *A. palmata* in the upper Florida Keys declined by half from 2004–2010 and 30% of this loss was attributable to partial mortality caused by WPX and other tissue loss diseases (Williams and Miller, 2011). The aim of this dissertation was to elucidate disease dynamics and potential pathogenicity of contemporary white pox disease (WPX) outbreaks in *Acropora palmata*. The studies presented here are the first to investigate the association of *Vibrio* bacteria with WPX.

Chapter 3 shows that the concentration of cultivable *Vibrio* was consistently greater in WPX samples compared to healthy samples over three years of sampling. Based on quantitative real-time PCR (qPCR), the relative abundance of *Vibrio* bacteria to total bacteria was four times higher in samples from WPX lesions. The lesions sampled during this study were active (tissue was sloughing and skeleton was bright white), but of unknown age. It was determined that further studies, with higher temporal resolution, were needed to understand whether *Vibrio* are directly involved in WPX onset and progression. Accordingly, high resolution sampling of *A. palmata* was conducted during

a WPX outbreak, and revealed unique spatiotemporal dynamics in microbial communities at the front (or margins) of lesions ≤ 24 h old, as well as blooming of potential *Vibrio* pathobionts and a reduction of beneficial taxa (Chapter 4). Additionally, Chapter 4 identifies the combined environmental factors of low wind speed and high seawater temperature as important thresholds that may serve as tipping points leading to host stress and disruption of microbiome homeostasis. Together, these two chapters frame *Vibrio* as conditionally rare taxa (CRT) (Shade *et al.*, 2014) in the coral microbiome that are capable of blooming under certain conditions.

In Chapter 3 the diversity of 69 *Vibrio* isolates collected from diseased and apparently healthy *A. palmata* colonies and the surrounding seawater by multilocus sequence analysis (MLSA). There was no strong association of particular *Vibrio* species with health status or sample type; however, 86% of total isolates were closely related to *Vibrio* species with known pathogenicity to corals. In Chapter 5, a functional approach pangenome analysis was done on all 69 *Vibrio* isolates. No evidence of health status or sample type influenced the distribution of orthologous protein clusters. Taken together, this indicates that *Vibrio* may be part of a non-specific, heterotrophic bloom in WPX disease lesions. Chapter 4 showed that WPX lesions healed rapidly, decreasing in size by ~29% after just 8–13 d. Moreover, as lesions age they form a cluster with healthy samples in ordination space, indicating that communities return close to their original state as lesions heal. This suggests (1) either the coral host and/or the commensal microbiota are resilient to ephemeral *Vibrio* blooms and (2) that the microbiome may return to the original "healthy" state within days of lesion formation. Although *A.*

palmata in the Florida Keys develop WPX signs, they may now be resilient to tissue-loss progression due to WPX.

Chapter 4 indicates that high seawater temperature combined with low wind speed may result in stressful conditions that suppress coral health and immunity and promote blooms of opportunistic pathogens and pathobionts (i.e., *Vibrio*) in the coral microbiome. However, samples were only collected during a single outbreak event at the beginning of the disease season. Disease dynamics may change after multiple rounds of doldrum conditions and new WPX lesion formation; a ratcheting-down affect may occur in which coral health an immunity are reduced with each outbreak round, while the microbiome becomes less resilient to opportunistic blooms of potentially pathogenic bacteria (via mechanisms like HGT of virulence genes and the loss of keystone stabilizers) (Stecher *et al.*, 2013). Alternatively, the coral host and its microbiome may be robust to repeated disease outbreaks, even gaining resistance with exposure. Further field and manipulative studies are needed to examine these scenarios.

Chapter 5 presents 69 draft genome sequences of *Vibrio* spp. isolated from the surface mucus layer of *A. palmata* colonies afflicted with WPX, apparently healthy colonies showing no disease signs, and the surrounding seawater to advance our understanding of the genetic features underlying coral reef associated vibrios. There has been recent interest in examining the genomic content, life history strategies, and ecological roles of CRT within seawater microbial communities in the coastal environments (Lauro *et al.*, 2009; Shade *et al.*, 2014). CRT capable of bloom formation, such as *Vibrio*, have been less explored in marine host-microbiome systems. The

availability of the genomes presented in this study will provide an important foundation for understanding *Vibrio* blooming in the coral microbiome.

References

Lauro FM, McDougald D, Thomas T, Williams TJ, Egan S, Rice S, *et al.* (2009). The genomic basis of trophic strategy in marine bacteria. *Proc Natl Acad Sci* **106**: 15527–15533.

Shade A, Jones SE, Caporaso JG, Handelsman J, Knight R, Fierer N, *et al.* (2014). Conditionally rare taxa disproportionately contribute to temporal changes in microbial diversity. *mBio* **5**: e01371–14–e01371–14.

Stecher B, Maier L, Hardt W-D. (2013). 'Blooming' in the gut: how dysbiosis might contribute to pathogen evolution. *Nat Rev Micro* **11**: 277–284.

Weil E, Rogers CS. (2011). Coral reef diseases in the Atlantic-Caribbean. In: Dubinsky Z, Stambler N (eds). *Coral Reefs: An Ecosystem in Transition*. Springer Netherlands: Dordrecht, pp 465–491.

Williams DE, Miller MW. (2011). Attributing mortality among drivers of population decline in *Acropora palmata* in the Florida Keys (USA). *Coral Reefs* **31**: 369–382.

APPENDIX A

SUPPLEMENTARY MATERIALS FOR CHAPTER 3

Table S3.1. List of reference strains and sequence accession numbers.

Strain	Accession no.							
	gapA	ftsZ	mreB	gyrB	pyrH	recA	rpoA	topA
E. coli str. K-12 substr. W3110	WGS Accession: GCF_001878695.1 (Patric ID: 316407.41) [b]							
E. coralii CAIM 912 = LMG 22228	DQ907268.1	DQ907329.1	DQ907396.1	AB298198.1	JF739392.1	AJ842456	AJ842530.1	EF114217
G. hollisae CAIM 625 = LMG 117719	DQ907317.1	EF027348.1	DQ907398.1	AB298259.1	JF739393.1	AJ842351.1	AJ842535.1	AB298259
P. damselae subsp. damselae ATCC 33539	WGS Accession: GCF_000950315.1 (Patric ID: 85581.9) [b]							
V. alginolyticus 40B	WGS Accession: GCA_000176055.1 (Patric ID: 674977.3) [b]							
V. alginolyticus ANC4-19	WGS Accession: GCA_001584265.1 (Patric ID: 663.91) [b]							
V. alginolyticus LMG 4409	DQ907274.1	EF027344.1	DQ907405.1	AB298202.1	GU266285.1	AJ842373.1	AJ842558.1	AB298202
V. anguillarum LMG 4437	DQ907275.1	DQ907334.1	DQ907406.1	AB298203.1	KU755175.1	AJ842375.1	AJ842561.1	AB298203
V. antiquarius Ex25	WGS Accession: GCF_001909305.1 (Patric ID: 150340.30) [b]							
V. brasiliensis LMG 20546	DQ449613.1	DQ907335.1	DQ907407.1	AB298204.1	HM771374.1	AJ580884.1	AJ842563.1	AB298204
V. campbellii LMG 11216	EF596565.1	DQ907337.1	DQ907408.1	AB298205.1	EF596641.1	AJ842377.1	AJ842564.1	AB298205
V. chagasii LMG 21353	DQ481611.1	DQ996590.1	DQ481637.1	AB298206.1	EU118252.1	AJ842385.1	AJ842572.1	AB298206
V. cholerae O1 biovar El Tor str. N16961	WGS Accession: GCA_000006745.1 (Patric ID: 243277.26) [b]							
V. coralliilyticus 58	WGS Accession: GCF_001693615.1 (Patric ID: 190893.24) [b]							
V. coralliilyticus LMG 20984	DQ907279.1	DQ907341.1	DQ907412.1	AB298210.1	GU266292.1	AJ842402.1	AJ842587.1	AB298210
V. coralliilyticus OCN008	WGS Accession: GCA_000461895.1 (Patric ID: 1384040.4) [b]							
V. coralliilyticus OCN014	WGS Accession: GCA_000763535.2 (Patric ID: 190893.12) [b]							
V. coralliilyticus P1	WGS Accession: GCA_000195475.2 (Patric ID: 909421.4) [b]							
V. coralliilyticus RE22	WGS Accession: GCF_001297935.1 (Patric ID: 190893.21) [b]							
V. coralliilyticus S2043	WGS Accession: GCF_000967485.1 (Patric ID: 190893.15) [b]							

V. diabolicus CNCM I-1629 = LMG 19805	WGS Accession: GCF_001048675.1 (Patric ID: 50719.6) [b]							
V. diazotrophicus CECT 627 = LMG 7893	DQ907280.1	DQ907342.1	DQ907413.1	AB298212.1	HE805632.1	AJ580856.1	AJ842598.1	AB298212
V. fortis LMG 21557	DQ907282.1	DQ907346.1	DQ907417.1	AB298216.1	LMG 21557T [a]	AJ842421.1	AJ842609.1	AB298216
V. gazogenes ATCC 29988 = LMG 19540	KF697264.1	KF697255.1	KF697280.1	KF697272.1	KF697288.1	AJ842429.1	KF697306.1	AB298258
V. genomosp. F10 ZF-129	WGS Accession: GCA_000287055.1 (Patric ID: 1187848.3) [b]							
V. halioticoli LMG 18542	AY546638.1	DQ907349.1	DQ907421.1	AB298220.1	LMG 18542T [a]	AJ842430.1	AJ842617.1	AB298220
V. harveyi 74F	WGS Accession: GCF_001185565.1 (Patric ID: 669.39) [b]							
V. harveyi AOD131	WGS Accession: GCA_000347555.1 (Patric ID: 1287887.3) [b]							
V. harveyi CAIM 1792	WGS Accession: GCA_000259935.1 (Patric ID: 1125980.3) [b]							
V. harveyi E385	WGS Accession: GCA_000493315.1 (Patric ID: 1352943.3) [b]							
V. harveyi LMG 4044	DQ449616.1	DQ907350.1	DQ907422.1	AB298221.1	LMG 4044T [a]	AJ842440.1	AJ842627.1	AB298221
V. harveyi VHJR4	WGS Accession: GCF_001050875.1 (Patric ID: 1300144.3) [b]							
V. harveyi VHJR7	WGS Accession: GCA_000442925.1 (Patric ID: 1300145.3) [b]							
V. harveyi ZJ0603	WGS Accession: GCA_000275705.1 (Patric ID: 1191522.3) [b]							
V. hepatarius LMG 20362	DQ907285.1	DQ907352.1	DQ907424.1	AB298222.1	LMG 20362T [a]	AJ842444.1	AJ842631.1	DQ481649.1
V. jasicida CAIM 1864 = LMG 25398	WGS Accession: GCA_000400365.1 (Patric ID: 1229494.3) [b]							
V. maritimus R-40493 = CAIM 1455	KF666681.1	GU929927.1	GU929931.1	KF666700.1	GU929933.1	GU929935.1	GU929937.1	DQ907485.1
V. mediterranei LMG 11258	DQ907290.1	DQ907356.1	DQ907428.1	AB298228.1	LMG 11258T [a]	AJ842459.1	AJ842644.1	KF697314.1
V. mediterranei AK1 = LMG 19703	DQ907310.1	DQ907310	DQ907449.1	NZ_ABCH01000001	GU266289.1	AJ842507	JN039148.1	KF697315.1
V. mytili LMG 19157	DQ907293.1	DQ907358.1	DQ907431.1	AB298231.1	LMG 19157T [a]	AJ842472.1	AJ842657.1	DQ907491.1
V. natriegens LMG 10935	DQ907294.1	DQ907359.1	DQ907432.1	AB298232.1	LMG 10935T [a]	AJ842473.1	AJ842658.1	DQ907492.1
V. neptunius LMG 20536	DQ907296.1	DQ907361.1	DQ907435.1	AB298234.1	LMG 20536T [a]	AJ842478.1	AJ842663.1	AB298234
V. nereis LMG 3895	DQ449617.1	DQ907362.1	DQ907436.1	AB298235.1	JN968379.1	AJ842479.1	AJ842666.1	DQ481657.1
V. nigripulchritudo LMG 3896	DQ907297.1	EF027347.1	DQ907437.1	AB298236.1	LMG 3896T [a]	AJ842480.1	AJ842667.1	DQ481659.1

V. orientalis LMG 7897	DQ907299.1	DQ907365.1	DQ907439.1	AB298238.1	LMG 7897T[a]	AJ842485.1	AJ842672.1	GU929939.1
V. owensii 47666-1	WGS Accession: GCA_000818255.1 (Patric ID: 696485.16)[b]							
V. owensii ATCC 25919	WGS Accession: GCA_000400225.1 (Patric ID: 1280000.3)[b]							
V. owensii LMG 25430	WGS Accession: GCA_000400325.1 (Patric ID: 1280004.3)[b]							
V. owensii OCN002	WGS Accession: GCA_000818275.1 (Patric ID: 696485.17)[b]							
V. owensii R-40901	AB609125.1	GU078679.1	GU078686.1	GU078680.1	GU078692.1	GU078693.1	GU078697.1	DQ907503.1
V. owensii SH14	WGS Accession: GCF_001310575.1 (Patric ID: 696485.20)[b]							
V. parahaemolyticus LMG 2850	DQ449618.1	DQ907367.1	DQ907440.1	AB298239.1	LMG 2850T[a]	AJ842490.1	AJ842677.1	DQ907505.1
V. pectenicida LMG 19642	DQ907301.1	DQ907368.1	DQ907441.1	AB298240.1	LMG 19642T[a]	AJ842491.1	AJ842678.1	DQ907506.1
V. pelagia ATCC 25916 = LMG 3897	DQ907302.1	DQ907369.1	DQ907442.1	AB298241.1	LMG 3897T[a]	AJ580872.1	AJ842682.1	DQ907507.1
V. porteresiae MSSRF30	KF697266.1	KF697257.1	KF697282.1	KF697274.1	KF697290.1	KF697299	KF697308.1	DQ907510.1
V. proteolyticus LMG 3772	DQ907305.1	EF114210.1	DQ907444.1	AB298261.1	LMG 3772T[a]	AJ842499.1	AJ842686.1	DQ907511.1
V. rotiferianus LMG 21460	DQ449619.1	DQ907372.1	DQ907445.1	AB298244.1	LMG 21460T	AJ842688.1	AJ842688.1	KF697317.1
V. rumoiensis LMG 20038	DQ907307.1	DQ907374.1	DQ907446.1	AB298245.1	LMG 20038T[a]	AJ842503.1	AJ842690.1	KF697318.1
V. sinaloensis DSM 21326	WGS Accession: GCA_000189275.2 (Patric ID: 945550.3)[b]							
V. splendidus LMG 19031	DQ481622.1	DQ481635.1	DQ481647.1	AB298248.1	LMG 19031T[a]	AJ842725.1	AJ842725.1	AB298248
V. tapetis LMG 19706	DQ907311.1	DQ907379.1	DQ907451.1	AB298249.1	HE795189.1	HE795219.1	AJ842730.1	KF697320.1
V. tubiashii LMG 10936	DQ907312.1	DQ907381.1	DQ907453.1	AB298251.1	LMG 10936T[a]	AJ842734.1	AJ842734.1	GU969227.1
V. tubiashii T33	WGS Accession: GCA_000775715.1 (Patric ID: 29498.5)[b]							
V. variabilis R-40492 = CAIM 1454	KF666686.1	GU929926.1	GU929930.1	GU929928.1	GU929932.1	GU929934.1	GU929936.1	GU929938.1
V. vulnificus LMG 13545	DQ907313.1	DQ907382.1	DQ907454.1	AB298252.1	GQ382226.1	AJ842523.1	AJ842737.1	DQ907522.1
Vibrio sp. EJY3	WGS Accession: GCA_000241385.1 (Patric ID: 1116375.3)[b]							

[a] Sequence retrieved from http://www.taxvibrio.lncc.br/project

[b] Sequence retrieved from https://www.patricbrc.org

Table S3.2. Data for calculation of the weighted mean 16S gene copy number for *Acropora palmata* surface mucus layer bacterial communities.

Qiime taxa[a]	taxa mean[a]	rrnDB taxonomic level[b]	16s copy no.[b]	mean*copy no.
k__Bacteria;Other;Other;Other;Other	4.70E-03	Bacteria	4.6	2.16E-02
k__Bacteria;p__[Thermi];c__Deinococci;o__Deinococcales;f__Trueperaceae	0.00E+00	Trueperaceae	2	0.00E+00
k__Bacteria;p__Acidobacteria;c__Acidobacteria-6;o__CCU21;f__	1.91E-05	Acidobacteria_Gp6	1	1.91E-05
k__Bacteria;p__Acidobacteria;c__Acidobacteriia;o__Acidobacteriales;f__Acidobacteriaceae	0.00E+00	Acidobacteria	1.28	0.00E+00
k__Bacteria;p__Acidobacteria;c__AT-s2-57;o__;f__	0.00E+00	Acidobacteria	1.28	0.00E+00
k__Bacteria;p__Acidobacteria;c__AT-s54;o__;f__	0.00E+00	Acidobacteria	1.28	0.00E+00
k__Bacteria;p__Acidobacteria;c__RB25;o__;f__	3.51E-05	Acidobacteria	1.28	4.49E-05
k__Bacteria;p__Acidobacteria;c__Solibacteres;o__Solibacterales;f__PAUC26f	0.00E+00	Acidobacteria	1.28	0.00E+00
k__Bacteria;p__Acidobacteria;c__Sva0725;o__Sva0725;f__	0.00E+00	Acidobacteria	1.28	0.00E+00
k__Bacteria;p__Actinobacteria;c__Acidimicrobiia;o__Acidimicrobiales;f__	1.63E-05	Acidimicrobiales	1.5	2.44E-05
k__Bacteria;p__Actinobacteria;c__Acidimicrobiia;o__Acidimicrobiales;f__C111	1.79E-04	Acidimicrobiales	1.5	2.68E-04
k__Bacteria;p__Actinobacteria;c__Acidimicrobiia;o__Acidimicrobiales;f__JdFBGBact	0.00E+00	Acidimicrobiales	1.5	0.00E+00
k__Bacteria;p__Actinobacteria;c__Acidimicrobiia;o__Acidimicrobiales;f__koll13	2.87E-05	Acidimicrobiales	1.5	4.30E-05
k__Bacteria;p__Actinobacteria;c__Acidimicrobiia;o__Acidimicrobiales;f__ntu14	7.52E-05	Acidimicrobiales	1.5	1.13E-04
k__Bacteria;p__Actinobacteria;c__Acidimicrobiia;o__Acidimicrobiales;f__OCS155	4.59E-02	Acidimicrobiales	1.5	6.88E-02
k__Bacteria;p__Actinobacteria;c__Acidimicrobiia;o__Acidimicrobiales;f__SC3-41	0.00E+00	Acidimicrobiales	1.5	0.00E+00
k__Bacteria;p__Actinobacteria;c__Acidimicrobiia;o__Acidimicrobiales;f__wb1_P06	2.47E-04	Acidimicrobiales	1.5	3.70E-04
k__Bacteria;p__Actinobacteria;c__Acidimicrobiia;o__Acidimicrobiales;Other	1.04E-04	Acidimicrobiales	1.5	1.56E-04
k__Bacteria;p__Actinobacteria;c__Actinobacteria;o__Actinomycetales;f__	2.74E-04	Actinomycetales	3.44	9.43E-04
k__Bacteria;p__Actinobacteria;c__Actinobacteria;o__Actinomycetales;f__Actinomycetaceae	1.22E-04	Actinomycetaceae	2.73	3.33E-04
k__Bacteria;p__Actinobacteria;c__Actinobacteria;o__Actinomycetales;f__Corynebacteriaceae	3.25E-04	Corynebacteriaceae	4.44	1.44E-03
k__Bacteria;p__Actinobacteria;c__Actinobacteria;o__Actinomycetales;f__Dietziaceae	2.40E-03	Actinomycetales	3.44	8.26E-03
k__Bacteria;p__Actinobacteria;c__Actinobacteria;o__Actinomycetales;f__Gordoniaceae	0.00E+00	Actinomycetales	3.44	0.00E+00
k__Bacteria;p__Actinobacteria;c__Actinobacteria;o__Actinomycetales;f__Intrasporangiaceae	2.47E-05	Intrasporangiaceae	2	4.95E-05
k__Bacteria;p__Actinobacteria;c__Actinobacteria;o__Actinomycetales;f__Microbacteriaceae	2.50E-03	Microbacteriaceae	2.28	5.70E-03
k__Bacteria;p__Actinobacteria;c__Actinobacteria;o__Actinomycetales;f__Micrococcaceae	9.11E-04	Micrococcaceae	3.1	2.82E-03
k__Bacteria;p__Actinobacteria;c__Actinobacteria;o__Actinomycetales;f__Micromonosporaceae	3.15E-05	Micromonosporaceae	3.44	1.08E-04
k__Bacteria;p__Actinobacteria;c__Actinobacteria;o__Actinomycetales;f__Mycobacteriaceae	0.00E+00	Mycobacteriaceae	2.1	0.00E+00
k__Bacteria;p__Actinobacteria;c__Actinobacteria;o__Actinomycetales;f__Nocardiaceae	1.34E-03	Nocardiaceae	3.39	4.55E-03
k__Bacteria;p__Actinobacteria;c__Actinobacteria;o__Actinomycetales;f__Nocardioidaceae	6.57E-05	Nocardioidaceae	2.11	1.39E-04

k__Bacteria;p__Actinobacteria;c__Actinobacteria;o__Actinomycetales;f__Nocardiopsaceae	4.31E-04	Nocardiopsaceae	4.5	1.94E-03
k__Bacteria;p__Actinobacteria;c__Actinobacteria;o__Actinomycetales;f__Propionibacteriaceae	4.08E-04	Propionibacteriaceae	2.03	8.29E-04
k__Bacteria;p__Actinobacteria;c__Actinobacteria;o__Actinomycetales;f__Sanguibacteraceae	3.26E-05	Sanguibacteraceae	4	1.30E-04
k__Bacteria;p__Actinobacteria;c__Actinobacteria;o__Actinomycetales;f__Sporichthyaceae	0.00E+00	Actinomycetales	3.44	0.00E+00
k__Bacteria;p__Actinobacteria;c__Actinobacteria;o__Actinomycetales;Other	3.02E-04	Actinomycetales	3.44	1.04E-03
k__Bacteria;p__Actinobacteria;c__Thermoleophilia;o__Gaiellales;f__Gaiellaceae	2.49E-05	Actinobacteria	1.89	4.70E-05
k__Bacteria;p__Bacteroidetes;c__[Rhodothermi];o__[Rhodothermales];f__[Balneolaceae]	4.24E-03	Bacteroidetes	1.73	7.34E-03
k__Bacteria;p__Bacteroidetes;c__[Rhodothermi];o__[Rhodothermales];f__Rhodothermaceae	2.49E-05	Rhodothermaceae	1	2.49E-05
k__Bacteria;p__Bacteroidetes;c__[Saprospirae];o__[Saprospirales];f__	1.71E-03	Bacteroidetes	1.73	2.96E-03
k__Bacteria;p__Bacteroidetes;c__[Saprospirae];o__[Saprospirales];f__Chitinophagaceae	1.21E-04	Chitinophagaceae	3	3.64E-04
k__Bacteria;p__Bacteroidetes;c__[Saprospirae];o__[Saprospirales];f__Saprospiraceae	9.52E-04	Saprospiraceae	2.5	2.38E-03
k__Bacteria;p__Bacteroidetes;c__Bacteroidia;o__Bacteroidales;f__	2.77E-04	Bacteroidales	3.32	9.20E-04
k__Bacteria;p__Bacteroidetes;c__Bacteroidia;o__Bacteroidales;f__Bacteroidaceae	1.20E-04	Bacteroidaceae	5.62	6.76E-04
k__Bacteria;p__Bacteroidetes;c__Bacteroidia;o__Bacteroidales;f__Marinilabiaceae	6.36E-05	Bacteroidales	3.32	2.11E-04
k__Bacteria;p__Bacteroidetes;c__Bacteroidia;o__Bacteroidales;f__Porphyromonadaceae	3.19E-04	Porphyromonadaceae	3.64	1.16E-03
k__Bacteria;p__Bacteroidetes;c__Bacteroidia;o__Bacteroidales;f__Rikenellaceae	1.72E-04	Rikenellaceae	2	3.44E-04
k__Bacteria;p__Bacteroidetes;c__Bacteroidia;o__Bacteroidales;Other	7.67E-04	Bacteroidales	3.32	2.55E-03
k__Bacteria;p__Bacteroidetes;c__BME43;o__;f__	1.02E-04	Bacteroidetes	1.73	1.77E-04
k__Bacteria;p__Bacteroidetes;c__Cytophagia;o__Cytophagales;f__[Amoebophilaceae]	3.59E-04	Cytophagia	3.02	1.08E-03
k__Bacteria;p__Bacteroidetes;c__Cytophagia;o__Cytophagales;f__Cytophagaceae	2.47E-05	Cytophagaceae	2.99	7.39E-05
k__Bacteria;p__Bacteroidetes;c__Cytophagia;o__Cytophagales;f__Flammeovirgaceae	2.56E-03	Flammeovirgaceae	4.5	1.15E-02
k__Bacteria;p__Bacteroidetes;c__Cytophagia;o__Cytophagales;Other	6.51E-05	Cytophagia	3.02	1.97E-04
k__Bacteria;p__Bacteroidetes;c__Flavobacteriia;o__Flavobacteriales;f__	7.29E-03	Flavobacteriales	1.4	1.02E-02
k__Bacteria;p__Bacteroidetes;c__Flavobacteriia;o__Flavobacteriales;f__[Weeksellaceae]	3.53E-04	Flavobacteriales	1.4	4.95E-04
k__Bacteria;p__Bacteroidetes;c__Flavobacteriia;o__Flavobacteriales;f__Cryomorphaceae	1.99E-02	Cryomorphaceae	2	3.97E-02
k__Bacteria;p__Bacteroidetes;c__Flavobacteriia;o__Flavobacteriales;f__Flavobacteriaceae	1.94E-01	Flavobacteriaceae	3.22	6.25E-01
k__Bacteria;p__Bacteroidetes;c__Flavobacteriia;o__Flavobacteriales;f__NS9	6.37E-03	Flavobacteriales	1.4	8.92E-03
k__Bacteria;p__Bacteroidetes;c__Flavobacteriia;o__Flavobacteriales;Other	2.51E-03	Flavobacteriales	1.4	3.51E-03
k__Bacteria;p__Bacteroidetes;c__Sphingobacteriia;o__Sphingobacteriales;f__	1.50E-03	Sphingobacteriales	2.79	4.18E-03
k__Bacteria;p__Bacteroidetes;c__Sphingobacteriia;o__Sphingobacteriales;f__NS11-12	3.78E-04	Sphingobacteriales	2.79	1.06E-03
k__Bacteria;p__Bacteroidetes;c__Sphingobacteriia;o__Sphingobacteriales;f__Sphingobacteriacea	2.22E-03	Sphingobacteriaceae	4.67	1.03E-02
k__Bacteria;p__Bacteroidetes;c__Sphingobacteriia;o__Sphingobacteriales;Other	1.95E-03	Sphingobacteriales	2.79	5.44E-03

k__Bacteria;p__Bacteroidetes;Other;Other;Other	1.98E-03	Bacteroidetes	1.73	3.43E-03
k__Bacteria;p__Caldithrix;c__Caldithrixae;o__Caldithrixales;f__Caldithrixaceae	2.47E-05	Bacteria	4.6	1.14E-04
k__Bacteria;p__Chlorobi;c__OPB56;o__;f__	1.63E-05	Chlorobi	1.63	2.65E-05
k__Bacteria;p__Chloroflexi;c__Anaerolineae;o__Ardenscatenales;f__Ardenscatenaceae	0.00E+00	Anaerolineae	2	0.00E+00
k__Bacteria;p__Chloroflexi;c__Anaerolineae;o__Caldilineales;f__Caldilineaceae	0.00E+00	Caldilineaceae	2	0.00E+00
k__Bacteria;p__Chloroflexi;c__Anaerolineae;o__MSB-1E9;f__	0.00E+00	Anaerolineae	2	0.00E+00
k__Bacteria;p__Chloroflexi;c__Anaerolineae;o__O4D2Z37;f__	1.63E-05	Anaerolineae	2	3.26E-05
k__Bacteria;p__Chloroflexi;c__Ellin6529;o__;f__	3.82E-05	Chloroflexi	1.79	6.85E-05
k__Bacteria;p__Chloroflexi;c__S085;o__;f__	1.63E-05	Chloroflexi	1.79	2.91E-05
k__Bacteria;p__Chloroflexi;c__SAR202;o__;f__	1.86E-04	Chloroflexi	1.79	3.32E-04
k__Bacteria;p__Chloroflexi;Other;Other;Other	2.87E-05	Chloroflexi	1.79	5.13E-05
k__Bacteria;p__Cyanobacteria;c__4C0d-2;o__MLE1-12;f__	4.38E-04	Cyanobacteria	2.35	1.03E-03
k__Bacteria;p__Cyanobacteria;c__4C0d-2;o__SM2F09;f__	0.00E+00	Cyanobacteria	2.35	0.00E+00
k__Bacteria;p__Cyanobacteria;c__4C0d-2;o__YS2;f__	7.02E-05	Cyanobacteria	2.35	1.65E-04
k__Bacteria;p__Cyanobacteria;c__Gloeobacterophycideae;o__Gloeobacterales;f__Gloeobacterace	3.26E-05	Cyanobacteria	2.35	7.65E-05
k__Bacteria;p__Cyanobacteria;c__Nostocophycideae;o__Nostocales;f__Nostocaceae	0.00E+00	Cyanobacteria	2.35	0.00E+00
k__Bacteria;p__Cyanobacteria;c__Nostocophycideae;o__Stigonematales;f__Rivulariaceae	8.60E-05	Cyanobacteria	2.35	2.02E-04
k__Bacteria;p__Cyanobacteria;c__Oscillatoriophycideae;o__Chroococcales;f__Cyanobacteriaceae	0.00E+00	Cystobacteraceae	2.33	0.00E+00
k__Bacteria;p__Cyanobacteria;c__Oscillatoriophycideae;o__Chroococcales;f__Spirulinaceae	3.51E-05	Cyanobacteria	2.35	8.25E-05
k__Bacteria;p__Cyanobacteria;c__Oscillatoriophycideae;o__Chroococcales;f__Xenococcaceae	2.23E-04	Cyanobacteria	2.35	5.24E-04
k__Bacteria;p__Cyanobacteria;c__Oscillatoriophycideae;o__Chroococcales;Other	5.83E-04	Cyanobacteria	2.35	1.37E-03
k__Bacteria;p__Cyanobacteria;c__Oscillatoriophycideae;o__Oscillatoriales;f__Phormidiaceae	0.00E+00	Cyanobacteria	2.35	0.00E+00
k__Bacteria;p__Cyanobacteria;c__Oscillatoriophycideae;o__Oscillatoriales;Other	0.00E+00	Cyanobacteria	2.35	0.00E+00
k__Bacteria;p__Cyanobacteria;c__Oscillatoriophycideae;Other;Other	0.00E+00	Cyanobacteria	2.35	0.00E+00
k__Bacteria;p__Cyanobacteria;c__Synechococcophycideae;o__Pseudanabaenales;f__Pseudanabae	2.46E-04	Cyanobacteria	2.35	5.78E-04
k__Bacteria;p__Cyanobacteria;c__Synechococcophycideae;o__Synechococcales;f__Acaryochlori	0.00E+00	Cyanobacteria	2.35	0.00E+00
k__Bacteria;p__Cyanobacteria;c__Synechococcophycideae;o__Synechococcales;f__Synechococc	1.58E-01	Cyanobacteria	2.35	3.71E-01
k__Bacteria;p__Cyanobacteria;c__Synechococcophycideae;Other;Other	0.00E+00	Cyanobacteria	2.35	0.00E+00
k__Bacteria;p__Cyanobacteria;Other;Other;Other	1.33E-03	Cyanobacteria	2.35	3.12E-03
k__Bacteria;p__Fibrobacteres;c__Fibrobacteria;o__Ucp1540;f__	8.60E-05	Fibrobacteria	3	2.58E-04
k__Bacteria;p__Firmicutes;c__Bacilli;o__Bacillales;f__[Exiguobacteraceae]	0.00E+00	Bacillales	7.71	0.00E+00
k__Bacteria;p__Firmicutes;c__Bacilli;o__Bacillales;f__Bacillaceae	4.83E-03	Bacillales	7.71	3.72E-02
k__Bacteria;p__Firmicutes;c__Bacilli;o__Bacillales;f__Paenibacillaceae	3.72E-03	Bacillales	7.71	2.87E-02

k__Bacteria;p__Firmicutes;c__Bacilli;o__Bacillales;f__Planococcaceae	0.00E+00	Planococcaceae	10.29	0.00E+00
k__Bacteria;p__Firmicutes;c__Bacilli;o__Bacillales;f__Staphylococcaceae	2.47E-05	Staphylococcaceae	4.5	1.11E-04
k__Bacteria;p__Firmicutes;c__Bacilli;o__Bacillales;f__Thermoactinomycetaceae	3.12E-05	Bacillales	7.71	2.41E-04
k__Bacteria;p__Firmicutes;c__Bacilli;o__Bacillales;Other	1.63E-05	Bacillales	7.71	1.25E-04
k__Bacteria;p__Firmicutes;c__Bacilli;o__Lactobacillales;f__	5.12E-03	Lactobacillales	5.19	2.66E-02
k__Bacteria;p__Firmicutes;c__Bacilli;o__Lactobacillales;f__Aerococcaceae	5.74E-05	Aerococcaceae	4.75	2.72E-04
k__Bacteria;p__Firmicutes;c__Bacilli;o__Lactobacillales;f__Enterococcaceae	8.79E-04	Enterococcaceae	4.72	4.15E-03
k__Bacteria;p__Firmicutes;c__Bacilli;o__Lactobacillales;f__Lactobacillaceae	3.06E-05	Lactobacillaceae	4.68	1.43E-04
k__Bacteria;p__Firmicutes;c__Bacilli;o__Lactobacillales;f__Leuconostocaceae	3.59E-04	Leuconostocaceae	4.06	1.46E-03
k__Bacteria;p__Firmicutes;c__Bacilli;o__Lactobacillales;f__Streptococcaceae	3.53E-04	Streptococcaceae	5.44	1.92E-03
k__Bacteria;p__Firmicutes;c__Bacilli;o__Turicibacterales;f__Turicibacteraceae	0.00E+00	Bacilli	6.45	0.00E+00
k__Bacteria;p__Firmicutes;c__Bacilli;Other;Other	2.74E-04	Bacilli	6.45	1.77E-03
k__Bacteria;p__Firmicutes;c__Clostridia;o__Clostridiales;f__[Tissierellaceae]	1.12E-04	Clostridiales	5.36	6.00E-04
k__Bacteria;p__Firmicutes;c__Clostridia;o__Clostridiales;f__Clostridiaceae	3.39E-04	Clostridiales	5.36	1.81E-03
k__Bacteria;p__Firmicutes;c__Clostridia;o__Clostridiales;f__Lachnospiraceae	1.17E-04	Lachnospiraceae	6	7.04E-04
k__Bacteria;p__Firmicutes;c__Clostridia;o__Clostridiales;f__Ruminococcaceae	1.46E-04	Ruminococcaceae	2.94	4.30E-04
k__Bacteria;p__Firmicutes;c__Clostridia;o__Clostridiales;f__Veillonellaceae	5.73E-05	Clostridiales	5.36	3.07E-04
k__Bacteria;p__Firmicutes;c__Clostridia;o__Clostridiales;Other	3.27E-04	Clostridiales	5.36	1.75E-03
k__Bacteria;p__Firmicutes;c__Clostridia;o__Thermoanaerobacterales;f__Caldicellulosiruptoracea	0.00E+00	Clostridia	3.4	0.00E+00
k__Bacteria;p__Firmicutes;c__Erysipelotrichi;o__Erysipelotrichales;f__Erysipelotrichaceae	7.02E-05	Erysipelotrichaceae	9.15	6.42E-04
k__Bacteria;p__Firmicutes;Other;Other;Other	5.54E-05	Firmicutes	4.04	2.24E-04
k__Bacteria;p__Fusobacteria;c__Fusobacteriia;o__Fusobacteriales;f__Fusobacteriaceae	5.19E-03	Fusobacteriaceae	6.27	3.26E-02
k__Bacteria;p__Fusobacteria;c__Fusobacteriia;o__Fusobacteriales;f__Leptotrichiaceae	0.00E+00	Leptotrichiaceae	4.17	0.00E+00
k__Bacteria;p__Gemmatimonadetes;c__Gemm-2;o__;f__	3.06E-05	Gemmatimonadetes	1.67	5.10E-05
k__Bacteria;p__Gemmatimonadetes;c__Gemm-4;o__;f__	0.00E+00	Gemmatimonadetes	1.67	0.00E+00
k__Bacteria;p__GN02;c__;o__;f__	1.48E-04	Bacteria	4.6	6.79E-04
k__Bacteria;p__GN02;c__3BR-5F;o__;f__	2.49E-04	Bacteria	4.6	1.14E-03
k__Bacteria;p__GN02;c__BD1-5;o__;f__	3.94E-04	Bacteria	4.6	1.81E-03
k__Bacteria;p__GN02;c__GKS2-174;o__;f__	3.19E-04	Bacteria	4.6	1.47E-03
k__Bacteria;p__GN02;c__GN07;o__;f__	3.26E-05	Bacteria	4.6	1.50E-04
k__Bacteria;p__GN02;c__GN10;o__;f__	0.00E+00	Bacteria	4.6	0.00E+00
k__Bacteria;p__GN02;c__IIB17;o__;f__	1.41E-04	Bacteria	4.6	6.48E-04
k__Bacteria;p__GN02;Other;Other;Other	4.46E-03	Bacteria	4.6	2.05E-02
k__Bacteria;p__Lentisphaerae;c__[Lentisphaeria];o__Lentisphaerales;f__	0.00E+00	Bacteria	4.6	0.00E+00

k__Bacteria;p__Lentisphaerae;c__[Lentisphaeria];o__Lentisphaerales;f__Arctic95B-10	4.88E-05	Bacteria	4.6	2.25E-04
k__Bacteria;p__Lentisphaerae;c__[Lentisphaeria];o__Lentisphaerales;f__Lentisphaeraceae	3.52E-04	Bacteria	4.6	1.62E-03
k__Bacteria;p__Lentisphaerae;c__[Lentisphaeria];o__Lentisphaerales;Other	7.02E-05	Bacteria	4.6	3.23E-04
k__Bacteria;p__Lentisphaerae;c__[Lentisphaeria];o__Victivallales;f__Victivallaceae	1.30E-04	Bacteria	4.6	5.96E-04
k__Bacteria;p__Lentisphaerae;c__[Lentisphaeria];Other;Other	3.51E-05	Bacteria	4.6	1.61E-04
k__Bacteria;p__Nitrospirae;c__Nitrospira;o__Nitrospirales;f__Nitrospiraceae	2.49E-05	Nitrospiraceae	1.42	3.53E-05
k__Bacteria;p__OD1;c__;o__;f__	6.86E-05	Bacteria	4.6	3.15E-04
k__Bacteria;p__OD1;c__ABY1;o__;f__	2.49E-05	Bacteria	4.6	1.14E-04
k__Bacteria;p__OD1;c__ZB2;o__;f__	8.65E-04	Bacteria	4.6	3.98E-03
k__Bacteria;p__OD1;Other;Other;Other	2.47E-05	Bacteria	4.6	1.14E-04
k__Bacteria;p__OP3;c__koll11;o__GIF10;f__kpj58rc	7.46E-05	Bacteria	4.6	3.43E-04
k__Bacteria;p__Planctomycetes;c__;o__;f__	6.51E-05	Planctomycetes	1.85	1.20E-04
k__Bacteria;p__Planctomycetes;c__028H05-P-BN-P5;o__;f__	0.00E+00	Planctomycetes	1.85	0.00E+00
k__Bacteria;p__Planctomycetes;c__BD7-11;o__;f__	0.00E+00	Planctomycetes	1.85	0.00E+00
k__Bacteria;p__Planctomycetes;c__C6;o__d113;f__	5.74E-05	Deinococcales	2.75	1.58E-04
k__Bacteria;p__Planctomycetes;c__C6;o__MVS-107;f__	7.65E-05	Planctomycetes	1.85	1.42E-04
k__Bacteria;p__Planctomycetes;c__OM190;o__;f__	0.00E+00	Planctomycetes	1.85	0.00E+00
k__Bacteria;p__Planctomycetes;c__OM190;o__agg27;f__	7.91E-05	Planctomycetes	1.85	1.46E-04
k__Bacteria;p__Planctomycetes;c__OM190;o__CL500-15;f__	1.90E-04	Planctomycetes	1.85	3.52E-04
k__Bacteria;p__Planctomycetes;c__Phycisphaerae;o__Phycisphaerales;f__	9.72E-03	Phycisphaerales	1	9.72E-03
k__Bacteria;p__Planctomycetes;c__Phycisphaerae;o__Phycisphaerales;f__Phycisphaeraceae	4.49E-05	Phycisphaeraceae	1	4.49E-05
k__Bacteria;p__Planctomycetes;c__Pla3;o__;f__	1.63E-05	Planctomycetes	1.85	3.01E-05
k__Bacteria;p__Planctomycetes;c__vadinHA49;o__DH61;f__	2.87E-05	Planctomycetes	1.85	5.30E-05
k__Bacteria;p__Proteobacteria;c__Alphaproteobacteria;o__;f__	8.48E-02	Alphaproteobacteria	2.07	1.76E-01
k__Bacteria;p__Proteobacteria;c__Alphaproteobacteria;o__BD7-3;f__	1.27E-04	Alphaproteobacteria	2.07	2.63E-04
k__Bacteria;p__Proteobacteria;c__Alphaproteobacteria;o__Caulobacterales;f__Caulobacteraceae	8.50E-04	Caulobacteraceae	2	1.70E-03
k__Bacteria;p__Proteobacteria;c__Alphaproteobacteria;o__Kiloniellales;f__	2.33E-03	Alphaproteobacteria	2.07	4.83E-03
k__Bacteria;p__Proteobacteria;c__Alphaproteobacteria;o__Kiloniellales;f__Kiloniellaceae	0.00E+00	Alphaproteobacteria	2.07	0.00E+00
k__Bacteria;p__Proteobacteria;c__Alphaproteobacteria;o__Kordiimonadales;f__	0.00E+00	Alphaproteobacteria	2.07	0.00E+00
k__Bacteria;p__Proteobacteria;c__Alphaproteobacteria;o__Kordiimonadales;f__Kordiimonadacea	4.10E-05	Alphaproteobacteria	2.07	8.49E-05
k__Bacteria;p__Proteobacteria;c__Alphaproteobacteria;o__Kordiimonadales;Other	0.00E+00	Alphaproteobacteria	2.07	0.00E+00
k__Bacteria;p__Proteobacteria;c__Alphaproteobacteria;o__Rhizobiales;f__Aurantimonadaceae	1.34E-04	Aurantimonadaceae	2	2.68E-04
k__Bacteria;p__Proteobacteria;c__Alphaproteobacteria;o__Rhizobiales;f__Beijerinckiaceae	0.00E+00	Beijerinckiaceae	2.33	0.00E+00
k__Bacteria;p__Proteobacteria;c__Alphaproteobacteria;o__Rhizobiales;f__Bradyrhizobiaceae	1.15E-03	Bradyrhizobiaceae	1.39	1.60E-03

k__Bacteria;p__Proteobacteria;c__Alphaproteobacteria;o__Rhizobiales;f__Brucellaceae	1.59E-03	Brucellaceae	3.64	5.81E-03
k__Bacteria;p__Proteobacteria;c__Alphaproteobacteria;o__Rhizobiales;f__Cohaesibacteraceae	0.00E+00	Rhizobiales	2.38	0.00E+00
k__Bacteria;p__Proteobacteria;c__Alphaproteobacteria;o__Rhizobiales;f__Hyphomicrobiaceae	2.72E-03	Hyphomicrobiaceae	1.83	4.98E-03
k__Bacteria;p__Proteobacteria;c__Alphaproteobacteria;o__Rhizobiales;f__Methylobacteriaceae	7.49E-03	Methylobacteriaceae	5.82	4.36E-02
k__Bacteria;p__Proteobacteria;c__Alphaproteobacteria;o__Rhizobiales;f__Phyllobacteriaceae	1.47E-02	Phyllobacteriaceae	2	2.94E-02
k__Bacteria;p__Proteobacteria;c__Alphaproteobacteria;o__Rhizobiales;f__Rhizobiaceae	2.21E-04	Rhizobiaceae	3.08	6.82E-04
k__Bacteria;p__Proteobacteria;c__Alphaproteobacteria;o__Rhizobiales;Other	2.51E-04	Rhizobiales	2.38	5.97E-04
k__Bacteria;p__Proteobacteria;c__Alphaproteobacteria;o__Rhodobacterales;f__Hyphomonadacea	2.87E-05	Hyphomonadaceae	1.67	4.79E-05
k__Bacteria;p__Proteobacteria;c__Alphaproteobacteria;o__Rhodobacterales;f__Rhodobacteraceae	6.82E-02	Rhodobacteraceae	2.86	1.95E-01
k__Bacteria;p__Proteobacteria;c__Alphaproteobacteria;o__Rhodobacterales;Other	2.47E-05	Rhodobacterales	2.86	7.07E-05
k__Bacteria;p__Proteobacteria;c__Alphaproteobacteria;o__Rhodospirillales;f__	7.46E-05	Rhodospirillales	3.62	2.70E-04
k__Bacteria;p__Proteobacteria;c__Alphaproteobacteria;o__Rhodospirillales;f__Acetobacteraceae	0.00E+00	Acetobacteraceae	4.06	0.00E+00
k__Bacteria;p__Proteobacteria;c__Alphaproteobacteria;o__Rhodospirillales;f__Rhodospirillaceae	5.07E-03	Rhodospirillaceae	3.19	1.62E-02
k__Bacteria;p__Proteobacteria;c__Alphaproteobacteria;o__Rhodospirillales;Other	0.00E+00	Rhodospirillales	3.62	0.00E+00
k__Bacteria;p__Proteobacteria;c__Alphaproteobacteria;o__Rickettsiales;f__	3.12E-03	Rickettsiales	1	3.12E-03
k__Bacteria;p__Proteobacteria;c__Alphaproteobacteria;o__Rickettsiales;f__AEGEAN_112	2.04E-02	Rickettsiales	1	2.04E-02
k__Bacteria;p__Proteobacteria;c__Alphaproteobacteria;o__Rickettsiales;f__Pelagibacteraceae	5.05E-02	Rickettsiales	1	5.05E-02
k__Bacteria;p__Proteobacteria;c__Alphaproteobacteria;o__Rickettsiales;f__Rickettsiaceae	2.72E-04	Rickettsiaceae	1	2.72E-04
k__Bacteria;p__Proteobacteria;c__Alphaproteobacteria;o__Rickettsiales;Other	1.25E-03	Rickettsiales	1	1.25E-03
k__Bacteria;p__Proteobacteria;c__Alphaproteobacteria;o__Sphingomonadales;f__	0.00E+00	Sphingomonadales	1.68	0.00E+00
k__Bacteria;p__Proteobacteria;c__Alphaproteobacteria;o__Sphingomonadales;f__Erythrobacterac	1.05E-04	Erythrobacteraceae	1.17	1.23E-04
k__Bacteria;p__Proteobacteria;c__Alphaproteobacteria;o__Sphingomonadales;f__Sphingomonada	6.31E-04	Sphingomonadaceae	2.2	1.39E-03
k__Bacteria;p__Proteobacteria;c__Alphaproteobacteria;Other;Other	2.75E-02	Alphaproteobacteria	2.07	5.68E-02
k__Bacteria;p__Proteobacteria;c__Betaproteobacteria;o__Burkholderiales;f__Alcaligenaceae	1.55E-03	Alcaligenaceae	2.8	4.33E-03
k__Bacteria;p__Proteobacteria;c__Betaproteobacteria;o__Burkholderiales;f__Burkholderiaceae	6.61E-04	Burkholderiaceae	3.56	2.35E-03
k__Bacteria;p__Proteobacteria;c__Betaproteobacteria;o__Burkholderiales;f__Comamonadaceae	1.95E-03	Comamonadaceae	2.68	5.23E-03
k__Bacteria;p__Proteobacteria;c__Betaproteobacteria;o__Burkholderiales;f__Oxalobacteraceae	1.29E-02	Oxalobacteraceae	3.16	4.07E-02
k__Bacteria;p__Proteobacteria;c__Betaproteobacteria;o__Burkholderiales;Other	3.51E-05	Burkholderiales	3.4	1.19E-04
k__Bacteria;p__Proteobacteria;c__Betaproteobacteria;o__EC94;f__	3.06E-05	Betaproteobacteria	2.48	7.58E-05
k__Bacteria;p__Proteobacteria;c__Betaproteobacteria;o__Methylophilales;f__Methylophilaceae	1.37E-03	Methylophilaceae	2	2.75E-03
k__Bacteria;p__Proteobacteria;c__Betaproteobacteria;o__MWH-UniP1;f__	3.16E-04	Betaproteobacteria	2.48	7.83E-04
k__Bacteria;p__Proteobacteria;c__Betaproteobacteria;o__Neisseriales;f__Neisseriaceae	0.00E+00	Neisseriaceae	6.43	0.00E+00
k__Bacteria;p__Proteobacteria;c__Betaproteobacteria;o__Nitrosomonadales;f__Nitrosomonadacea	2.87E-05	Nitrosomonadaceae	1	2.87E-05
k__Bacteria;p__Proteobacteria;c__Betaproteobacteria;o__Rhodocyclales;f__Rhodocyclaceae	1.20E-04	Rhodocyclaceae	2.89	3.47E-04

k__Bacteria;p__Proteobacteria;c__Betaproteobacteria;Other;Other	0.00E+00	Betaproteobacteria	2.48	0.00E+00
k__Bacteria;p__Proteobacteria;c__Deltaproteobacteria;o__;f__	1.20E-04	Deltaproteobacteria	2.2	2.64E-04
k__Bacteria;p__Proteobacteria;c__Deltaproteobacteria;o__Bdellovibrionales;f__Bacteriovoracace	1.38E-03	Bacteriovoracaceae	2	2.75E-03
k__Bacteria;p__Proteobacteria;c__Deltaproteobacteria;o__Bdellovibrionales;f__Bdellovibrionace	0.00E+00	Bdellovibrionaceae	1.8	0.00E+00
k__Bacteria;p__Proteobacteria;c__Deltaproteobacteria;o__Desulfobacterales;f__Desulfobacterace	1.05E-04	Desulfobacteraceae	3.25	3.42E-04
k__Bacteria;p__Proteobacteria;c__Deltaproteobacteria;o__Desulfobacterales;f__Desulfobulbacea	3.14E-04	Desulfobulbaceae	3.5	1.10E-03
k__Bacteria;p__Proteobacteria;c__Deltaproteobacteria;o__Desulfovibrionales;f__Desulfovibriona	1.82E-04	Desulfovibrionaceae	2.73	4.96E-04
k__Bacteria;p__Proteobacteria;c__Deltaproteobacteria;o__Desulfuromonadales;f__Desulfuromona	3.06E-05	Desulfuromonadaceae	2	6.11E-05
k__Bacteria;p__Proteobacteria;c__Deltaproteobacteria;o__GMD14H09;f__	3.21E-05	Deltaproteobacteria	2.2	7.06E-05
k__Bacteria;p__Proteobacteria;c__Deltaproteobacteria;o__MIZ46;f__	0.00E+00	Deltaproteobacteria	2.2	0.00E+00
k__Bacteria;p__Proteobacteria;c__Deltaproteobacteria;o__Myxococcales;f__	3.06E-05	Myxococcales	2.66	8.13E-05
k__Bacteria;p__Proteobacteria;c__Deltaproteobacteria;o__Myxococcales;f__0319-6G20	7.64E-05	Myxococcales	2.66	2.03E-04
k__Bacteria;p__Proteobacteria;c__Deltaproteobacteria;o__Myxococcales;f__Cystobacterineae	1.82E-04	Myxococcales	2.66	4.85E-04
k__Bacteria;p__Proteobacteria;c__Deltaproteobacteria;o__Myxococcales;f__Haliangiaceae	1.63E-05	Haliangiaceae	2	3.26E-05
k__Bacteria;p__Proteobacteria;c__Deltaproteobacteria;o__Myxococcales;f__Nannocystaceae	5.53E-05	Myxococcales	2.66	1.47E-04
k__Bacteria;p__Proteobacteria;c__Deltaproteobacteria;o__Myxococcales;f__OM27	1.20E-03	Myxococcales	2.66	3.19E-03
k__Bacteria;p__Proteobacteria;c__Deltaproteobacteria;o__Myxococcales;f__Polyangiaceae	2.49E-05	Polyangiaceae	3.5	8.71E-05
k__Bacteria;p__Proteobacteria;c__Deltaproteobacteria;o__Myxococcales;Other	0.00E+00	Myxococcales	2.66	0.00E+00
k__Bacteria;p__Proteobacteria;c__Deltaproteobacteria;o__NB1-j;f__	3.12E-05	Deltaproteobacteria	2.2	6.87E-05
k__Bacteria;p__Proteobacteria;c__Deltaproteobacteria;o__NB1-j;f__JTB38	0.00E+00	Deltaproteobacteria	2.2	0.00E+00
k__Bacteria;p__Proteobacteria;c__Deltaproteobacteria;o__NB1-j;f__NB1-i	1.63E-05	Deltaproteobacteria	2.2	3.58E-05
k__Bacteria;p__Proteobacteria;c__Deltaproteobacteria;o__NB1-j;Other	0.00E+00	Deltaproteobacteria	2.2	0.00E+00
k__Bacteria;p__Proteobacteria;c__Deltaproteobacteria;o__PB19;f__	2.95E-03	Deltaproteobacteria	2.2	6.50E-03
k__Bacteria;p__Proteobacteria;c__Deltaproteobacteria;o__Spirobacillales;f__	2.78E-04	Deltaproteobacteria	2.2	6.11E-04
k__Bacteria;p__Proteobacteria;c__Deltaproteobacteria;o__Sva0853;f__	4.22E-02	Deltaproteobacteria	2.2	9.29E-02
k__Bacteria;p__Proteobacteria;c__Deltaproteobacteria;o__Sva0853;f__JTB36	3.12E-05	Deltaproteobacteria	2.2	6.87E-05
k__Bacteria;p__Proteobacteria;c__Deltaproteobacteria;o__Sva0853;f__S25_1238	1.58E-03	Deltaproteobacteria	2.2	3.48E-03
k__Bacteria;p__Proteobacteria;c__Deltaproteobacteria;o__Syntrophobacterales;f__Syntrophobact	0.00E+00	Syntrophobacteraceae	2	0.00E+00
k__Bacteria;p__Proteobacteria;c__Deltaproteobacteria;Other;Other	5.35E-04	Deltaproteobacteria	2.2	1.18E-03
k__Bacteria;p__Proteobacteria;c__Epsilonproteobacteria;o__Campylobacterales;f__	1.99E-02	Campylobacterales	3.11	6.17E-02
k__Bacteria;p__Proteobacteria;c__Epsilonproteobacteria;o__Campylobacterales;f__Campylobacte	4.44E-04	Campylobacteraceae	3.24	1.44E-03
k__Bacteria;p__Proteobacteria;c__Epsilonproteobacteria;o__Campylobacterales;f__Helicobactera	6.42E-05	Helicobacteraceae	2.98	1.91E-04
k__Bacteria;p__Proteobacteria;c__Epsilonproteobacteria;o__Campylobacterales;Other	3.51E-05	Campylobacterales	3.11	1.09E-04
k__Bacteria;p__Proteobacteria;c__Gammaproteobacteria;o__;f__	6.57E-05	Gammaproteobacteria	2.78	1.83E-04

k__Bacteria;p__Proteobacteria;c__Gammaproteobacteria;o__[Marinicellales];f__[Marinicellaceae	3.51E-05	Gammaproteobacteria	2.78	9.76E-05
k__Bacteria;p__Proteobacteria;c__Gammaproteobacteria;o__Aeromonadales;f__Aeromonadaceae	0.00E+00	Aeromonadaceae	8.33	0.00E+00
k__Bacteria;p__Proteobacteria;c__Gammaproteobacteria;o__Alteromonadales;f__	0.00E+00	Alteromonadales	7.46	0.00E+00
k__Bacteria;p__Proteobacteria;c__Gammaproteobacteria;o__Alteromonadales;f__Alteromonadace	7.56E-04	Alteromonadaceae	4.18	3.16E-03
k__Bacteria;p__Proteobacteria;c__Gammaproteobacteria;o__Alteromonadales;f__Colwelliaceae	3.99E-04	Colwelliaceae	9	3.59E-03
k__Bacteria;p__Proteobacteria;c__Gammaproteobacteria;o__Alteromonadales;f__Ferrimonadacea	8.74E-05	Ferrimonadaceae	7	6.12E-04
k__Bacteria;p__Proteobacteria;c__Gammaproteobacteria;o__Alteromonadales;f__HTCC2188	6.38E-05	Alteromonadales	7.46	4.76E-04
k__Bacteria;p__Proteobacteria;c__Gammaproteobacteria;o__Alteromonadales;f__OM60	7.24E-04	Alteromonadales	7.46	5.40E-03
k__Bacteria;p__Proteobacteria;c__Gammaproteobacteria;o__Alteromonadales;f__Shewanellaceae	0.00E+00	Shewanellaceae	9.5	0.00E+00
k__Bacteria;p__Proteobacteria;c__Gammaproteobacteria;o__Alteromonadales;Other	1.63E-05	Alteromonadales	7.46	1.21E-04
k__Bacteria;p__Proteobacteria;c__Gammaproteobacteria;o__Chromatiales;f__	4.11E-04	Chromatiales	1.62	6.65E-04
k__Bacteria;p__Proteobacteria;c__Gammaproteobacteria;o__Chromatiales;f__Ectothiorhodospirac	2.49E-05	Ectothiorhodospiraceae	1.5	3.73E-05
k__Bacteria;p__Proteobacteria;c__Gammaproteobacteria;o__Enterobacteriales;f__Enterobacteriac	3.60E-03	Enterobacteriaceae	6.39	2.30E-02
k__Bacteria;p__Proteobacteria;c__Gammaproteobacteria;o__HOC36;f__	0.00E+00	Gammaproteobacteria	2.78	0.00E+00
k__Bacteria;p__Proteobacteria;c__Gammaproteobacteria;o__HTCC2188;f__	2.47E-05	Gammaproteobacteria	2.78	6.88E-05
k__Bacteria;p__Proteobacteria;c__Gammaproteobacteria;o__HTCC2188;f__HTCC2089	5.49E-04	Gammaproteobacteria	2.78	1.53E-03
k__Bacteria;p__Proteobacteria;c__Gammaproteobacteria;o__Legionellales;f__	2.48E-04	Legionellales	2.02	5.01E-04
k__Bacteria;p__Proteobacteria;c__Gammaproteobacteria;o__Legionellales;f__Coxiellaceae	2.19E-03	Coxiellaceae	1	2.19E-03
k__Bacteria;p__Proteobacteria;c__Gammaproteobacteria;o__Legionellales;f__Endoecteinascidiac	6.84E-05	Legionellales	2.02	1.38E-04
k__Bacteria;p__Proteobacteria;c__Gammaproteobacteria;o__Legionellales;f__Francisellaceae	5.54E-05	Francisellaceae	2.92	1.62E-04
k__Bacteria;p__Proteobacteria;c__Gammaproteobacteria;o__Legionellales;f__Legionellaceae	4.37E-05	Legionellaceae	3.05	1.33E-04
k__Bacteria;p__Proteobacteria;c__Gammaproteobacteria;o__Legionellales;Other	7.26E-04	Legionellales	2.02	1.47E-03
k__Bacteria;p__Proteobacteria;c__Gammaproteobacteria;o__Oceanospirillales;f__	8.23E-04	Oceanospirillales	3.99	3.28E-03
k__Bacteria;p__Proteobacteria;c__Gammaproteobacteria;o__Oceanospirillales;f__Endozoicimona	6.00E-05	Oceanospirillales	3.99	2.39E-04
k__Bacteria;p__Proteobacteria;c__Gammaproteobacteria;o__Oceanospirillales;f__Halomonadacea	1.06E-02	Halobacteriaceae	1.44	1.53E-02
k__Bacteria;p__Proteobacteria;c__Gammaproteobacteria;o__Oceanospirillales;f__Oceanospirillac	0.00E+00	Oceanospirillaceae	5.67	0.00E+00
k__Bacteria;p__Proteobacteria;c__Gammaproteobacteria;o__Oceanospirillales;Other	5.73E-05	Oceanospirillales	3.99	2.29E-04
k__Bacteria;p__Proteobacteria;c__Gammaproteobacteria;o__Pasteurellales;f__Pasteurellaceae	0.00E+00	Pasteurellaceae	5.93	0.00E+00
k__Bacteria;p__Proteobacteria;c__Gammaproteobacteria;o__Pseudomonadales;f__Moraxellaceae	0.00E+00	Moraxellaceae	4.61	0.00E+00
k__Bacteria;p__Proteobacteria;c__Gammaproteobacteria;o__Pseudomonadales;f__Pseudomonada	1.13E-03	Pseudomonadaceae	4.38	4.93E-03
k__Bacteria;p__Proteobacteria;c__Gammaproteobacteria;o__Thiohalorhabdales;f__	0.00E+00	Gammaproteobacteria	2.78	0.00E+00
k__Bacteria;p__Proteobacteria;c__Gammaproteobacteria;o__Thiohalorhabdales;f__Thiohalorhabd	1.63E-05	Gammaproteobacteria	2.78	4.53E-05
k__Bacteria;p__Proteobacteria;c__Gammaproteobacteria;o__Thiotrichales;f__Piscirickettsiaceae	1.91E-04	Piscirickettsiaceae	3	5.73E-04
k__Bacteria;p__Proteobacteria;c__Gammaproteobacteria;o__Thiotrichales;f__Thiotrichaceae	1.63E-05	Thiotrichaceae	2	3.26E-05

k__Bacteria;p__Proteobacteria;c__Gammaproteobacteria;o__Vibrionales;f__Pseudoalteromonadac	1.03E-04	Pseudoalteromonadaceae	9.45	9.73E-04
k__Bacteria;p__Proteobacteria;c__Gammaproteobacteria;o__Vibrionales;f__Vibrionaceae	7.62E-05	Vibrionaceae	9.16	6.98E-04
k__Bacteria;p__Proteobacteria;c__Gammaproteobacteria;o__Vibrionales;Other	6.69E-05	Vibrionales	9.16	6.13E-04
k__Bacteria;p__Proteobacteria;c__Gammaproteobacteria;o__Xanthomonadales;f__Xanthomonada	1.98E-02	Xanthomonadaceae	2.33	4.60E-02
k__Bacteria;p__Proteobacteria;c__Gammaproteobacteria;Other;Other	3.85E-03	Gammaproteobacteria	2.78	1.07E-02
k__Bacteria;p__Proteobacteria;c__TA18;o__PHOS-HD29;f__	0.00E+00	Proteobacteria	2.26	0.00E+00
k__Bacteria;p__Proteobacteria;Other;Other;Other	1.86E-03	Proteobacteria	2.26	4.20E-03
k__Bacteria;p__SAR406;c__AB16;o__Arctic96B-7;f__A714017	1.86E-02	Bacteria	4.6	8.57E-02
k__Bacteria;p__SBR1093;c__A712011;o__;f__	6.47E-04	Bacteria	4.6	2.98E-03
k__Bacteria;p__Spirochaetes;c__[Brachyspirae];o__[Brachyspirales];f__Brachyspiraceae	6.00E-05	Brachyspiraceae	1	6.00E-05
k__Bacteria;p__Spirochaetes;c__[Leptospirae];o__[Leptospirales];f__Leptospiraceae	0.00E+00	Leptospiraceae	2	0.00E+00
k__Bacteria;p__Spirochaetes;c__Spirochaetes;o__Spirochaetales;f__Spirochaetaceae	5.02E-03	Spirochaetaceae	1.63	8.18E-03
k__Bacteria;p__Tenericutes;c__Mollicutes;o__;f__	3.21E-05	Mollicutes	1.73	5.55E-05
k__Bacteria;p__Tenericutes;c__Mollicutes;o__Mycoplasmatales;f__Mycoplasmataceae	0.00E+00	Mycoplasmataceae	1.49	0.00E+00
k__Bacteria;p__TM6;c__;o__;f__	2.87E-05	Bacteria	4.6	1.32E-04
k__Bacteria;p__TM6;c__SBRH58;o__;f__	0.00E+00	Bacteria	4.6	0.00E+00
k__Bacteria;p__TM6;c__SJA-4;o__;f__	0.00E+00	Bacteria	4.6	0.00E+00
k__Bacteria;p__TM6;Other;Other;Other	1.63E-05	Bacteria	4.6	7.49E-05
k__Bacteria;p__TM7;c__;o__;f__	3.25E-04	Bacteria	4.6	1.50E-03
k__Bacteria;p__TM7;c__TM7-3;o__EW055;f__	2.90E-02	Bacteria	4.6	1.33E-01
k__Bacteria;p__TM7;c__TM7-3;Other;Other	7.32E-05	Verrucomicrobia	1.52	1.11E-04
k__Bacteria;p__Verrucomicrobia;c__Opitutae;o__Puniceicoccales;f__Puniceicoccaceae	3.77E-04	Puniceicoccaceae	2	7.53E-04
k__Bacteria;p__Verrucomicrobia;c__Verruco-5;o__R76-B128;f__	1.84E-04	Verrucomicrobia	1.52	2.80E-04
k__Bacteria;p__Verrucomicrobia;c__Verruco-5;o__SS1-B-03-39;f__	0.00E+00	Verrucomicrobia	1.52	0.00E+00
k__Bacteria;p__Verrucomicrobia;c__Verruco-5;Other;Other	3.06E-05	Verrucomicrobia	1.52	4.64E-05
k__Bacteria;p__Verrucomicrobia;c__Verrucomicrobiae;o__Verrucomicrobiales;f__Verrucomicrobi	0.00E+00	Verrucomicrobiaceae	3	0.00E+00
k__Bacteria;p__WS3;c__PRR-12;o__GN03;f__KSB4	0.00E+00	Bacteria	4.6	0.00E+00
k__Bacteria;p__WS3;c__PRR-12;o__GN03;Other	7.65E-05	Bacteria	4.6	3.52E-04
k__Bacteria;p__WS6;c__B142;o__;f__	0.00E+00	Bacteria	4.6	0.00E+00
k__Bacteria;p__ZB3;c__BS119;o__;f__	2.16E-04	Bacteria	4.6	9.93E-04

[a] Qiime taxa and mean from the file “subset_L5.biom” available at http://portal.nersc.gov/dna/MEP/oldcores/CoralPaper2015/testresults.tar.gz

[b] Based on rrnDB version 5.0 (updated 12/23/2016) available at https://rrndb.umms.med.umich.edu 2/1/2017

Table S3.3 Sea temperatures during late summer sampling periods.

	2012			2013			2014		
Week	Mean	Stdev.	N	Mean	Stdev.	N	Mean	Stdev.	N
29	28.2	1.2	766.0	28.0	1.5	417.0	30.2	1.0	753.0
30	28.7	1.5	842.0	29.7	1.2	1236.0	29.6	0.8	987.0
31	29.9	0.8	1330.0	29.1	1.6	714.0	31.0	1.4	656.0
32	28.8	1.3	984.0	29.2	1.3	734.0	30.6	1.1	1259.0

Data downloaded from: http://optics.marine.usf.edu/cgi-bin/vb?area=FK&station=07

APPENDIX B

SUPPLEMENTARY MATERIALS FOR CHAPTER 4

S4.1. Disease survey results.

	Date						
Colony	6/25	7/3	7/12	7/13	7/14	7/22	7/24
LK-Apal-13	0	0	—	0	0	0	0
LK-Apal-18	0	0	—	0	0	—	6
LK-Apal-19	0	3	—	0	0	6	5
LK-Apal-21	0	0	—	0	0	0	0
LK-Apal-24	0	2	—	0	1	17	
LK-Apal-30	0	4	—	0	4	—	21
LK-Apal-57	0	1	—	0	0	10	12
LK-Apal-59	0	2	0	0	0	—	7
LK-Apal-60	0	3	0	0	0	—	7
LK-Apal-62	0	0	0	0	1	—	17
LK-Apal-64	0	0	0	0	0	—	9
LK-Apal-65	0	0	—	1	1	—	4
LK-Apal-66	0	1	—	2	2	—	32
LK-Apal-68	0	0	—	1	1	4	—
LK-Apal-70	0	0	0	0	0	1	—
LK-Apal-71	0	0	0	0	0	15	—
LK-Apal-72	0	0	0	0	0	0	0
LK-Apal-73	0	1	—	0	3	—	7
LK-Apal-74	0	1	—	0	0	18	—
Total number of lesions	0	18	0	4	13	0	127
Prevalence (% colonies diseased)	0	47.4	0	15.8	36.8	70.0	78.6
Severity (no. lesions per diseased colony)	0	2	0	1.3	1.9	10.1	11.5
Severity (no. lesions per colony)	0	1	0	0.22	0.7	3.9	7.1

Table S4.2. List of barcodes and metadata.

Sample_ID	I5_Index	I7_Index	Collection date	Sample type	Colony id	Lesion age	Distance
LKTS.24h.126	CTACAGCA	ATCGTTGG	7.14.15	Pox	Apl-73	24h.PX	front
LKTS.24h.127	GACACTGT	ATCGTTGG	7.14.15	DH	Apl-73	24h.PX	2.cm
LKTS.24h.128	TCTGTGTC	ATCGTTGG	7.14.15	DH	Apl-73	24h.PX	10.cm
LKTS.24h.29	AGTCGACT	TAGCAACC	7.14.15	Pox	Apl-24	24h.PX	front
LKTS.24h.30	CCATCCTA	TAGCAACC	7.14.15	DH	Apl-24	24h.PX	2.cm
LKTS.24h.31	GTCAAGAG	TAGCAACC	7.14.15	DH	Apl-24	24h.PX	10.cm
LKTS.24h.44	TTCGTTCG	GTGACTCA	7.14.15	DH	Apl-30	24h.PX	10.cm
LKTS.24h.65	AACCAACC	TTCGTTCG	7.14.15	Pox	Apl-62	24h.PX	front
LKTS.24h.66	CCAACCAA	TTCGTTCG	7.14.15	DH	Apl-62	24h.PX	2.cm
LKTS.24h.67	GGTTGGTT	TTCGTTCG	7.14.15	DH	Apl-62	24h.PX	10.cm
LKTS.24h.74	CGTTCGTT	TTCGTTCG	7.13.15	Pox	Apl-65	24h.PX	front
LKTS.24h.75	TAGGTTGC	TCACAGAC	7.13.15	DH	Apl-65	24h.PX	2.cm
LKTS.24h.87	GTCAAGAG	ACACAGTC	7.13.15	Pox	Apl-66	24h.PX	front
LKTS.24h.88	TAGGTTGC	ACACAGTC	7.13.15	DH	Apl-66	24h.PX	2.cm
LKTS.24h.89	AAGCAAGC	ACACAGTC	7.13.15	DH	Apl-66	24h.PX	10.cm
LKTS.24h.96	TCTGTGTC	ACACAGTC	7.13.15	Pox	Apl-68	24h.PX	front
LKTS.24h.97	AACCAACC	CGATGGTT	7.13.15	DH	Apl-68	24h.PX	2.cm
LKTS.3.5d.107	GCAAGCAA	CGATGGTT	7.19.15	Pox	Apl-71	3.5d.PX	front
LKTS.3.5d.108	TTCGTTCG	CGATGGTT	7.19.15	DH	Apl-71	3.5d.PX	2.cm
LKTS.3.5d.109	AGGTGAAC	CGATGGTT	7.19.15	DH	Apl-71	3.5d.PX	10.cm
LKTS.3.5d.68	TTGGTTGG	TTCGTTCG	7.19.15	Pox	Apl-62	3.5d.PX	front
LKTS.3.5d.69	AGTCGACT	TTCGTTCG	7.19.15	DH	Apl-62	3.5d.PX	2.cm
LKTS.3.5d.70	CCATCCTA	TTCGTTCG	7.19.15	DH	Apl-62	3.5d.PX	10.cm
LKTS.3.5d.71	GTCAAGAG	TTCGTTCG	7.20.15	Pox	Apl-62	3.5d.PX	front
LKTS.3.5d.72	TAGGTTGC	TTCGTTCG	7.20.15	DH	Apl-62	3.5d.PX	2.cm
LKTS.3.5d.73	AAGCAAGC	TTCGTTCG	7.20.15	DH	Apl-62	3.5d.PX	10.cm
LKTS.3.5d.77	AGGTGAAC	TTCGTTCG	7.19.15	Pox	Apl-65	3.5d.PX	front
LKTS.3.5d.78	CTACAGCA	TTCGTTCG	7.19.15	DH	Apl-65	3.5d.PX	2.cm
LKTS.3.5d.79	GACACTGT	TTCGTTCG	7.19.15	DH	Apl-65	3.5d.PX	10.cm
LKTS.3.5d.84	TTGGTTGG	ACACAGTC	7.19.15	Pox	Apl-66	3.5d.PX	front
LKTS.3.5d.85	AGTCGACT	ACACAGTC	7.19.15	DH	Apl-66	3.5d.PX	2.cm
LKTS.3.5d.86	CCATCCTA	ACACAGTC	7.19.15	DH	Apl-66	3.5d.PX	10.cm
LKTS.3.5d.98	CCAACCAA	CGATGGTT	7.19.15	Pox	Apl-68	3.5d.PX	front
LKTS.3.5d.99	GGTTGGTT	CGATGGTT	7.19.15	DH	Apl-68	3.5d.PX	2.cm
LKTS.8.10d.101	AGTCGACT	CGATGGTT	7.29.15	Pox	Apl-68	8.10d.PX	front
LKTS.8.10d.103	GTCAAGAG	CGATGGTT	7.29.15	DH	Apl-68	8.10d.PX	10.cm
LKTS.8.10d.114	CCAACCAA	ATCGTTGG	7.29.15	Pox	Apl-71	8.10d.PX	front
LKTS.8.10d.115	GGTTGGTT	ATCGTTGG	7.29.15	DH	Apl-71	8.10d.PX	2.cm
LKTS.8.10d.116	TTGGTTGG	ATCGTTGG	7.29.15	DH	Apl-71	8.10d.PX	10.cm

LKTS.8.10d.133	AGTCGACT	AGTGTCTG	7.29.15	Pox	Apl-73	8.10d.PX	front
LKTS.8.10d.134	CCATCCTA	AGTGTCTG	7.29.15	DH	Apl-73	8.10d.PX	2.cm
LKTS.8.10d.135	GTCAAGAG	AGTGTCTG	7.29.15	DH	Apl-73	8.10d.PX	10.cm
LKTS.8.10d.93	AGGTGAAC	ACACAGTC	7.29.15	Pox	Apl-66	8.10d.PX	front
LKTS.8.10d.94	CTACAGCA	ACACAGTC	7.29.15	DH	Apl-66	8.10d.PX	2.cm
LKTS.8.10d.95	GACACTGT	ACACAGTC	7.29.15	DH	Apl-66	8.10d.PX	10.cm
LKTS.H.117	AGTCGACT	ATCGTTGG	6.27.15	healthy	Apl-72		
LKTS.H.118	CCATCCTA	ATCGTTGG	7.3.15	healthy	Apl-72		
LKTS.H.119	GTCAAGAG	ATCGTTGG	7.13.15	healthy	Apl-13		
LKTS.H.120	TAGGTTGC	ATCGTTGG	6.27.15	healthy	Apl-73		
LKTS.H.125	AGGTGAAC	ATCGTTGG	7.12.15	healthy	Apl-73		
LKTS.H.143	CTACAGCA	AGTGTCTG	6.27.15	healthy	Apl-29		
LKTS.H.32	TAGGTTGC	TAGCAACC	7.3.15	healthy	Apl-13		
LKTS.H.39	GTCAAGAG	CCAACGTA	7.13.15	healthy	Apl-21		
LKTS.H.40	TAGGTTGC	CCAACGTA	7.3.15	healthy	Apl-21		
LKTS.H.54	CCATCCTA	CGTAGCAT	6.27.15	healthy	Apl-57		
LKTS.H.59	GCAAGCAA	CGTAGCAT	7.12.15	healthy	Apl-57		
LKTS.H.63	GACACTGT	CGTAGCAT	7.3.15	healthy	Apl-62		
LKTS.H.64	TCTGTGTC	CGTAGCAT	7.12.15	healthy	Apl-62		
LKTS.H.76	TTCGTTCG	TTCGTTCG	7.12.15	healthy	Apl-64		
LKTS.H.80	TCTGTGTC	TTCGTTCG	6.27.15	healthy	Apl-66		
LKTS.H.82	CCAACCAA	ACACAGTC	7.12.15	healthy	Apl-66		
LKTS.H.83	GGTTGGTT	ACACAGTC	7.12.15	healthy	Apl-72		
LKTS.W.1	AACCAACC	GTGTGTGT	6.27.15	water			
LKTS.W.10	CGTTCGTT	GTGTGTGT	7.13.15	water			
LKTS.W.11	GCAAGCAA	GTGTGTGT	7.13.15	water			
LKTS.W.12	TTCGTTCG	GTGTGTGT	7.13.15	water			
LKTS.W.14	CTACAGCA	GTGTGTGT	7.14.15	water			
LKTS.W.15	GACACTGT	GTGTGTGT	7.19.15	water			
LKTS.W.16	TCTGTGTC	GTGTGTGT	7.19.15	water			
LKTS.W.18	CCAACCAA	TGTCTCAC	7.20.15	water			
LKTS.W.19	AACCAACC	TCACAGAC	7.20.15	water			
LKTS.W.2	CCAACCAA	GTGTGTGT	6.27.15	water			
LKTS.W.21	AGTCGACT	TGTCTCAC	7.24.15	water			
LKTS.W.22	CCATCCTA	TGTCTCAC	7.24.15	water			
LKTS.W.23	GTCAAGAG	TGTCTCAC	7.29.15	water			
LKTS.W.24	TAGGTTGC	TGTCTCAC	7.29.15	water			
LKTS.W.25	AACCAACC	TAGCAACC	7.29.15	water			
LKTS.W.3	GGTTGGTT	GTGTGTGT	6.27.15	water			
LKTS.W.4	TTGGTTGG	GTGTGTGT	7.3.15	water			
LKTS.W.5	AGTCGACT	GTGTGTGT	7.3.15	water			
LKTS.W.6	CCATCCTA	GTGTGTGT	7.3.15	water			
LKTS.W.7	GTCAAGAG	GTGTGTGT	7.12.15	water			

LKTS.W.8	TAGGTTGC	GTGTGTGT	7.12.15	water
LKTS.W.9	AAGCAAGC	GTGTGTGT	7.12.15	water

Table S4.3. Significant Lefse indicator families (LDA > 2) for each sample type.

Sample	Taxa	LDA	$P_{(KW)}$*
healthy	p__Proteobacteria.c__Gammaproteobacteria.o__Oceanospirillales.f__Halomonadaceae	4.64	0.016
	p__Bacteroidetes.c__Flavobacteriia.o__Flavobacteriales.f__Flavobacteriaceae	4.39	0.003
	p__Proteobacteria.c__Alphaproteobacteria.o__Rhodobacterales.f__Rhodobacteraceae	4.09	0.000
≤ 24 h			
front	p__Proteobacteria.c__Gammaproteobacteria.o__Vibrionales.f__Vibrionaceae	5.26	0.007
front	p__Proteobacteria.c__Epsilonproteobacteria.o__Campylobacterales.f__Campylobacteraceae	4.01	0.008
front	p__Proteobacteria.c__Gammaproteobacteria.o__Alteromonadales.f__Ferrimonadaceae	3.82	0.021
front	p__Firmicutes.c__Clostridia.o__Clostridiales.f__Acidaminobacteraceae_	3.55	0.028
10 cm	p__Proteobacteria.c__Gammaproteobacteria.o__Legionellales.f__Francisellaceae	4.14	0.004
10 cm	p__Bacteroidetes.c__Flavobacteriia.o__Flavobacteriales.f__Cryomorphaceae	3.91	0.021
3−5 d			
front	p__Proteobacteria.c__Gammaproteobacteria.o__Oceanospirillales.f__Oceanospirillaceae	3.87	0.040
front	p__Firmicutes.c__Clostridia.o__Clostridiales.f__Lachnospiraceae	2.89	0.021
front	p__Proteobacteria.c__Alphaproteobacteria.o__Kiloniellales.f__Kiloniellaceae	2.84	0.013
front	p__Proteobacteria.c__Alphaproteobacteria.o__Rhodobacterales.f__Hyphomonadaceae	2.82	0.000
2 cm	p__Proteobacteria.c__Deltaproteobacteria.o__Desulfobacterales.f__Desulfobacteraceae	3.12	0.040
2 cm	p__Tenericutes.c__Mollicutes.o__Acholeplasmatales.f__Acholeplasmataceae	2.98	0.003
10 cm	p__Proteobacteria.c__Alphaproteobacteria.o__Rickettsiales.f__Pelagibacteraceae	4.57	0.008
10 cm	p__Proteobacteria.c__Alphaproteobacteria.o__Rickettsiales.f__AEGEAN_112	3.79	0.000
8−10 d			
front	p__Proteobacteria.c__Gammaproteobacteria.o__Alteromonadales.f__Colwelliaceae	3.85	0.000
front	p__Bacteroidetes.c__Cytophagia.o__Cytophagales.f__Flammeovirgaceae	3.84	0.003
front	p__Verrucomicrobia.c__Verrucomicrobiae.o__Verrucomicrobiales.f__Verrucomicrobiaceae	3.83	0.017
front	p__Proteobacteria.c__Gammaproteobacteria.o__Alteromonadales.f__Alteromonadaceae	3.76	0.001
front	p__Proteobacteria.c__Gammaproteobacteria.o__Alteromonadales.f__OM60	3.67	0.002
front	p__Proteobacteria.c__Gammaproteobacteria.o__Vibrionales.f__Pseudoalteromonadaceae	3.67	0.000
front	p__Proteobacteria.c__Deltaproteobacteria.o__Bdellovibrionales.f__Bacteriovoracaceae	3.64	0.025
front	p__Proteobacteria.c__Gammaproteobacteria.o__Oceanospirillales.f__Endozoicimonaceae	3.31	0.015
front	p__Bacteroidetes.c__Saprospirae_.o__Saprospirales_.f__Saprospiraceae	3.12	0.040
front	p__Proteobacteria.c__Alphaproteobacteria.o__Sphingomonadales.f__Erythrobacteraceae	3.02	0.007
2 cm	p__Actinobacteria.c__Acidimicrobiia.o__Acidimicrobiales.f__OCS155	4.52	0.020
2 cm	p__SAR406.c__AB16.o__Arctic96B_7.f__A714017	3.79	0.031
2 cm	p__Proteobacteria.c__Gammaproteobacteria.o__Legionellales.f__Coxiellaceae	3.10	0.010
2 cm	p__Verrucomicrobia.c__Opitutae.o__Pelagicoccales_.f__Pelagicoccaceae	3.08	0.018
10 cm	p__Bacteroidetes.c__Sphingobacteriia.o__Sphingobacteriales.f__NS11_12	3.38	0.004
10 cm	p__Actinobacteria.c__Acidimicrobiia.o__Acidimicrobiales.f__C111	3.22	0.009
10 cm	p__Actinobacteria.c__Acidimicrobiia.o__Acidimicrobiales.f__wb1_P06	3.20	0.001
10 cm	p__Proteobacteria.c__Gammaproteobacteria.o__Alteromonadales.f__HTCC2188	3.05	0.001
10 cm	p__Actinobacteria.c__Actinobacteria.o__Actinomycetales.f__Microbacteriaceae	2.94	0.006

**P*-values are from a Kruskal-Wallace (KW) rank-sum test.

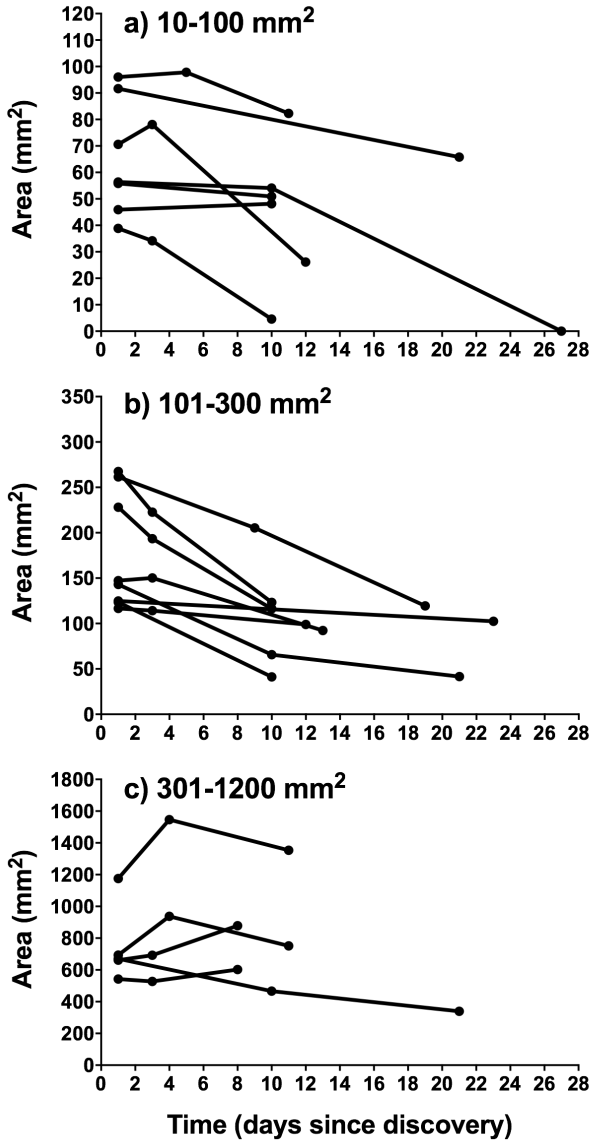

Figure S4.1. Lesion size change with time from day of discovery ($t = 0$).

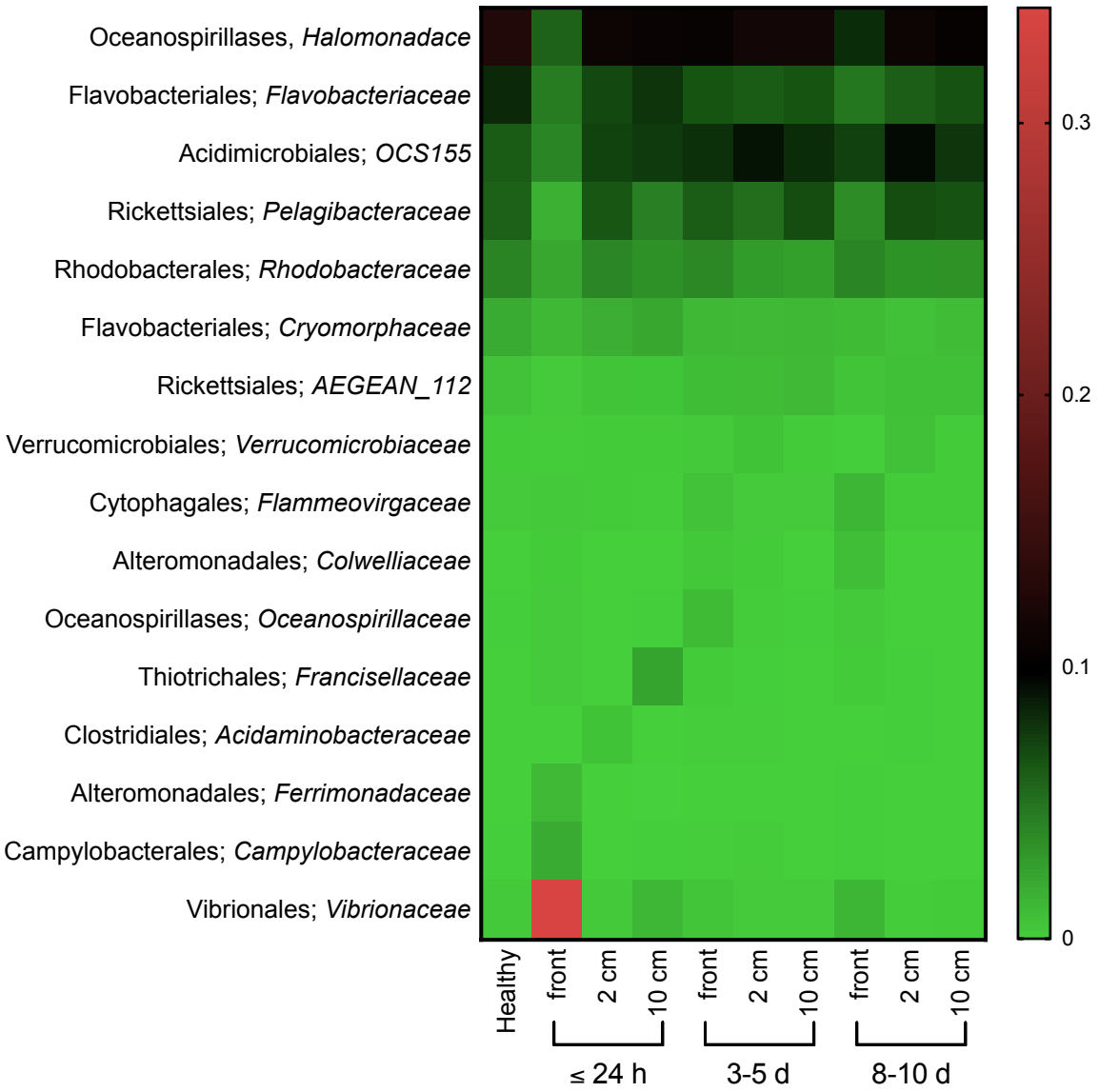

Figure S4.2. Differential relative abundance for the top 16 most abundant indicator families with significant Lefse LDA effect scores ($P < 0.05$).